



www.micore.eu



WP1 Historical storms

REVIEW OF CLIMATE CHANGE IMPACTS ON STORM OCCURRENCE

Deliverable D1.4





Project 202798

**REVIEW OF CLIMATE CHANGE IMPACTS ON
STORM OCCURRENCE**

**Edited by O. Ferreira (UALG), M. Vousdoukas (UALG)
and P. Ciavola (UniFe)**

Deliverable D1.4

Delivery date Month 12 (June 2009)

Version: 16/ 07/ 09

Authors (addresses to be found on outside covers)

Belgium

Piet Haerens (IMDC) and Renaat De Sutter (IMDC)

Bulgaria

Nikolay Valchev (IO-BAS), Ekaterina Trifonova (IO-BAS), Nataliya Andreeva (IO-BAS)

France-Aquitaine

Gonéri Le Cozannet (BRGM), Sophie Lecacheux (BRGM), Etienne Del vallee (BRGM), Nicolas Desramaut (BRGM), Elodie Charles (BRGM), Carlos Oliveros (BRGM), Yann Balouin (BRGM)

France-Mediterranean

Yann Balouin (BRGM), Rémi Belon (BRGM), Gonéri Le Cozannet (BRGM) and Mathieu Gervais (BRGM)

Italy-Northern Adriatic

Paolo Ciavola (UniFe), Andrea Valentini (ARPA-SIM), Marinella Masina (UniFe) and Clara Armaroli (UniFe)

Netherlands

Fedor Baart (TUD), Marije Smit (TUD) and Mark van Koningsveld (TUD)

Poland

Kazimierz Furmanczyk (USZ), Joanna Dudzinska-Nowak (USZ), Barbara Paplinska-Swerpel (USZ), Maciej Marek (USZ), Monika Kodrans-Nsiah (USZ)

Portugal-Western coast

Alexandre Quadrio (FFCUL) and Rui Taborda (FFCUL)

Portugal-Southern coast

Luis Pedro Almeida (UALG), Michalis Vousdoukas (UALG) and Óscar Ferreira (UALG)

Spain-Atlantic Andalusia

Pedro Ribera (UPO), D. Gallego (UPO), and C. Peña (UPO)

Spain-Catalan coast

José A. Jiménez (UniFe) and Eva Bosom (UniFe)

UK

Luciana S. Esteves (UoP), Jon J. Williams (UoP) and Jenny Brown (POL)

Executive Summary

The main objective of the European-funded MICORE project¹ is to develop and demonstrate on-line tools for the reliable prediction of storm impacts on coastlines and to develop and enhance existing civil protection strategies. Using available datasets, the magnitude and frequency of storms had been analysed at 9 diverse Europe sites in order to determine storm trends over a period spanning between 30 and 100 years. Meteorological and marine data available at national and European level were included in the analysis. Here the aim was to improve understanding of coastal responses to changes in storminess and only events above a locally defined storm threshold were considered. This overcame the problems associated with the integration and comparison of information from widely dispersed geographical locations in Europe.

The storm duration analysis performed for France (Aquitaine and Mediterranean), Italy (Northern Adriatic), Portugal (West Coast), Spain (Catalonia) and UK (Eastern Irish Sea) did not find any statistically significant change during the studied period. Similarly, no significant trends were observed for the Bulgarian and southern Portugal sites. The Polish site was the exception, showing a slight increase in storminess over the period studied. No clear trends in storm intensity were found for Italy–Northern Adriatic (waves and winds), Portugal–West Coast, and UK – Eastern Irish Sea. Similarly, Belgium, the Netherlands and Spain–Atlantic Andalusia (waves) did not detect any statistically significant trends. However, data from the Bulgarian and southern Portuguese coastlines indicated a slightly decreasing storminess trend. In contrast, a slight increase in storm frequency was observed in France–Aquitaine and Mediterranean (from the 1970s till 1990s), Italy–Northern Adriatic (only surges), Poland (significant both for surges and waves) and Spain–Andalusia (significant for wind). Results from the coastal regions in this study therefore support the conclusion that there are no significant trends detected in the magnitude or frequency of storms in Europe during the study period.

The study provided some evidence that storminess variability is much higher than the observed trends at the time-scales used in this work (i.e. more than 3 decades). For example, data from France–Aquitaine and Spain–Andalusia indicated a direct relationship between storminess and the NAO (North Atlantic Oscillation) index. It was, however, not possible to observe any clear association between storminess changes and changes in the global climate. This does not imply that global climate change consequences (e.g., sea temperature increase, sea level rise etc.) will not have an influence on European storminess and on storminess impacts in the future. However, for the existing and available data sets at a European level, those impacts have not been detected in this study

¹ Morphological Impacts and Coastal Risks Induced by Extreme storm events

An absence in many countries of measured wave data presented a significant problem in this study. Although wave hindcast data exists, its reliability is limited, and thus it is recommended that all EU countries initiate and contribute to a European database of wave measurements to be made available for research purposes. Further, since a project on the scale of MICORE could not include all European coastlines, some of the uncertainties in the interpretation of temporal changes to storminess could be reduced through consideration at a regional-scale. It is important to note also that although no clear trends in storminess emerge from the present study, this result does not necessarily imply that longer-term trends are absent. The study has thus far not considered changes in the occurrence of “clusters” of events, i.e. the occurrence of several medium-energy events over a short time-scale. With respect to coastal evolution such storm ‘sequencing’ can have a major role in depleting beach sediments and decreasing resilience of dune ridges. Understanding and predicting this impact using innovative approaches will form the next area of work in the MICORE project and will provide a basis for the development of future coastal storm warning systems.

Disclaimer

The research leading to these results has received funding from the European Community's Seventh Framework Programme under grant agreement n° 202798. The views expressed in the report are the responsibility of the authors. No parts of this report could be extracted or reproduced without the permit of the authors. For further information contact the Project's Coordinator (Prof. Paolo Ciavola) at cvp@unife.it.

Contents

1	INTRODUCTION.....	10
1.1	REFERENCES.....	11
1.2	WEBSITES.....	11
2	BELGIUM.....	12
2.1	INTRODUCTION.....	12
2.2	METHODS.....	12
2.3	RESULTS.....	13
2.3.1	<i>Wind</i>	13
2.3.2	<i>Waves</i>	16
2.3.3	<i>Sea level</i>	19
2.4	CONCLUSIONS.....	22
2.4.1	<i>Wind</i>	22
2.4.2	<i>Waves</i>	22
2.4.3	<i>Sea level</i>	22
2.4.4	<i>Storminess</i>	22
2.5	REFERENCES.....	23
3	BULGARIA.....	25
3.1	METHODS.....	25
3.2	RESULTS.....	27
3.3	CONCLUSIONS.....	30
3.4	REFERENCES.....	30
4	FRANCE-AQUITAINE.....	32
4.1	METHODOLOGY.....	32
4.2	RESULTS.....	34
4.3	CONCLUSION.....	36

4.4	REFERENCES.....	37
5	FRANCE-MEDITERRANEAN.....	39
5.1	METHODS	39
5.2	RESULTS	40
5.2.1	<i>Short-term tendencies</i>	40
5.2.2	<i>Mid-term tendencies</i>	41
5.3	CONCLUSIONS	44
5.4	REFERENCES.....	45
6	ITALY-NORTHERN ADRIATIC.....	46
6.1	METHODS	46
6.1.1	<i>Meteo, wave and tidal data-sets</i>	46
6.1.2	<i>Meteo storminess analysis</i>	49
6.1.3	<i>Wave storminess analysis</i>	50
6.2	RESULTS	50
6.2.1	<i>Analysis of storm occurrence: long-term wind observations</i>	50
6.2.2	<i>Analysis of storm occurrence: medium-term wave records</i>	51
6.2.3	<i>Occurrence of storm surges</i>	53
6.3	CONCLUSIONS	53
6.4	CONSULTED WEBSITES	54
6.5	REFERENCES.....	55
7	NETHERLANDS	57
7.1	INTRODUCTION.....	57
7.2	METHODS	57
7.2.1	<i>Observations over the last decades</i>	57
7.2.2	<i>Modelled climate change effects</i>	58
7.3	RESULTS	58

7.3.1	<i>Observations over the last decades</i>	58
7.3.2	<i>Modelled climate change effects</i>	60
7.4	CONCLUSIONS	61
7.5	REFERENCES.....	62
8	POLAND	63
8.1	METHODS	63
8.2	RESULTS	64
8.3	CONCLUSIONS	69
8.4	REFERENCES:.....	69
9	PORTUGAL-WESTERN COAST	71
9.1	METHODS	71
9.1.1	<i>Storm definition</i>	71
9.1.2	<i>Model validation</i>	72
9.2	RESULTS	73
9.3	CONCLUSIONS	78
9.4	REFERENCES.....	78
10	PORTUGAL-SOUTHERN COAST	79
10.1	METHODS	79
10.2	RESULTS	80
10.2.1	<i>Validation/modification of Hindcast data (HIPOCAS)</i>	80
10.2.2	<i>Historical Storminess Analysis</i>	82
10.3	CONCLUSIONS	86
10.4	REFERENCES.....	86
11	SPAIN-ATLANTIC ANDALUSIA	87
11.1	INTRODUCTION.....	87
11.2	DATA AND METHODS.....	87

11.3	RESULTS	88
11.3.1	<i>Storm definition</i>	88
11.3.2	<i>NAO relationship</i>	89
11.3.3	<i>Transfer function</i>	90
11.4	SUMMARY	92
11.5	REFERENCES.....	93
12	SPAIN-CATALAN COAST	94
12.1	INTRODUCTION.....	94
12.2	STUDY AREA AND DATA	94
12.3	STORMINESS VARIABLES	96
12.3.1	<i>Wave variables</i>	96
12.3.2	<i>Storm-induced hazards</i>	96
12.4	RESULTS	98
12.5	SUMMARY AND CONCLUSIONS	105
12.6	ACKNOWLEDGEMENTS.....	106
12.7	REFERENCES.....	106
13	UK.....	107
13.1	METHODS OF ANALYSIS	107
13.1.1	<i>Measured water level and surge - Tide Gauges</i>	107
13.1.2	<i>Measured wind, barometric pressure and waves</i>	107
13.1.3	<i>POLCOMS-WAM model</i>	107
13.1.4	<i>ERA-40 waves, wind and barometric pressure</i>	108
13.2	RESULTS	108
13.3	SUMMARY	112
13.4	REFERENCES.....	113
14	FINAL CONSIDERATIONS.....	115



14.1	DIFFERENCES IN THE AVAILABLE DATASETS	115
14.2	DIFFERENCES IN THE USED PROXIES	116
14.3	DIFFERENCES IN THE ANALYSIS	116
14.4	STORMINESS ANALYSIS	116
14.4.1	<i>Storm duration</i>	117
14.4.2	<i>Storm intensity</i>	117

1 Introduction

Severe storms have historically affected European coastlines but the knowledge on changes on storminess for the last decades is still restricted. Climate change is assumed to be a main driving factor with a potential to induce changes on the intensity, duration and frequency of powerful storm events, including a long-term increase/decrease on peak wind speeds, surges and waves. It is therefore important to know if the magnitude of storms, their duration and frequency has changed in the last decades. The understanding of trends in storminess in the last decades will help to better prepare coastal managers for future events, taking into account potential changes on storm occurrence and magnitude to improve planning of mitigation and adaptation strategies.

One main goal of MICORE, within the objectives of WP1, is to undertake an analysis of change in storm occurrence and to consider future variability in the context of climate change. This analysis includes the study of trends in meteorological data (e.g. changes in storminess proxies) and intends to provide guidance for the understanding of the response of coastlines to potential changes in the forcing agents. The analysis presented hereafter is based on the study of existing databases available at national and European level for different forcing agents. The considered driving factors include storm waves, wave energy, winds and surge levels, depending on data availability and on the specific conditions of exposure of each coastline. A main factor limiting the analysis is the unavailability of representative (mostly measured) data sets for the last 40 years or more. Measured data, i.e. waves, only recently have become available (2-3 decades at the most) and rarely allows a comprehensive analysis of storminess changes when used alone. Therefore, it was necessary to incorporate model predictions (e.g. hindcast models) that were previously validated to assure a quality control.

In the original MICORE WP1 description it was mentioned that historical data (last 150 years) would be used for this analysis. However, it was found that already compiled or existing information on meteorological and oceanographic forcing was available for the last 150 years only for a few countries from the MICORE Consortium. Moreover, the data quality was generally low, with several gaps in time series, small accuracy and large number of uncertainties in the measurements. For most of the cases it was also almost impossible to compare these datasets with measured or hindcasted data from the last 40-50 years. As a consequence, it was decided to focus the study mainly on the last decades (generally 40 to 50 years datasets) where the available data was found to have good quality standards.

The storminess analysis was made for all study areas of MICORE (for further details see Ferreira et al. 2009 and www.micore.eu). Three additional areas (Aquitaine-France, Catalonia-Spain, and Portuguese West Coast) considered relevant for the goals of this deliverable and not included in the defined study areas were also incorporated in this analysis. The coastal regions where storminess was studied are:

- Belgium – The entire coastal area

- Bulgaria – The entire coastal area
- France – Aquitaine
- France – Mediterranean
- Italy – Northern Adriatic
- Netherlands – The entire coastal area
- Poland – The entire coastal area
- Portugal – South Coast
- Portugal – West Coast
- Spain – Atlantic Andalusia
- Spain – Catalonia
- United Kingdom – Eastern Irish Sea

The main scopes of this deliverable are:

- To present different proxies and approaches to study storminess changes;
- To identify potential storminess changes for the studied European countries;
- To evaluate if there is any general trend of storminess change for Europe;

1.1 References

Ferreira, Ó., Ciavola, P., Armaroli, C., Balouin, Y., Benavente, J., Del Río, L., Deserti, M., Esteves, L.S., Furmanczyk, K., Haerens, P., Matias, A., Perini, L., Taborda, R., Terefenko, P., Trifonova, E., Trouw, K., Valchev, N., Van Dongeren, A., Van Koningsveld, M. and Williams, J.J., 2009. Coastal Storm Risk Assessment in Europe: Examples from 9 study sites. *Journal of Coastal Research*, SI 56, 1632-1636.

1.2 Websites

MICORE Project (www.micore.eu)

2 Belgium

Piet Haerens and Renaat De Sutter

2.1 Introduction

The effects of climate change on marine systems are manifold (Van den Eynde, De Sutter et al., 2008). Sea level rise is an important indicator of climate change in coastal regions. It increases the likelihood of storm surges, coastal erosion, land-water salt intrusion and it endangers coastal ecosystems, etc. Changes in the sediment transport cycles will occur and cause, together with the changing hydrodynamic conditions, secondary effects, e.g., on dredging activities, marine transport and harbour activities. Ocean warming can increase zoo- and phytoplankton productivity (CO₂-uptake), increase risks for human health, change the marine species composition, stress the fishery activities, etc.

This document reports on the state of the art of climate change impact assessment of the marine hydrodynamic environment of the Belgian Part of the North Sea (BPNS). More specifically, the report deals with wind, waves and water level but focussing on storm conditions and hence the extreme conditions for these parameters.

For the BPNS, ongoing scientific work is being carried out within the CLIMAR project (<http://www.arcadisbelgium.be/climar/>) which was used as the main source of information for this document. As the author of this document, R. De Sutter, is - besides his main activities for IMDC - also part-time active for Gent University and in that position involved in the CLIMAR project, up-to-date data and information regarding the CLIMAR activities could be used and evaluated for this report. All CLIMAR partners, especially MUMM (<http://www.mumm.ac.be/>), are greatly acknowledged for the use of their work. Besides that project, also short reference is made to the SEAMOCS project (<http://www.maths.lth.se/seamocs/index.html>) for what concerns storm surges. Unfortunately, no detailed project reports are publicly available at the moment.

2.2 Methods

For the BPNS, ongoing scientific work is being carried out within the CLIMAR project and this project is the main source of information for this document. The objective of CLIMAR is the elaboration of an evaluation framework for adaptation scenarios/measures as a response to climate induced ecological, social and economical impacts and this for the Belgian North Sea environment. One of the objectives is the definition and modelling of climate change induced primary impacts at North Sea scale: sea level rise, increased storminess, possible increased rainfall, temperature, etc.

Besides that project, also short reference is made to the SEAMOCS project dealing with storm surge. The European research and training network SeaMocs deals with the application of stochastic models for coastal currents, climate and safe transportation

(www.maths.lth.se/seamocs). Unfortunately, no detailed project reports are publicly available at the moment.

This document provides an evaluation of the available literature information, additional data analysis within the MICORE project has not been performed.

2.3 Results

2.3.1 Wind

2.3.1.1 Introduction and average values

An analysis of wind data was carried out in the framework of the Climar project: a statistical analysis of the data available for wind measurements in the (near) the Belgian Part of the North Sea for a period from the first available to the most recent measurements (Van den Eynde et al., 2008). All results are reported in (Van den Eynde et al., 2008).

A first set of analysed data (Westhinder) were measured by the Flemish Community, Agency of Maritime Service and Coast (MDK). A second set of measurements (Brouwershavense Gat 2 and the Vlakte van de Raan) was obtained from the Hydro Meteo Centrum Zeeland (<http://www.hmcz.nl>), where data may be downloaded. From the Norwegian Meteorological Institute (DNMI), wind field data for atmospheric pressure and wind vectors were obtained for the period 1955 to 2006. Based on these wind fields, a time series for the station Westhinder was constructed.

There is no clear increasing or decreasing trend detected in the average wind speed. The analysis of average wind speed is not further documented here, as the focus of the Micore project is on storminess.

Results on wind direction are as follows: both the wind component to the North and the wind component to the East are increasing over time, but the wind component to the East at a higher pace. This indicates therefore a change over time of the wind direction moving from West winds to South-West winds. The analysis also shows that the strongest winds occur in the months November to February, but no clear seasonal difference in wind direction occurs. More details on variation in wind direction can be found at (Van den Eynde et al., 2008).

2.3.1.2 Frequency of extreme wind conditions

The occurrence of high wind speeds was analysed and revealed the following results. As an example, in Fig. 1 and Fig. 2, the percentage of occurrence of wind speeds greater than or equal to respectively 6 Bft. and 8 Bft. for the meteorological predictions of DNMI to Westhinder is shown. 6 Bft corresponds with a power-full wind with wind velocities greater than 10,8 m/s while 8 Bft. Corresponds to storm conditions with wind speeds greater than 17.2 m/s. Fig. 3 shows the maximum wind speeds for the same data set.

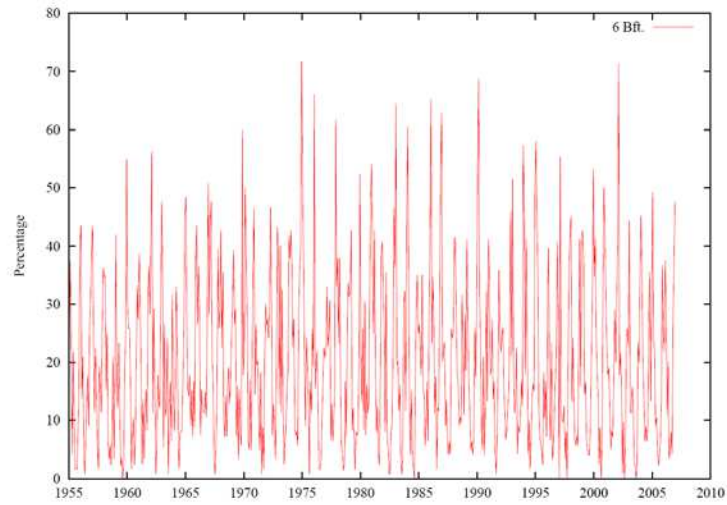


Figure 1. Percentage of occurrence of wind speeds over 6 Bft. at Westhinder in the meteorological forecasts of DNMI (Van den Eynde et al., 2008)

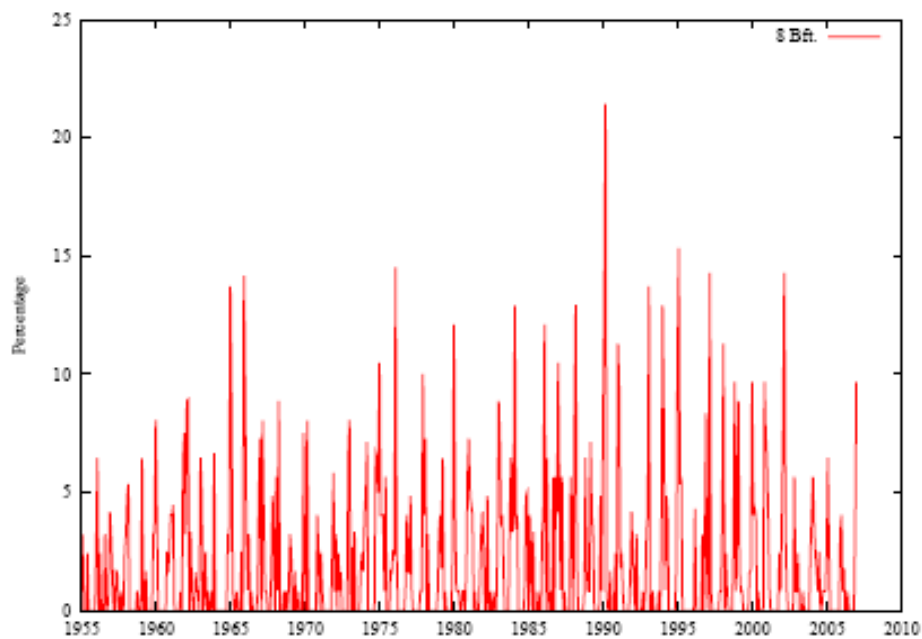


Figure 2. Percentage of occurrence of wind speeds over 8 Bft. at Westhinder in the meteorological forecasts of DNMI (Van den Eynde et al., 2008)

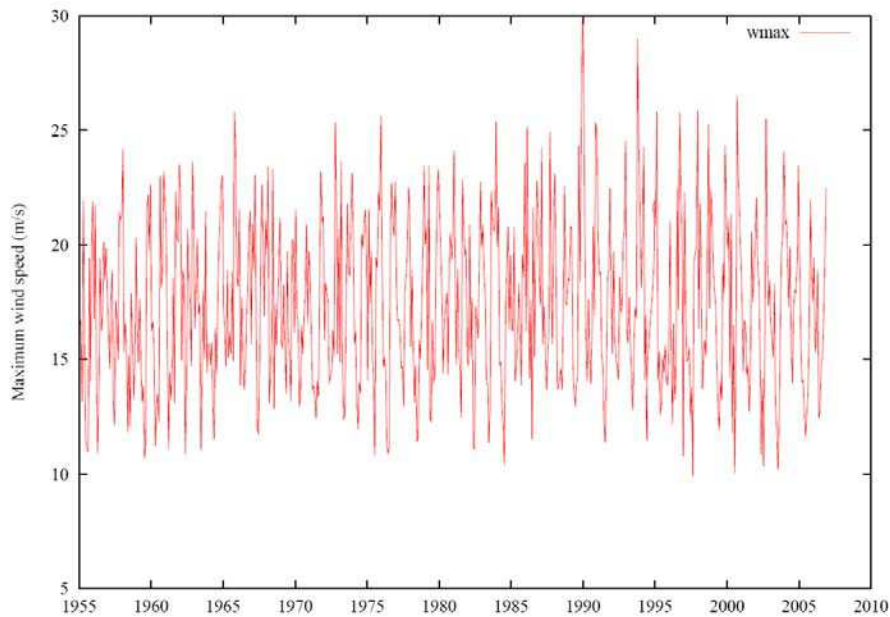


Figure 3. Occurrence of maximum wind speeds at Westhinder in the meteorological forecasts of DNMI (Van den Eynde et al., 2008)

In general, there is no clear trend observed for the occurrence frequency of high wind speeds or maximum wind speeds (Van den Eynde et al., 2008).

Table 1 Overview of the linear regression results for all 4 data sets : average (gemidd.), constant (constant a) and linear slope (helling b) for wind speeds greater than 6 Bft, greater than 8 Bft and the maximum wind speed

		Gemidd.	Const. a	Helling b
% $w_s > 6$ Bft.	Westhinder	29,94 %	32,09 %	-0,103 %/jaar
	Brouwersh. Gat 2	22,08 %	21,46 %	+0,042 %/jaar
	Vlakte van de Raan	21,30 %	16,93 %	+0,235 %/jaar
	Westhinder DNMI	20,10 %	20,09 %	+0,010 %/jaar
% $w_s > 8$ Bft.	Westhinder	3,43 %	5,44 %	-0,0966 %/jaar
	Brouwersh. Gat 2	1,28 %	1,40 %	-0,0082 %/jaar
	Vlakte van de Raan	1,12 %	0,74 %	+0,0204 %/jaar
	Westhinder DNMI	1,95 %	1,94 %	+0,0107 %/jaar
Max. w_s	Westhinder	21,14 m/s	20,54 m/s	+0,029 m/s/jaar
	Brouwersh. Gat 2	18,59 m/s	18,12 m/s	+0,032 m/s/jaar
	Vlakte van de Raan	18,68 m/s	17,53 m/s	+0,062 m/s/jaar
	Westhinder DNMI	17,39 m/s	17,39 m/s	-0,002 m/s/jaar

The report very cautiously proposes the conclusion that average wind speeds might be decreasing but that the maximum values could be increasing. The linear regression attempts however do not yield very reliable conclusions and data sets are limited (Van den Eynde, 2008).

In Siegismund and Schrum (2001), an evaluation of wind speed and wind direction for the entire North Sea based on data for the period 1958-1997 was carried out. In these results an increase in wind speed over the North Sea is observed by about 10%. Weisse et al (2005) obtained, via a regional climate model, the conclusion that there is a rising trend in the occurrence of storms for the period 1958 to 1990 in the Southern North Sea, followed by a decrease in the occurrence of storms since 1990-1995. A recent Dutch study (Smits et al., 2005) analyzed a number of high quality wind data in the Netherlands. These results indicate a continuous reduction in the number of storms in the Netherlands since 1962 to 2002.

2.3.2 Waves

2.3.2.1 Introduction and significant wave height

An analysis of wave data was carried out in the framework of the CLIMAR project: a statistical analysis of the data available for wave heights in the (near) the Belgian Part of the North Sea for a period from the first available to the most recent measurements (Van den Eynde et al., 2008). All results are reported in (Van den Eynde et al., 2008).

Wave measurements were carried out by the Flemish Community Services Agency Maritime and Coast (MDK) at the Bol van Heist (period 1978 – 2007), measurements carried out by Hydro Meteo Centrum Zeeland at 3 locations (Brouwershavense Gat 2 period 1980-2007, Deurloo and Scheur West both for the period 1985-2007).

As a method to quantify long-term trends, a linear regression on the different time series was applied. In Table 2 the results for the different measuring data are presented. At the stations Bol van Heist and Brouwershaven Gat 2 there is a decrease in monthly average significant wave height observed of -0.0013 m / year and -0.0027 m / year, respectively. This means that the average significant wave height at the Bol van Heist decreased from 0.7254 m in 1980 to 0.6905 m in mid-2007. Secondly, in station Deurloo no significant changes can be observed, and in station Scheur West even an increase in the monthly average significant wave heights is observed by 0.0024 m / year.

Table 2 Constant and slope in the linear regression for the average monthly significant wave height and corresponding standard deviations (Van den Eynde et al., 2008).

Location	Constant a (m)	Slope b (m/year)	STD a (m)	STD b (m/year)
Bol van Heist	0,7254	-1,3 10 ⁻³	2,3 10 ⁻⁴	9,0 10 ⁻⁷
Brouwershavensche Gat 2	0,9642	-2,7 10 ⁻³	1,3 10 ⁻³	4,9 10 ⁻⁶
Deurloo	0,8389	3,7 10 ⁻⁴	4,7 10 ⁻³	1,5 10 ⁻⁵
Scheur West	0,7733	2,4 10 ⁻³	5,0 10 ⁻³	1,6 10 ⁻⁵

2.3.2.2 Frequency of high waves and maximum wave heights

In Fig. 4 and Fig. 5 the percentage of significant wave heights that exceed 2 m and 3 m for the entire period at the Bol van Heist is given. From these Figures it may be inferred that there is a reduction in the incidence of the higher waves at the Bol van Heist. No reduction of the maximum significant wave height (Fig. 6) was observed.

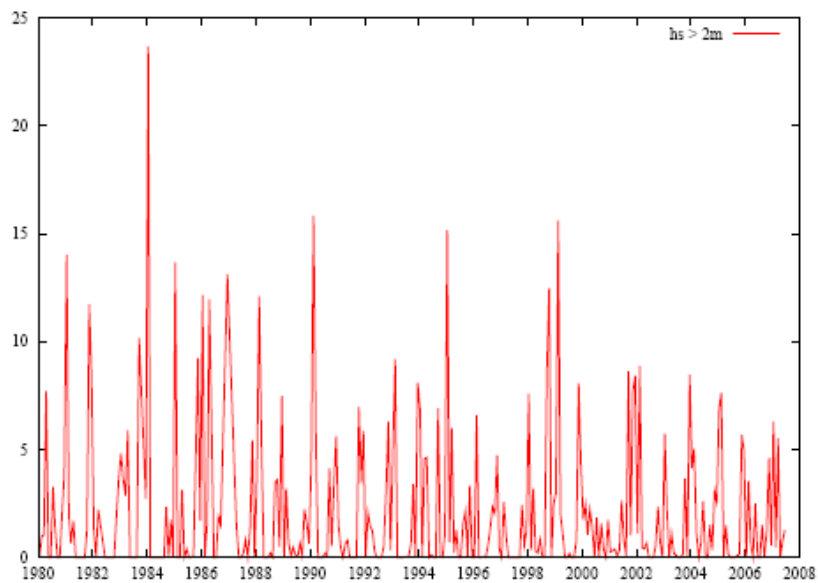


Figure 4. Percentage of occurrence of waves with significant wave height greater than 2 m, at the Bol van Heist. Measurements of MDK (Van den Eynde et al., 2008).

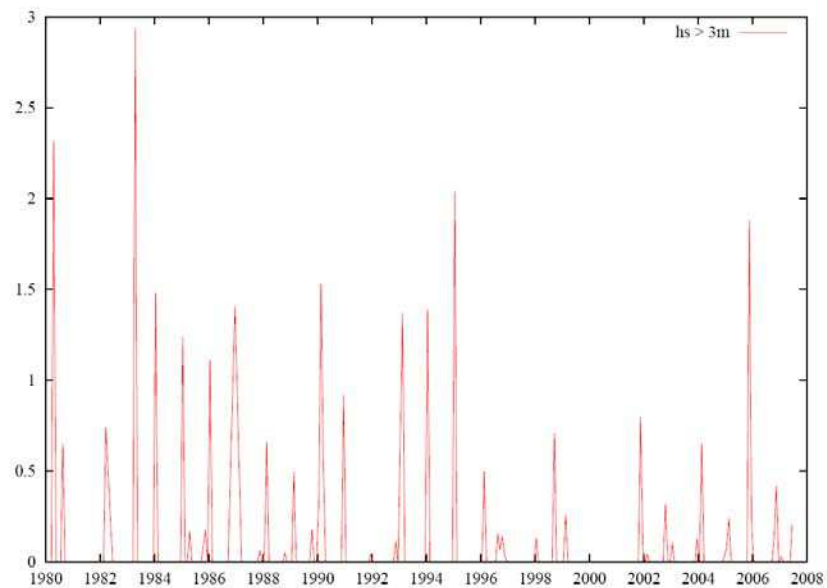


Figure 5. Percentage of occurrence of waves with significant wave height greater than 3 m, at the Bol van Heist. Measurements of MDK (Van den Eynde et al., 2008).

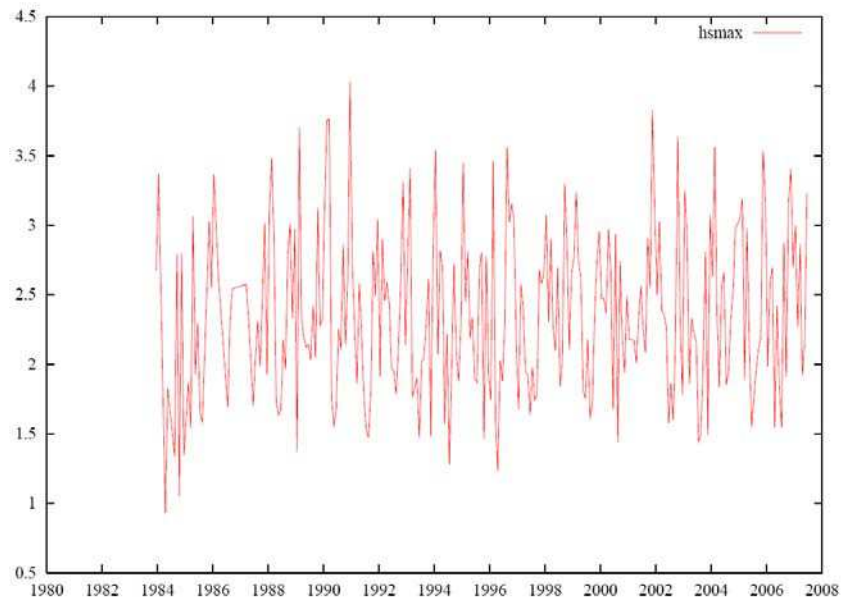


Figure 6. Maximum significant wave heights, at the Bol van Heist. Measurements of MDK (Van den Eynde et al., 2008).

For all data sets, a linear regression was applied to monthly averaged significant wave height data to confirm a possible long term trend.

Table 3 Overview of the linear regression results for all 4 data sets : average (gemidd.), constant (constant a) and linear slope (helling b) for significant wave heights greater than 2 m, than 3 m and the maximum significant wave height

		Gemidd.	Const. a	Helling b
% $H_s > 2$ m	Bol van Heist	2,111 %	2,597 %	-0.034 %/jaar
	Brouwersh. Gat 2	6,576 %	8,444 %	-0.136 %/jaar
	Deurloo	4,040 %	3,969 %	+0.004 %/jaar
	Scheur West	3,520 %	3,796 %	-0.017 %/jaar
% $H_s > 3$ m	Bol van Heist	0,093 %	0,157 %	-0.004 %/jaar
	Brouwersh. Gat 2	1,282 %	2,115 %	-0.061 %/jaar
	Deurloo	0,448 %	0,514 %	-0.004 %/jaar
	Scheur West	0,427 %	0,557 %	-0.008 %/jaar
Max. H_s	Bol van Heist	2,357 m	2,232 m	+0.0077 m/jaar
	Brouwersh. Gat 2	2,983 m	2,998 m	-0.0010 m/jaar
	Deurloo	2,694 m	2,715 m	-0.0013 m/jaar
	Scheur West	2,650 m	2,582 m	+0.0041 m/jaar

Except for the station Deurloo where the percentage of waves higher than 2 m remains about the same, there seems to be a slight decrease in the percentage of waves higher than 2 m or higher than 3 m. In the case of the percentage of waves higher than 2 m at the station Brouwershaven Gat 2, the decrease is clear: the rate fell from 8.44% in 1980 to 4.64% in mid 2007. For other stations, however, the decrease is limited.

The view on the monthly average maximum significant wave height is more divided, with a decrease in Brouwershaven Gat 2 and Deurloo, but an increase in the stations of Bol van Heist and Scheur West.

This may indicate that on average the waves are getting lower, but the 'extreme events' are getting more extreme (Van den Eynde et al., 2008).

2.3.3 Sea level

2.3.3.1 Introduction

There is now global consensus that sea level is continuously rising. In Europe, increases in sea level are measured between 0.8 and 3 mm per year (European Commission, 2006). This is partly the result of thermal expansion (volume increase with increasing temperature) and partly due to exchange of melting ice on land with the sea) In MIRA (2008) one can find more information about the causes, the reported changes at the global level, the evolution of sea level on a European scale, etc.

Not only will the mean sea level (MSL) rise, but also the extreme water levels. Changes in sea level and in storminess will increase the height of storm surges and the risk of coastal flooding.

In addition, vertical land movements will alter the relative height of extreme water events measured on land.

2.3.3.2 Mean sea level

The determination of the sea level rise is part of the research work scheduled in the work package 1 of the CLIMAR project (Ozer et al., 2008).

A time series of yearly mean sea level values (MSL) at the station Oostende has been used to investigate how MSL has evolved during the last 80 years.

The time series of yearly mean sea level values used in the cited study is presented on Fig. 7. The data are varying between 2.172 m (observed in 1929) and 2.357 m (observed in 2001). Even though the year to year variability is high, it is quite clear that MSL has risen over the period of interest. This is further confirmed by the fact the mean value, equal to 2.257 m, is well below the latest MSL value, equal to 2.294 m, computed by the Agency for Marine and Coastal Services (MDK) over the period 1982.3 – 2000.

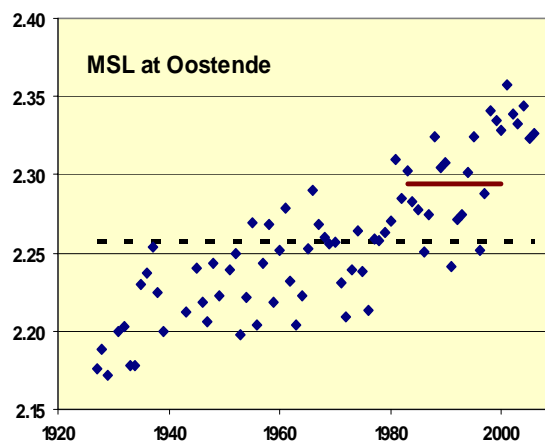


Figure 7. Time series of yearly mean sea level at Oostende for the period 1927-2006. The black dashed line shows the mean value of the dataset (2.257 m). The brown solid line shows the latest MSL value (2.294 m) published by the Agency for Marine and Coastal Services. This value has been computed over the period 1982.3 – 2000 (Ozer et al., 2008)

With the conventional linear regression line, MUMM derives a sea level rise equal to 1.69 mm/yr: a value greater than those reported in previous studies (Van Cauwenberghe, 1995, 1999) but in the meantime very close to the value (1.70 mm/yr) estimated by the Intergovernmental Panel on Climate Change (IPCC) (Bindoff et al., 2007) for the global average sea level rise during the 20th century. Models in which the sea level rise is allowed to vary in time (either by step or continuously) fit better with the data than the simple linear regression model. However, the gain is relatively limited and it is hard to conclude that there is an acceleration of the trend. The present SLR (e.g. based on a piecewise linear model) lies close to 4.4 mm/yr (Van den Eynde, De Sutter et al., 2008).

Meanwhile, in the Netherlands high-end climate change scenarios for flood protection are under further investigation. Very recent information (Katsman et al., 2009) project local sea level rises in between 0.5 m and 1.15 m or in between 0.05 m and 1.25 m for 2100, depending on the adopted impact of the elastic and gravity effects. For 2200 these ranges become respectively 1.5 – 4 m and 0.5 – 4 m.

If we look at the UK, for the first time uncertainty ranges are given, including uncertainty in current models and emission scenarios. They project the likely range of absolute SLR around the UK to range from 11.6 cm to 75.8 cm (the 5th percentile and the 95th percentile) by 2095 (Lowe et al., 2009).

2.3.3.3 Surge level

Within the Seamocs-project, long-term measurements of water levels along the Belgian coast (since 1925), divided into the astronomical tidal component and storm surge level, as well as wind speeds are analyzed and related to atmospheric circulation patterns.

Figure 8 shows the evolution of the yearly averaged surge level in Ostend. A rising trend can be observed.

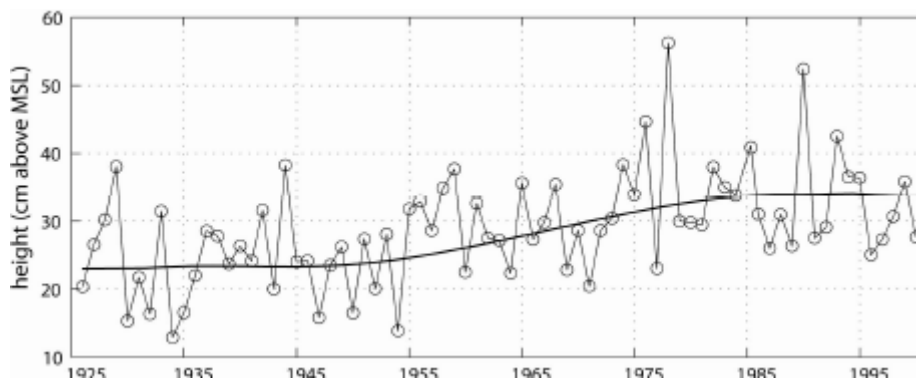


Figure 8. Evolution of the yearly averaged surge level at Ostend (Ullman, 2008)

Extreme surge heights are defined as surge heights above the 90th percentile of sea-surge height at Ostend (period 1925-2000), which is equal to 35 cm. More than 80% of the extreme surge heights at Ostend are associated with onshore North-westerly winds. A slight (linear) increase of the annual 90th percentile of sea surge at Ostend is noticed, with a value of + 1 mm/yr ($p > 99\%$) during the period 1925-2000.

Based on a historical analysis of the correlation between the surge level at Ostend and different weather patterns (atmospheric circulation patterns over the Northern Atlantic) for the period 1925-2000, it is shown that 70% of the surge levels greater than 65 cm are the result of one specific weather pattern, known as the "Atlantic Ridge" (AR) pattern with a north-westerly flow over the Belgian coast. There is a correlation between the frequency of occurrence of the AR-type weather in the winter and the occurrence of a high (99% percentile) surge level. This correlation has increased since 1965 and appears to be associated with a

corresponding increase in air pressure above the North Atlantic Ocean. While the occurrence of the AR pattern has not increased, the higher correlation leads to a higher “risk of occurrence” of very high surge levels (Monbaliu and Ullmann, 2009).

The project is still ongoing and detailed results are not publicly available yet.

2.4 Conclusions

2.4.1 Wind

There is no clear trend observed for the occurrence of high wind speeds or maximum wind speeds over the BPNS (Van den Eynde et al., 2008).

Also other recent literature (from the Netherlands or Germany) does not yield a clear response and a significant trend in extreme wind speeds cannot be put forward.

2.4.2 Waves

Based on the work of (Van den Eynde et al., 2008), no clear trend in significant wave heights or in the occurrence of higher waves can be demonstrated and yet implemented in a climate change scenario analysis.

2.4.3 Sea level

With the conventional linear regression line, MUMM derives a sea level rise equal to 1.69 mm/yr over the last 80 years (Ozer et al., 2008). The present SLR lies close to 4.4 mm/yr (Van den Eynde et al., 2008).

Specifically for Flanders, IMDC (2005) published the hydraulic boundary conditions for the Flemish Coast. This document should be considered as the standard during the design of constructions along the Belgium coast. IMDC states that a relative rise of the mean sea level of 22 cm is to be expected in the coming 50 years (2005 to 2055). For design purposes, however, the rise of the high tide level is more important. IMDC (2005) suggests considering a relative rise of the high tide level of 30 cm and a rise of the mean sea level of 25 cm in the coming 50 years (2005 to 2055).

Preliminary results from the Seamocs-project indicate that the yearly averaged surge levels at the Belgian coast and extreme surge levels are rising (Ullman, 2008).

2.4.4 Storminess

All literature sources do not yield a clear vision and do not confronting information ready to be implemented in a climate change scenario. There is currently not enough scientific evidence to support a scenario with increased storminess for the Flemish coast. There are no Flemish design guidelines yet for taking into account climate change induced changes in extreme wind or waves or changes in intensity and duration of storms.

2.5 References

Bindoff, N.L., J. Willebrand, V. Artale, A. Cazenave, J. Gregory, S. Gulev, K. Hanawa, C. Le Quéré, S. Levitu, Y. Nojiri, C.K. Shum, L.D. Talley and A. Unnikrishnan, 2007. Observations: Oceanic Climate Change and Sea Level. In: Climate Change 2007: The Physical Science Basis. Contribution of Working Group I to the Fourth Assessment Report of the Intergovernmental Panel on Climate Change [Solomon, S., D. Qin, M. Manning, Z. Chen, M. Marquis, K.B. Averyt, M. Tignor and H.L. Miller (eds)]. Cambridge University Press, Cambridge, United Kingdom and New York, NY, USA.

IMDC, 2005. Hydraulische randvoorwaardenboek Vlaamse kust. IMDC in opdracht van het Ministerie van de Vlaamse Gemeenschap, Departement Leefmilieu en Infrastructuur, Administratie Waterwegen en Zeewezen, Afdeling Waterwegen Kust. In Dutch.

IPCC, 2007. Fourth Assessment Report: Climate Change 2007_Synthesis Report (unedited copy) + Contribution of Working Group I_The Science of Climate Change + Contribution of Working Group II_Impacts, Adaptation and Vulnerability + Contribution of Working Group III_Mitigation of Climate Change.

Katsman C., Hazeleger W., Sterl A., Beersma J., 2009. Exploring high-end scenario's for flood protection of the Netherlands. Conference Climate change : global risks, challenges and decisions. Copenhagen, March 2009. IOP Conference series: Earth and Environmental Science 6 352004.

Lowe J., Tinker J., Howard T., De Gusmao D., Wolf J., Horsburgh K., Holt J., Reeder T., 2009. Informing adaptation : a new set of marine climate change scenario's. Conference Climate change : global risks, challenges and decisions. Copenhagen, March 2009. IOP Conference series: Earth and Environmental Science 6 352002.

MIRA, 2008. Milieurapport Vlaanderen, achtergronddocument klimaatverandering 2007. Brouwers J., De Nocker L., Schoeters K., Moorkens I., Jaspers K., Aernouts K., Beheydt D., Vanneuville W., Vlaamse Milieumaatschappij, april 2008. Downloadbaar op www.milieurapport.be.

Ozer J., Van den Eynde D. and Ponsar S., 2008. Evaluation of climate change impacts and adaptation responses for marine activities: CLIMAR. Trend analysis of the relative mean sea level at Oostende (Southern North Sea – Belgian coast), MUMM, 14 p.

Siegismund, F. and Schrum C., 2001. Decadal changes in the wind forcing over the North Sea. Climate Research, 18, 39-45.

Smits, A., S.M.G. Klein Tank and G.P. Können, 2005. Trends in storminess over the Netherlands, 1962-2002. International Journal of Climatology, 25 (10),1331-1344.

Ullman, A., 2008. Atmospheric circulation and sea-surge variation along the Belgian coast during the 20th century. Presentation at the SEAMOCs-conference in Høvik, Norway. 23-24 October 2008.

Ullmann, A. and Monbaliu, J., 2009. Changes in atmospheric circulation over the North Atlantic and sea-surge variations along the Belgian coast during the twentieth century, *International Journal of Climatology*, 29.

Van Cauwenberge, C., 1995. Relative sea level rise: further analyses and conclusions with respect to the high water, the mean sea and the low water levels along the Belgian coast. Report nr 37ter of the Hydrografische Dienst der Kust.

Van Cauwenberghe, C., 1999. Relative sea level rise along the Belgian coast: analyses and conclusions with respect to the high water, the mean sea and the low water levels. Report nr 46 of the Hydrografische Diensts der Kust.

Van den Eynde, D., De Sutter, R., Maes, F., Verwaest, T., van Bockstaele, E., 2008. Evaluation of climate change impacts and adaptation responses for marine activities: CLIMAR, Samenvattend rapport bij de Fase 1 van het CLIMAR project voor Federaal Wetenschapsbeleid, juli 2008, 33 p.

Van den Eynde, D., Francken F., Ponsar S. and Ozer J., 2008. Evaluation of climate change impacts and adaptation responses for marine activities: CLIMAR, Bepaling van de primaire impacten van klimaatsverandering: statistische analyse van metingen van golven, windsnelheid en –richting en van zeewatertemperatuur. MUMM.

Weisse, R., Von Storch H. and Feser F., 2005. Northeast Atlantic and North Sea storminess as simulated by a regional climate model during 1958-2001 and comparison with observations. *Journal of Climate*, 18, 465-479.

3 Bulgaria

Nikolay Valchev, Ekaterina Trifonova, Nataliya Andreeva

3.1 Methods

This analysis of climate impact on storm occurrence and intensity is based on long-term data series obtained by means of hindcast. This approach allows reconstruction of the wave field using continuous meteorological forcing. It was chosen because of the absence of long-lasting wave measurement in the Black Sea.

The global atmospheric pressure reanalysis spanning 61 years (1948-2008) carried out by the European Centre for Medium-range Weather Forecast (Uppala et al., 2005) and National Centre for Environmental Prediction (NCEP/NCAR) (Kalnay et al., 1996) was used to calculate the historical wind forcing for wave models. Since the atmospheric pressure fields have rather coarse resolution (2.5° spatial and 6 hours temporal), the wind input spatial resolution was downscaled to 0.5° through a regional atmospheric model (Lavrenov, 1998).

Two state-of-the-art models were used for wind wave hindcasting: WAM (Komen et al., 1994) and the SWAN model (SWAN Team, 2006). The WAM wave model was adapted for fetch-limited conditions and run for the whole Black Sea basin. SWAN was nested into WAM in order to simulate waves on the western shelf. Integrated parameters of total sea waves and swell were computed every hour. This coupled system is validated (Valchev et al., 2008) for the western Black Sea (Fig. 1).

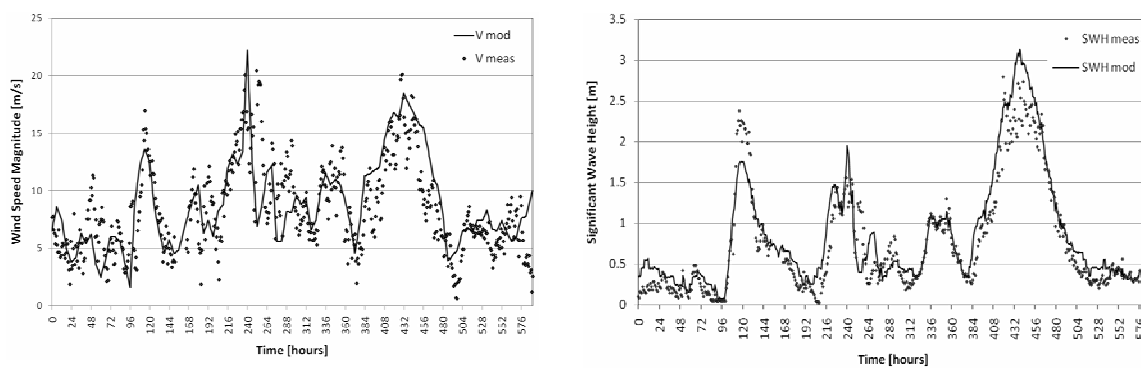


Figure 1. Validation of the wind forcing (left) and modelled significant wave height (right) against measurements during November, 2007 (after Valchev et al., 2008).

The wave climate was estimated for a grid point located approximately four kilometres offshore of the MICORE Bulgarian study site at a depth of about 30 m. Available series of parameters describe thoroughly the wave field over the studied 61-year period. In order to identify the wave events, the threshold for morphological impact, defined in Valchev and Trifonova (2009), was applied. A large number of wave events with duration ranging between

one and 500 hours exceed the threshold mentioned above. Therefore, it is necessary to distinguished storms from weak seas.

For this purpose, the integral wave index, obtained integrating the significant wave height over the events' duration, was estimated. Thus, comparatively mild but durable regimes, providing a significant energy input in the coastal zone, are taken into consideration along with distinctly severe events. In order to assess the trend, it is necessary that each year is represented by at least one event. Therefore, the integral wave index lowest value (130) obtained for a storm occurred in 1965 was chosen as limit over which a particular wave event could be considered storm. This limit is equivalent to the 1-year wave height return value, since this storm is in fact the strongest event during 1965, and the associated maximum significant wave height is the annual maximum. The storms' temporal limits are defined according to the lower threshold (Valchev and Trifonova, 2009).

According to the approach described above, 236 storms were selected over the entire period. The seasonal distribution of the total number of selected storms is presented in Fig. 2. The stormiest months appear to be January, February, December, March, and October, which provide about 86% of all storms. Hence, the storm season is assumed to last from October to March. Consequently, the year is regarded as beginning in July of a given year and ending in June of the following year. Thus, a misinterpretation of the storm season pattern is avoided. However, the available long-term series allow the identification of some April, May, August and September events that are considered important in the sense of their morphological impact. Storm events are divided into three types: severe, moderate and mild (as each one contains several subtypes), depending on their intensity, duration, storm development features as well as the typical wind pattern.

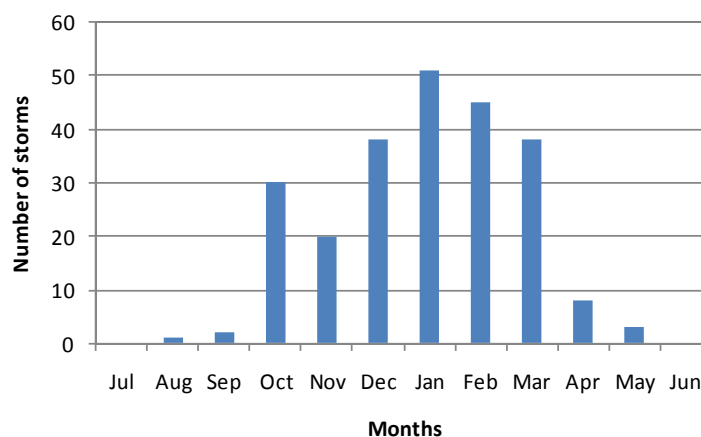


Figure 2. Distribution of the total number of selected storms per month for the period 1948-2008

Trends of storminess are assessed basing both on gross indexes such as storms and stormy days per season and more specific indicators such as the mean and specific wave energy per season. The coefficients of determination R^2 , estimated for each trend line and shown in captions of each figure, are relevant for the level of significance of 0.05.

3.2 Results

The number of storms per year shows a general trend of decrease (Fig. 3). The analysis reveals that the average annual storm occurrences during the 50s were five while after the year 2000 they decreased to three.

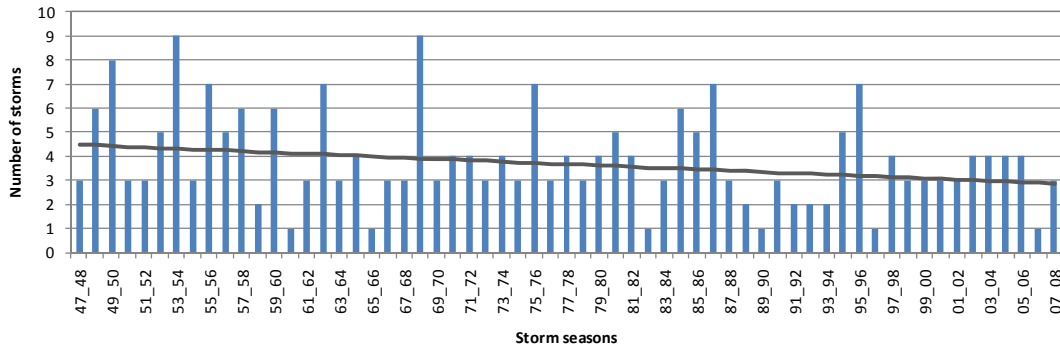


Figure 3. Number of storms over the storm seasons during 1948-2008 ($R^2=0.0841$)

It was found that the storm duration varies within rather wide range – two days for the shortest storm up to 23 days for the longest one, as the average duration is estimated to be approximately six days. The long-term variability of number of stormy days (Fig. 4) confirms the general trend of storminess decrease. In Fig. 3 and 4 three particularly energetic storm seasons stand out: 1953-1954, 1968-1969 and 1995-1996, which is confirmed by historical references. This fact implies there three periods of long-term storminess fluctuations can roughly be distinguished.

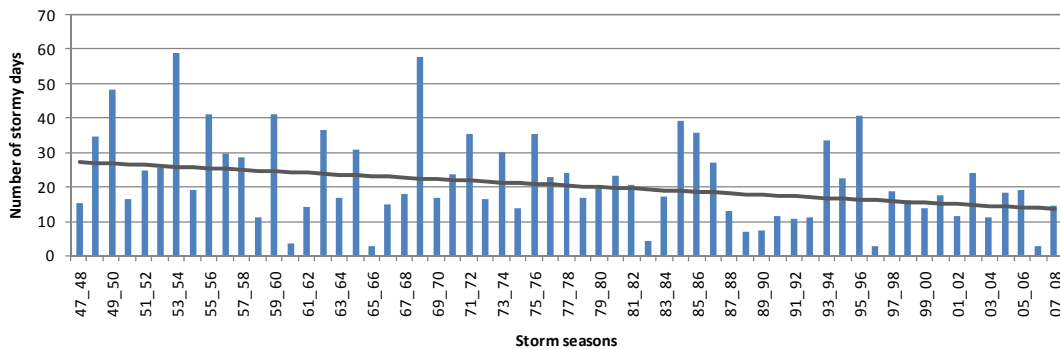


Figure 4. Number of stormy days over the storm seasons during 1948-2008 ($R^2=0.1391$)

On the other hand, the variability of storm intensity is assessed in terms of the mean waves a counter trend of increase of the mean storm intensity.

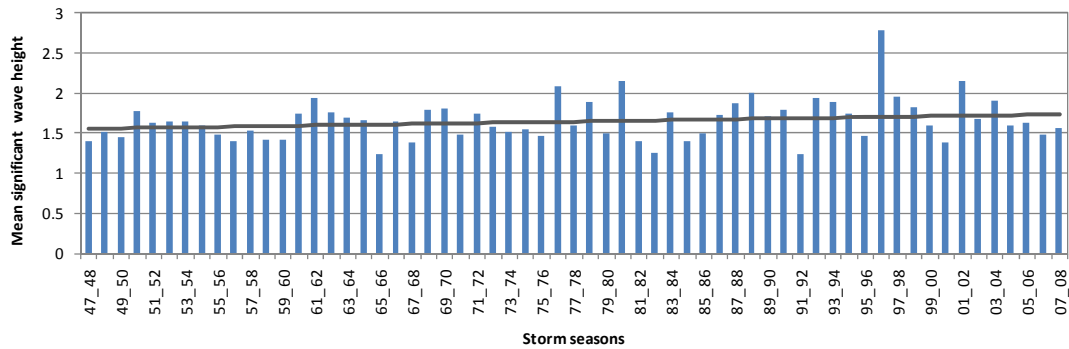


Figure 5. Average value of the mean significant wave height per storm season ($R^2=0.0702$).

Considering the morphological impact of storms, the amount of the wave energy entering the coastal zone is of particular relevance. For this reason, the wave energy of every storm event was integrated over its duration. Fig. 6 presents the long-term variability of the total storm energy. As a whole, the total wave energy per storm season exhibits a tendency for decrease. The results corroborate the hypothesis for three cycles of the wave energy fluctuations: up to 1966, 1966-1989 and after 1989. Furthermore, when a running average is used a stepwise decreasing trend becomes evident. It is noticed that generally every cycle consists of three sub-cycles of 7-9 years duration, as the absolute value of each succeeding maximum gradually decreases toward the end of the cycle. These maxima coincide with very cold winters in the eastern half of Bulgaria (Tishkov, 1991). The first maximum of the cycle stretched up to 1966 and probably corresponds to the winter of 1942, which was the coldest winter during 1899-1988. Respectively, in case of viability of this hypothesis, another sub-cycle of even lower storm intensity is forthcoming.

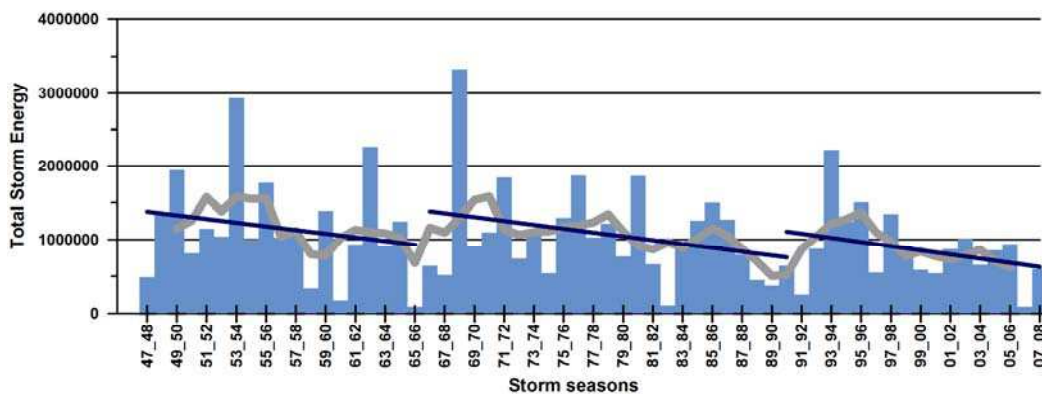


Figure 6. Long-term variability of the total storm energy: solid grey line - running average approximation; solid dark blue lines - linear trend lines for every sub-cycle.

Consequently, the total storm energy per storm season was divided by the corresponding total duration in order to calculate the mean storm energy per storm season over the entire period (Fig. 7). This time, a positive trend in the mean storm energy is observed similar to those of the mean wave height.

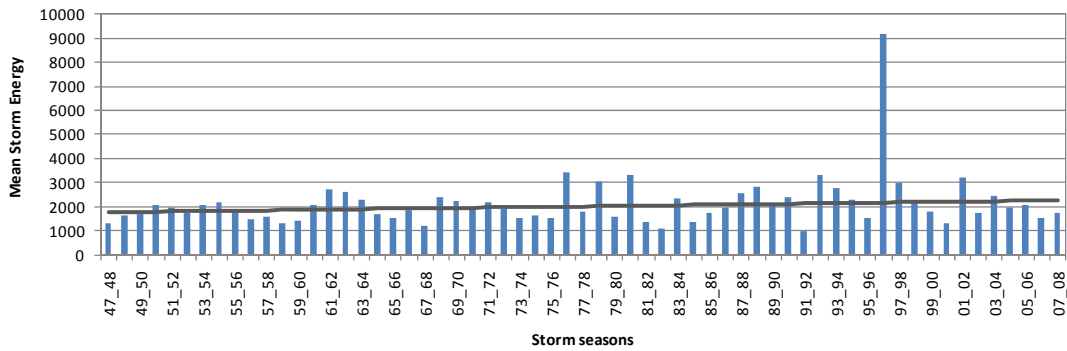


Figure 7. Mean storm energy of all storms per storm season ($R^2=0.0620$)

The results shown in Figs. 5 and 7 are very similar, but representing the storminess by the mean storm energy rather than mean wave height solely makes the contribution of severe storms more explicit.

In order to explain the increase of the mean significant wave height despite of overall decreasing trend of the storminess, the wave energy behaviour during the storm growth and decay is considered. The detailed review of storm types reveals that the storm pattern alters. It is ascertained that storms, characterized by rapid growth and decay, occurred more often during the second half of the 61-year period, which caused an increase of the averaged over the storm duration wave energy. Therefore, the ratio between the mean storm energy and the storm duration per storm season, called specific storm energy, is estimated. The variability of specific storm energy over the storm seasons is presented in Fig. 8.

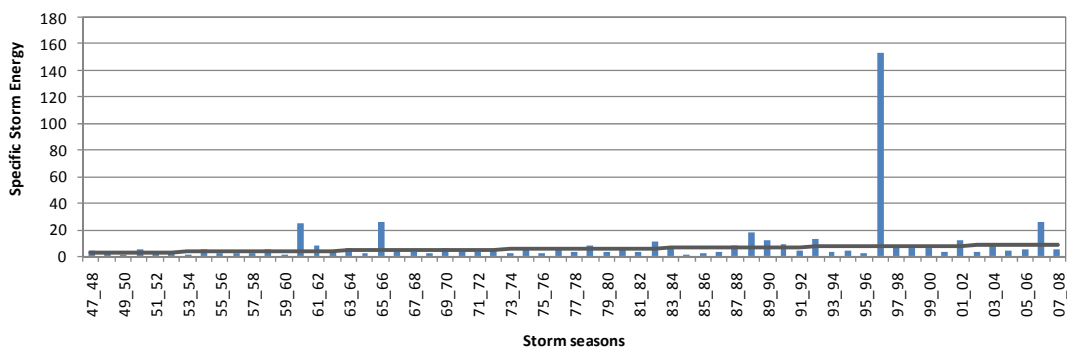


Figure 8. Specific storm energy per storm season ($R^2=0.1794$)

The positive trend implies that storms become more abrupt. In other words, wave energy is focusing over storms of shorter duration. These events are not notably less hazardous than those occurred in the beginning or in the middle parts of the studied period. An eloquent example of the alteration of storm pattern is presented in Fig. 9 on example of two of the most significant storms occurred in February 1979 and December 1996 (Belberov et al., 2009).

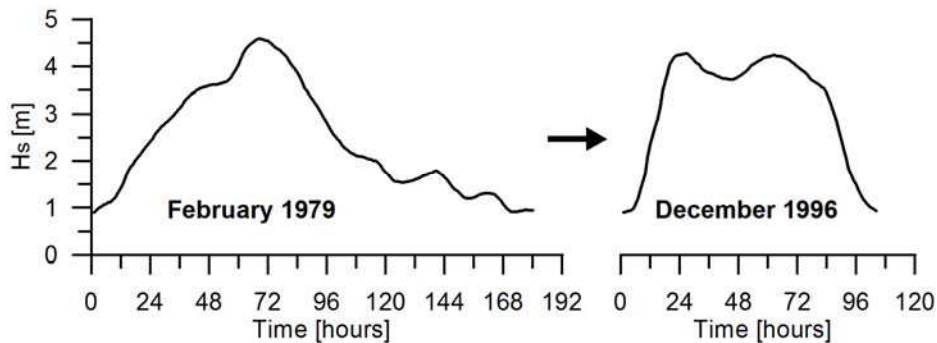


Figure 9. Alteration of storm pattern

3.3 Conclusions

Despite of the overall tendency for storminess decrease, there are no incontestable evidences corroborating a marked reduction of the storm intensity. While the total number of stormy hours diminishes, an increase of the mean wave energy is discernible. This causes a change of the storm pattern: storms with short growth stage, energetic stage of full development and fast decay are more frequently observed. This storm type still provides significant energy input in the coastal zone and is able of producing considerable morphological impact, including damages. Such storms develop abruptly therefore timely prediction and mitigation of hazard effects become more complex to tackle with.

Hence, little potential seems to exist for reducing the vulnerability to storms in the western Black Sea. That means the societies must begin to take such far-reaching implications into serious consideration during its strategic development and disaster avoidance planning processes.

3.4 References

Belberov, Z., E. Trifonova, N. Valchev, N. Andreeva, P. Eftimova, 2009. Contemporary reconstruction of the historical storm of February 1979 and assessment of its impact on the coastal zone infrastructure, Proc. of Int. Multidisciplinary Scientific GeoConference SGEM 2009, Vol. II, 243-250.

Kalnay, E., M. Kanamitsu, R. Kistler, W. Collins, D. Deaven, L. Gandin, M. Iredell, S. Saha, G. White, J. Woollen, Y. Zhu, M. Chelliah, W. Ebisuzaki, W. Higgins, J. Janowiak, K. C. Mo, C. Ropelewski, J. Wang, A. Leetmaa, R. Reynolds, R. Jenne, D. Joseph, 1996. The NCEP/NCAR reanalysis project. Bull. Am. Meteorol. Soc., 77, 437-471.

Komen, G. J., L. Cavaleri, M. Donelan, K. Hasselmann, S. Hasselmann, and P. A. E. M. Janssen, 1994. Dynamics and Modelling of Ocean Waves. Cambridge University Press, 532 pp

Lavrenov, I., 1998. Numerical modeling of wind waves in spatially heterogeneous ocean, Gidometeoizdat, St. Petersburg, 449 (in Russian).

The SWAN Team, 2006. SWAN User Manual, Delft University of Technology.

Tishkov, H. 1991. The winters in Bulgaria and their changing nature in the 20th century. Problems of Geography. Vol. 3, pp. 24-38. (In Bulgarian).

Uppala, S.M., Kallberg, P.W., Simmons, A.J., Andrae, U., Bechtold, V.D., Fiorino, M., Gibson, J.K., Haseler, J., Hernandez, A., Kelly, G.A., Li, X., Onogi, K., Saarinen, S., Sokka, N., Allan, R.P., Andersson, E., Arpe, K., Balmaseda, M.A., Beljaars, A.C.M., Van De Berg, L., Bidlot, J., Bormann, N., Caires, S., Chevallier, F., Dethof, A., Dragosavac, M., Fisher, M., Fuentes, M., Hagemann, S., Holm, E., Hoskins, B. J., Isaksen, L., Janssen, P.A.E.M., Jenne, R., McNally, A.P., Mahfouf, J.F., Morcrette, J.J., Rayner, N.A., Saunders, R.W., Simon, P., Sterl, A., Trenberth, K.E., Untch, A., Vasiljevic, D., Viterbo, P. and Woollen, J., 2005. The ERA-40 Re-analysis. Quart. J. Roy. Met. Soc., 131, pp. 2961-3012.

Valchev, N. and Trinonova, E., 2009. Wave climate clustering to define threshold values with respect to the expected morphological response. Journal of Coastal Research, SI 56 (Proceedings of the 10th International Coastal Symposium), 1666 – 1670. Lisbon, Portugal, ISSN 0749-0258.

Valchev, N., I. Davidan, Z. Belberov, A. Palazov, 2007. Practicability of wind waves simulations based on the global reanalysis wind fields in the Black Sea deep and shallow waters, 4th Int. Conf. "Port Development and Coastal Environment - 2007", 185-191.

4 France-Aquitaine

Gonéri Le Cozannet, Sophie Lecacheux, Etienne Delvallee, Nicolas Desramaut, Elodie Charles, Carlos Oliveros, Yann Balouin

4.1 Methodology

The morphology of linear sandy beaches of the Aquitaine coast depends on waves that are created in the northern Atlantic, spread up to the coast and create long-shore and cross-shore sand transport. In this very dynamical environment, possible modifications of wave height, period or direction are a matter of concern because of the potential consequences in terms of erosion and, in certain places, coastal inundations.

Many studies show that wave parameters are related with large scale atmospheric patterns (e.g. Bacon and Carter, 1993), particularly with the Northern Atlantic Oscillation, which is one of the important pattern of the climate variability in the Northern Atlantic (see Figure 1) The two modes of this oscillation are associated with different atmospheric conditions that account for:

- stronger winds, shifted northward during NAO+ phases
- weaker winds, shifted southward during NAO- phases

NAO index can be estimated by calculating the normalized difference between sea level Azores high pressure and Icelandic low pressures. NAO data used here were produced by the National Oceanic and Atmospheric Administration (NOAA) by applying a rotated principal component analysis of monthly mean standardized 500mb height anomalies for latitudes higher than 90°N (Barnston and Livezey, 1987).

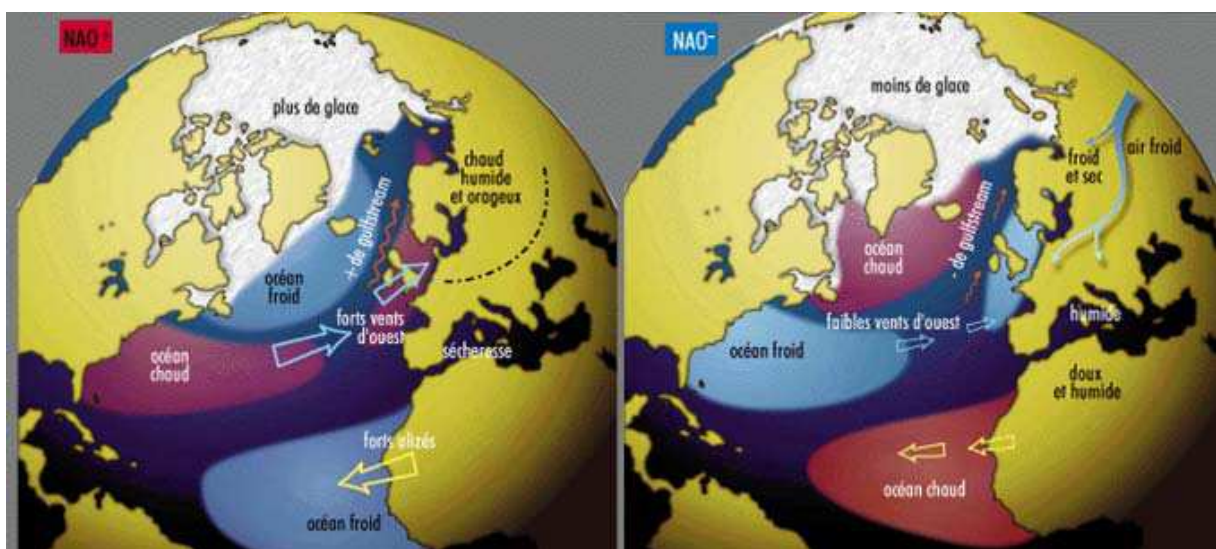


Figure 1 : Characteristics of the Northern Atlantic Oscillation. Source : Heinz Wanner, Institut de géographie climatologie et météorologie, Université de Berne.

Previous studies (Dupuis, 2006) established a link between the local wave conditions in the Bay of Biscay and the NAO index. Particularly, she found T_p to be positively correlated with this index. However, this study could not conclude on a possible trend of sea wave parameters because (1) the time series she used covered only 20 years and (2) establishing a link with a single wave parameter is not appropriate since the wave signal (H_s , T_m , D_m) is modal (Butel, 2002).

With respect to (1), the ERA-40 reanalysis (Uppala, 2005) of European Centre for Meteorological Weather Forecasts (ECMWF) provides 6 hourly ocean and atmospheric data at each node of a global 2.5° grid, from 1958 to 2001. Significant wave height (H_s), mean wave period (T_m) and direction (D_m) have been extracted for the $45^\circ\text{N}/5^\circ\text{W}$ node. The latter location was selected as:

- it is the longest time series available in the area of interest
- this data can be compared with in-situ data registered since 1998 by the Gascogne Buoy ($45.2^\circ\text{N}/5^\circ\text{W}$), which is operated by Météo-France and the UK Meteorological Office (<http://www.meteo.shom.fr/ancrees/gascogne.htm>)

The quality of data is satisfying, but a bias on H_s (Caires and Sterl, 2003) can be corrected by linear regression using the buoy data ($R^2=0.92$) (fig.2).

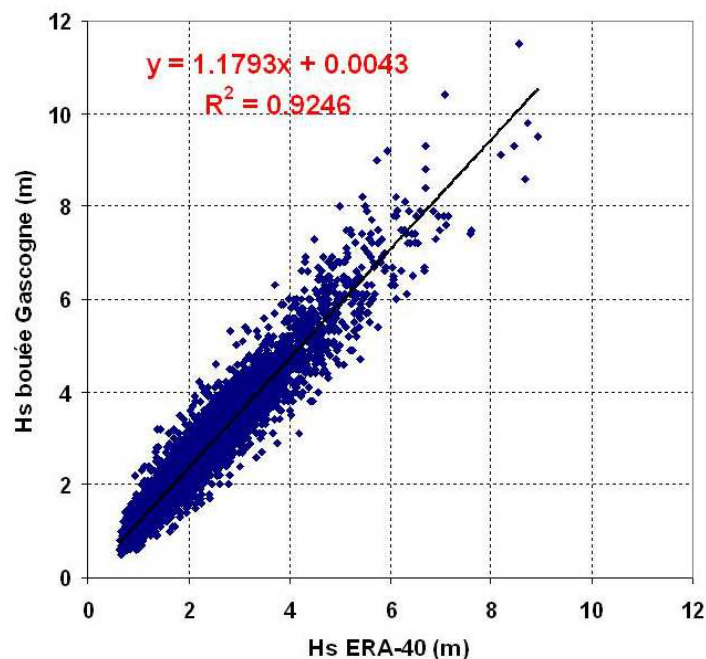


Figure 2 – Correlation between the wave significant height obtained from ERA-40 re-analysis and the Gascogne wave buoy dataset during the overlapping period 17/07/98 to 31/08/02 (13 incorrect values were deleted).

With respect to (2), another option to analyse the local wave climate is to use multivariate data analysis (Abadie, 2006). This assumes that the waves can be classified under several

modes. Butel (2002) used classification techniques to analyse together all wave components. Following that approach, wave data are classified into a limited number of modes that can be analysed in terms of occurrence, seasonality, etc., thus enabling easier wave data analysis.

The methodology is the following: the corrected ERA-40 data were classified using the classical K-Means algorithm. Then, wave climates were identified and the trends discussed. The relationship with NAO and other large scale atmospheric pattern is finally discussed.

4.2 Results

The 1958-2001 sea wave corrected data from ERA-40 were classified into 12 modes using the K-means algorithm (Table 1 and Fig. 3). Three principal groups appear (Butel, 2002):

Table 1. Classification and distribution of wave conditions in 3 groups.

Class	Description (Type / Incident direction / Seasonality)	Hs (m)	Tm (s)	Dm (°)	%
INT-1	INTER / NW / spring, summer, autumn	1.30	6.82	315.57	11.14
INT-2	INTER / N / annual	1.62	6.56	2.33	5.38
INT-3	INTER / W / spring, summer, autumn	1.78	6.87	270.97	7.08
INT-4	INTER / ENE / annual	1.97	6.18	61.90	3.37
INT-5	INTER / NW / spring, autumn, winter	2.68	8.72	319.49	7.23
INT-6	INTER / W / spring, autumn, winter	3.26	8.64	270.79	7.27
SW1-1	SWELL1 / WNW / spring, summer, autumn	1.34	8.29	294.03	16.63
SW1-2	SWELL 1 / WNW / annual	1.82	10.01	292.73	15.73
SW2-1	SWELL 2 / WNW / spring, autumn, winter	2.67	11.50	290.88	12.36
SW2-2	SWELL 2 / WNW / autumn, winter	4.13	13.00	290.99	4.74
SW2-3	SWELL 2 / WNW / spring, autumn, winter	4.78	10.08	284.61	6.45
SW2-4	SWELL 2 / WNW / autumn, winter	7.12	11.92	284.91	2.62

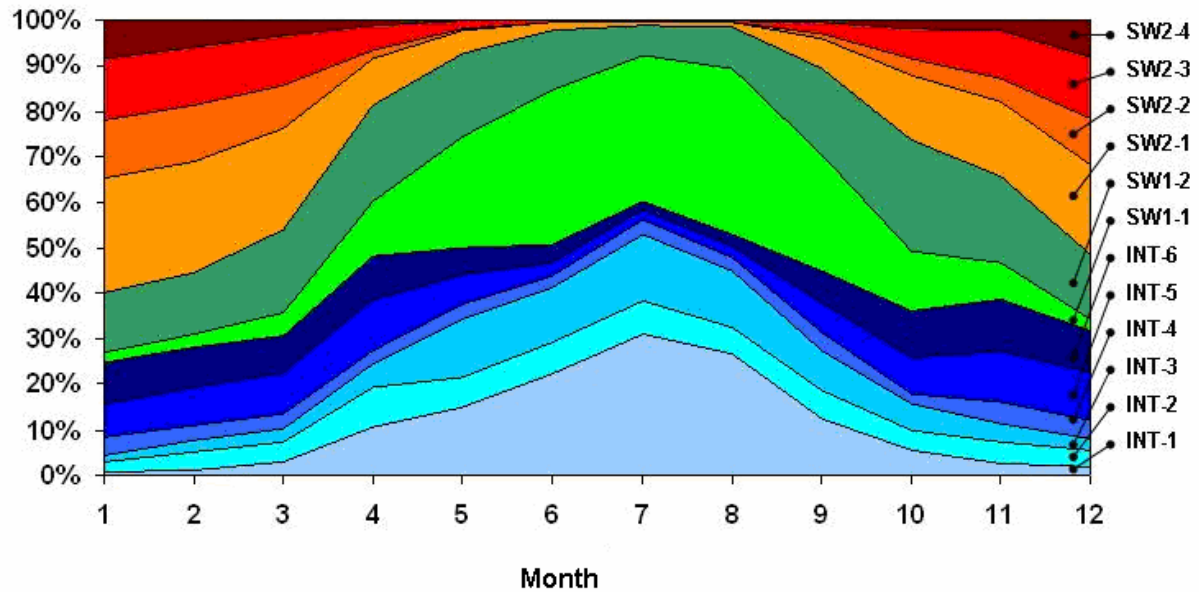


Figure 3. Seasonal occurrence of the 12 classes for the period 1958-2001.

- The first group (INT) consists of sea wind waves and intermediate sea conditions between swell and sea wind. They are characterized by low periods. INT is more frequent during the summer season.
- The second group (SW1) is made of low energy swell, characterized by relatively low wave height, long periods and north-west directions. SW1 is more frequent in winter.
- The third group (SW2) is made of energetic swell, characterized by long period, high wave height and north-west directions. SW2 is more frequent in winter.
- Sea storms occur when sea wave conditions fall within one of the SW2 classes.

While the yearly occurrence of SW1 remains relatively stable over the years, SW2 is highly non stationary. Moreover, the positive anomalies of SW2 occur generally during NAO+ years (Fig. 4). This relationship can be quantified: the correlation coefficient between the annual (civil year) NAO index and the annual proportion of SW2 is $R=0.63$, the significance of the correlation being higher than 95% (t-test).

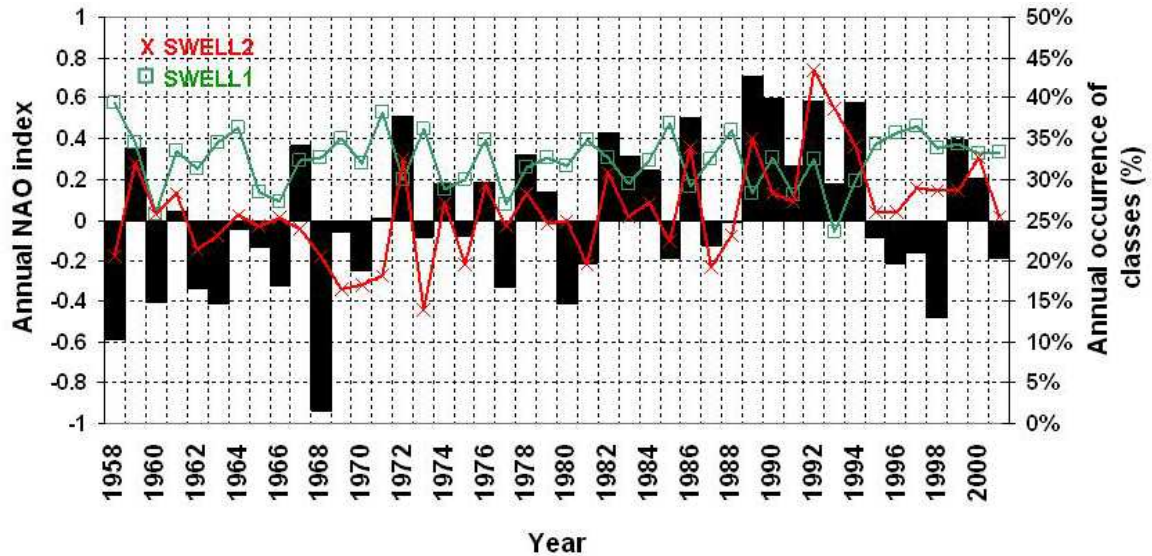


Figure 4. Time series of annual NAO index (histogram) and annual occurrence of SWELL2 (red crosses) and SWELL1 (green squares).

Other teleconnection patterns (see above) appear to be correlated with SW2 proportion and in particular the East-Atlantic pattern (EA) which is correlated with SW2 ($R=0.55$) in December. In January, NAO is correlated with SW2 proportion ($R=0.70$), while EA (see Barnston and Livezey, 1987) is correlated ($R=0.58$) with the residual variability of SW2 proportion.

From 1970 to 2001, a period characterized by positive NAO anomalies yearly means of significant sea wave height increased by $+0.008$ m/year at $45^{\circ}\text{N}/5^{\circ}\text{W}$ node. SW2 and SW1 waves significant heights did not vary significantly, and INTER waves increased by $+0.009$ m/year. Therefore, the growth of wave significant height is obviously due to the fact that the occurrence of most energetic waves (SW2) (i.e. the annual proportion of SW2) increased during this period.

Table 2: Trends of wave significant heights yearly means of from 1970 to 2001. Data: ERA40 ($45^{\circ}\text{N}/5^{\circ}\text{W}$ node) corrected by linear regression. P value of the model is the probability for a random dataset to have a slope equal or greater than the slope found for the parameter of interest.

Parameter	Dataset	Period	Slope	P value of the model
Hs	all	1970 – 2001	$+0,008$ m/year	0,7%
Hs	SW1 only	1970 - 2001	$+0,002$ m/year	10%
Hs	SW2 only	1970 – 2001	$-0,004$ m/year	41%
Hs	INTER only	1970 - 2001	$+0.009$ m/year	0,6%

4.3 Conclusion

These results show that the observed trend of wave height for the Bay of Biscay is $+0.008\text{m/year}$ at $45^{\circ}\text{N}/5^{\circ}\text{W}$ from 1970 to 2001. The climate variability in the Northern Atlantic and the local wave climate in the Bay of Biscay are correlated: the proportion of energetic sea waves is significantly correlated with two modes of climate variability of the Northern Atlantic

NAO, during the entire year but particularly during the winter season, and EA during the winter season. This is in agreement with other studies that analysed extreme sea waves and that established links between climate variability in the Northern Atlantic and sea wave height (Woolf, 2002; Wang and Swail, 2001 and 2002). Moreover, Wang and Swail (2006) showed that while the number of intense winter storm increased in the high latitudes of Northern Atlantic during the last 50 years, it decreased in the mid-latitudes. Bay of Biscay is located at an intermediate latitude where changes are more difficult to identify (Dupuis, 2006). The results of this study indicate that positive phases of the NAO are associated with atmospheric conditions that accounts for energetic sea waves spreading up to the Aquitaine coast. The observed trend of higher sea waves in the Bay of Biscay is consistent with the positive phases of NAO since 1970.

The wave climate analysis for the Atlantic Aquitaine coast based on ERA-40 datasets points out the strong correlation between storm occurrence and the North Atlantic Oscillation anomalies. The 1958-2002 period is actually too short to properly attribute wave climate changes to climate change. Nevertheless, climate modelling seems to indicate that the impact of man-made greenhouse effect to the persistence of the NAO+ weather regime occurrence is strong since 1980 and that both the ocean and greenhouse gas emissions probably explain NAO variability since last decades (Cassou, 2004). Moreover, projected climate change for the XXI century should favour the NAO+ weather regime. However, much work is still needed to investigate the link between climate change and wave climate, and even between weather regime and climate change² and as a result the presented increase of SW2 waves since 1970 should not be attributed to greenhouse gas emissions, without evidence from other/further studies.

4.4 References

Abadie, S.A., Butel R., Mauriet S., Morichon D., Dupuis H., 2006. Wave climate and longshore drift on the South Aquitaine coast. *Continental Shelf Research*, 26, pp. 1924-1939.

Bacon S., and Carter D. J. T., 1993. A connection between mean wave height and atmospheric pressure gradient in the North Atlantic. *International Journal of Climatology*, 13, 423-436.

Barnston, A. G., and R. E. Livezey, 1987. Classification, seasonality and persistence of low-frequency atmospheric circulation patterns. *Monthly Weather Review*, 115, 1083-1126.

Butel, R., Dupuis H., and Bonneton P., 2002. Spatial variability of wave conditions on the French Atlantic coast using in-situ data. *Journal of Coastal Research*, 36, 96-108.

² This work is actually part of a PhD (Elodie Charles, BRGM, Météo-France)

Caires, S., and A. Sterl, 2003. Validation of ocean wind and wave data using triple correlation. *J. Geophys. Res.*, 108, pages.

Cassou, C., 2004. Du changement climatique aux regimes de temps : l'oscillation nord-atlantique, *La Météorologie* n°45, 21–32.

Le.Cozannet.G., Lecacheux.S., Delvallée.E., Desmaraut.N., Oliveros.C., Pedreros.R., 2009. Influence de la NAO sur le climat de vague dans le Golfe de Gascogne., in *Ateliers de modélisation de l'atmosphère 2009 - Toulouse - France - 27-29 janvier 2009*.

Uppala, S.M., Kållberg, P.W., Simmons, A.J., Andrae, U., da Costa Bechtold, V., Fiorino, M., Gibson, J.K., Haseler, J., Hernandez, A., Kelly, G.A., Li, X., Onogi, K., Saarinen, S., Sokka, N., Allan, R.P., Andersson, E., Arpe, K., Balmaseda, M.A., Beljaars, A.C.M., van de Berg, L., Bidlot, J., Bormann, N., Caires, S., Chevallier, F., Dethof, A., Dragosavac, M., Fisher, M., Fuentes, M., Hagemann, S., Hólm, E., Hoskins, B.J., Isaksen, L., Janssen, P.A.E.M., Jenne, R., McNally, A.P., Mahfouf, J.-F., Morcrette, J.-J., Rayner, N.A., Saunders, R.W., Simon, P., Sterl, A., Trenberth, K.E., Untch, A., Vasiljevic, D., Viterbo, P., and Woollen, J. 2005. The ERA-40 re-analysis. *Quart. J. R. Meteorol. Soc.*, 131, 2961-3012.

Wang X.L. and V.R. Swail, 2001. Changes of extreme wave heights in northern hemisphere oceans and related atmospheric circulation regimes. *J. Climate*, 14, 2204-2221.

Wang X.L. and V.R. Swail, 2002. Trends of Atlantic wave extremes as simulated in a 40-year wave hindcast using kinematically reanalysed wind fields. *J. Climate*, 15(9), 1020-1035.

Wang X.L., V.R. Swail, F.Z. Zwiers, 2006. Climatologie and changes of Extratropical cyclone activity: Comparaison of ERA-40 with NCEP-NCAR Reanalysis for 1958-2001. *J. - Climate*, 19(13), 3145-3166.

Woolf, D.K., Cotton, P.D., Challenor, P.G., 2002. Variability and predictability of the North Atlantic wave climate. *Journal of Geophysical Research* 107 (C10), 3145.

5 France-Mediterranean

Yann Balouin, Rémi Belon, Gonéri Le Cozannet and Mathieu Gervais

5.1 Methods

Several studies were undertaken to evaluate recent evolution in storm occurrence and intensity on the French Mediterranean coast. These efforts were based on short-term wave measurements (Durand, 1999; Sabatier *et al.*, 2009), mid-term sea level evolution and meteorological parameters (Ulmann, 2008) and have shown evidence of a possible increase in storm frequency during the last decades. However, these works were not focused on morphogenic storm with morphological consequences and parameters used were not always applicable for the purpose of the present work.

As a consequence, available datasets and numerical modelling were identified and re-analysed to evaluate the possible effect of climate change on storminess in our coastal region.

In the Gulf of Lion region, wave and tide measurements were initiated recently and the longest timeseries covers less than 20 years. This data concerns:

- wave characteristics from a wave buoy located in front of Sète, where only wave height and period are available from 1989-2009 (data source: Regional Direction of Equipment of Languedoc-Roussillon DRE-LR);
- water level in the harbour of Sète from 1986 to 2000 (data source: DRE-LR)

Moreover, more qualitative information, obtained on storm characteristics during the historical review undertaken within MICORE, was used.

This information was re-analysed to evaluate the frequency and intensity of storm events as summarized in table 1. The complete dataset was used to evaluate the mean wave climate evolution. Moreover, significant wave height above 2 m was considered a storm threshold and was used to determine storminess changes. More than 350 events were identified.

Table 1: indicators used to evaluate evolution in storminess.

Dataset	Derived indicator
Wave measurements	Number of storm events/year or per winter period
	Storm peak wave Hs
	Mean annual Hs
	Duration of events
Water level measurements	Storm surge elevation
	Number of high surge events/year and per winter period

Due to the short period covered by the datasets, SIMAR simulations (HIPOCAS Project) were used to cover a longer time period. These model outputs covering the period 1958-2001 were

provided by Puertos del Estado (Spanish ports). Available measurements mentioned above were used to calibrate and validate the simulations. The wave heights and periods predicted at the point N 43.375 E 3.625, very close to the Lido of Sète, were compared with the Sète wave buoy for the overlapping period (11 years) (see fig. 1). The predicted values were underestimating wave heights and a linear correction was applied. The Pearson correlation coefficient between corrected and measured values is 0.75.

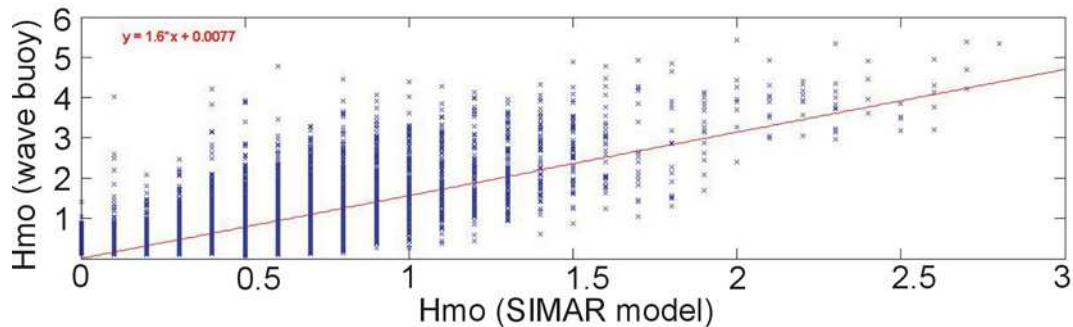


Figure 1. Comparison between measured and predicted values

A further comparison was done between the corrected SIMAR values and the measured storm characteristics. This analysis revealed that energetic conditions were well predicted and could be used to evaluate the occurrence of storm events. However, individual storm peak wave heights were not always fitting well (the event of 1997 with a return period of 50 years-T50 was predicted as a T10 event). Thus, evolution of storm intensities (on the grounds of wave heights) is submitted to caution.

Predicted wave direction was not calibrated because of the lack of field data. However, for the most important events when visual observations were available, a qualitative comparison was done. For these events, the predicted direction seemed to be correct.

5.2 Results

5.2.1 Short-term tendencies

The use of indicators derived from short-term measurements (less than 20 years) did not permit to attribute any tendency to a global climate change occurring at a larger time scale. However, the short-term analysis was important to confirm and validate the longer term tendencies that could be established with numerical simulations.

5.2.1.1 Storm waves

The 20 years time series of wave measurements in front of Sète was analysed. Over this period, the mean significant wave height was very stable (see Fig. 2a), with the annual mean showing a very low decrease. The maximum annual wave height was very variable and no clear tendency was observed (Fig. 2 b, c and d). The mean annual duration of storm events was quite stable (see Fig. 2b), while their frequency slightly increased (see Fig. 2c). This was particularly the case for the period 1998 to 2004, in which the number of events doubled.

However, the rate of increase is very low and cannot be considered as statistically significant. The total duration of stormy conditions per year (see Fig. 2d) did not show any significant tendency.

5.2.1.2 Surge level evolution

The surge level (defined as the water level measurements less the astronomical tide) in the Gulf of Lion presented a slight increase between 1986 and 1999. However, the observed increase was around 2.9 mm/y (see fig 3a), that is more or less equivalent to the sea level rise observed by satellites in this area (Cazenave et al., 2002). Storm surges along the Mediterranean coast were defined as positive surge levels exceeding 30 cm (Ullmann, 2008). Using this storm surge definition, it can be seen that the mean annual surge during the measured period, that is around 35 cm (see Fig. 3b), was stable. The maximum annual surge level, between 40 and 80 cm was very variable, without showing any dominant long term trend.

The analysis of the frequency of high water levels did not reveal any tendency. A very low increase in the frequency was observed (around 0.05 days/year) but was not statistically significant.

The analysis of changes in storm waves and storm frequency, were based on short-term measurements and consequently does not allow linking with global climate changes. Very low tendencies were observed on the datasets with a very low statistical significance. The main conclusion of this analysis is that the storminess during this short-term period can be considered as stable.

5.2.2 Mid-term tendencies

The 1958-2001 sea wave corrected data from SIMAR (HIPOCAS) were classified into 12 modes using the K-means algorithm (See Table 1). Four principal groups appear:

- The first group (Tramontane) consists of waves locally generated by winds coming from the land that consequently do not affect the coastline. They are characterized by low periods.
- The second group (INTER) is made of low energy swell, characterized by relatively low wave height, longer periods and SE directions. INTER is more frequent during the summer periods.
- The third group (SWELL) is made of energetic swell, characterized by long period, medium wave height and E, SE, and S directions. SWELL is more frequent in winter periods.
- The last group (STORM) consists of high energy swell characterised by long period, important wave heights and SE directions.

Sea storms occur when sea wave conditions can be classified into one of the SWELL2 and STORM groups described below.

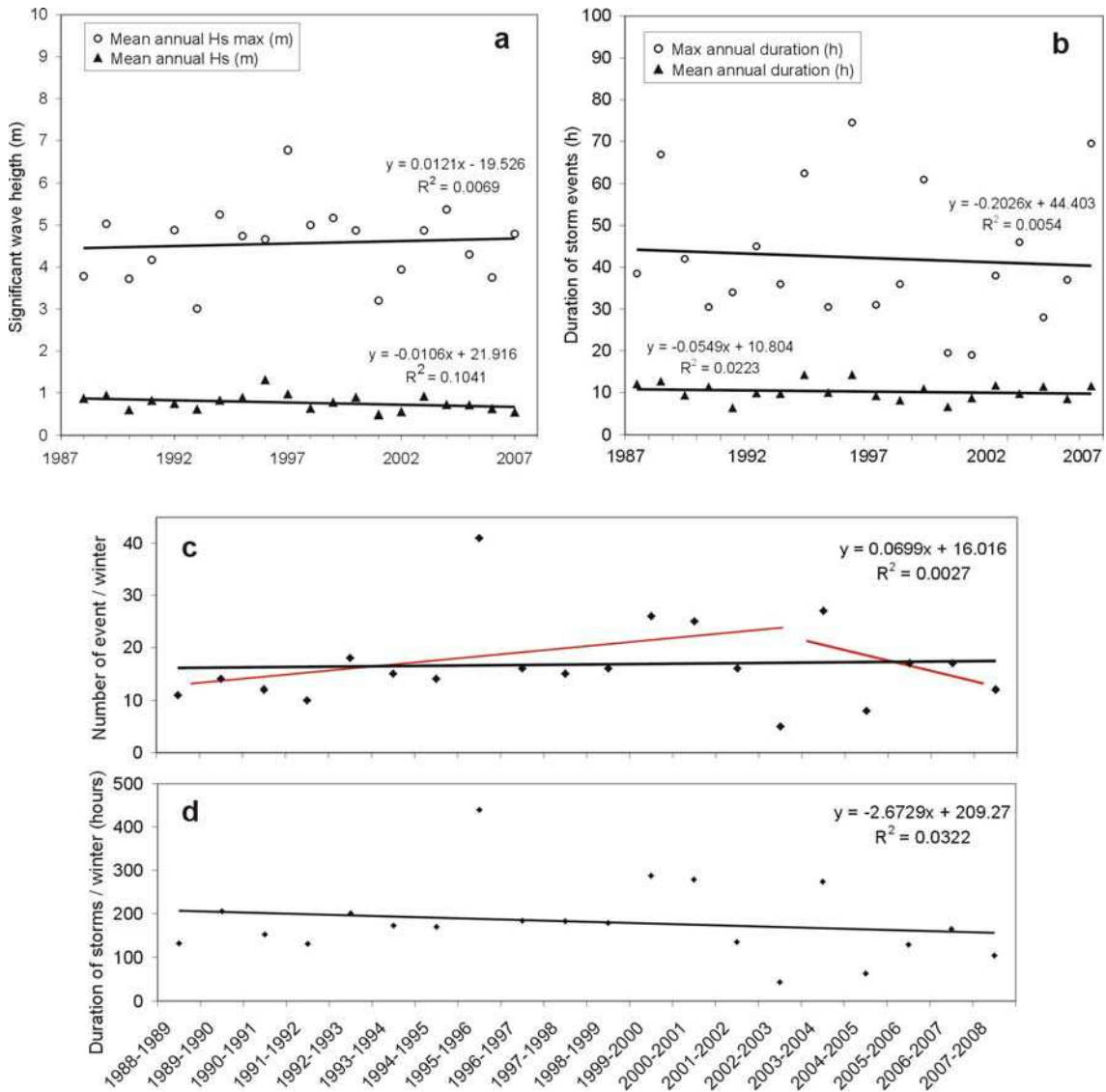


Figure 2. Evolution of storm wave climate during the last 20 years. a) Mean significant wave height; b) Mean and maximum duration of storm events; c) Number of storm events/winter (the red line indicates the best fit regression between 1988 and 2003, and between 2003 and 2008) and d) Total duration of stormy conditions / winter.

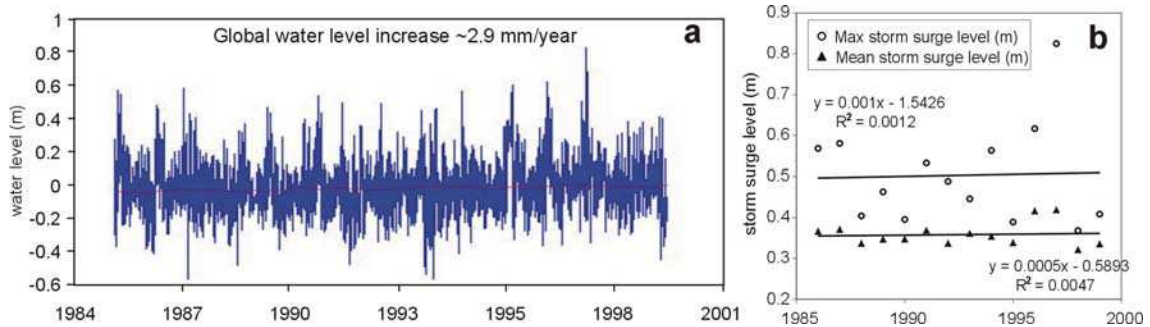


Figure 3. Evolution of storm surge levels. a) water level measurements indicating a global trend of 2.9 mm/y) and b) Annual mean and maximum storm surge level (m).

Table 1 - Classification and distribution in 4 groups.

Description	Hm0	Tp	Dm	Occurrence
Tramontane, N, annual	0.29	2.38	7	13.2%
Tramontane, NO, annual	0.47	2.56	315	14.8%
Tramontane, NO, annual	0.88	3.26	347	9.5%
Tramontane, NO, annual	0.93	3.22	310	6.7%
INTER, S, annual	0.34	5.91	167	7.8%
INTER, SE, annual	0.28	3.70	159	20.1%
INTER, SE, annual	0.72	4.14	150	13.0%
INTER, SE, annual	1.00	5.81	136	6.3%
SWELL1, E, autumn, winter, spring	0.84	9.20	96	1.7%
SWELL2, S, autumn, winter, spring	1.27	7.16	171	3.2%
SWELL2, SE, autumn, winter, spring	1.80	7.25	133	2.8%
STORM SE, november to march	3.13	9.00	124	0.7%

While no real tendency can be observed from the predicted significant wave heights, the analysis of the frequency of stormy conditions reveals a global increase since the 1970's (see Fig. 4). The trend suggests an increase of 0.3 days/year for the frequency of storm and swell2 classes. However, on a longer time period, a real tendency is quite difficult to be discerned from the dataset. From 1958 to 1970, the stormy conditions were more frequent, and decreasing at the end of the 60's.

However, STORM class alone (see Fig. 5) does not present any trend and the global increase of the most energetic classes is resulting from SWELL2 variability. As a consequence, no significant evolution can be deduced regarding the tendency of storm occurrence during the last 5 decades.

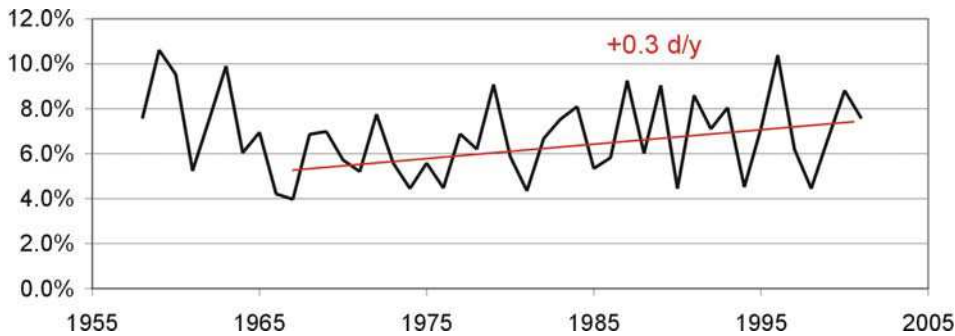


Figure 2. Cumulated frequency of Swell2 and Storm classes from 1958 to 2001.

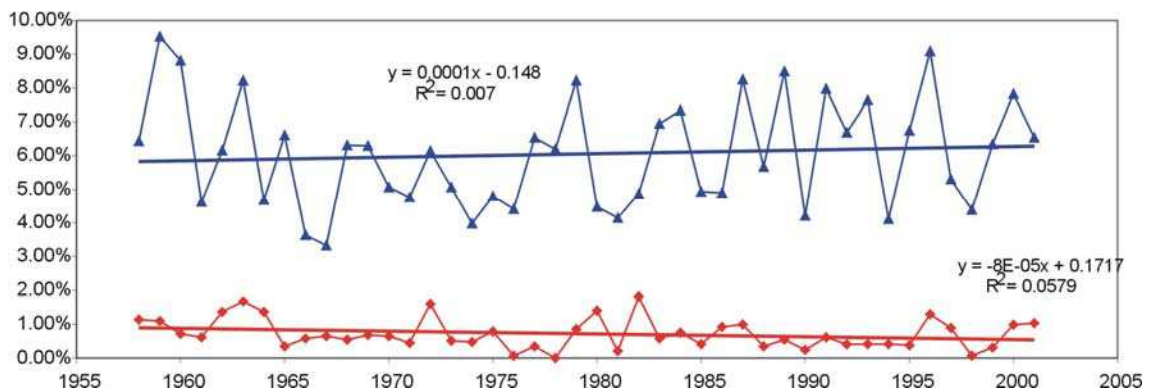


Figure 3. Frequency of Swell2 (blue) and Storm (red) classes from 1958 to 2001.

5.3 Conclusions

Wave buoy and tide gauge datasets as well as longer term simulations were used to evaluate a potential tendency in storm frequency and intensity during the last decades.

From the short term measurements and the HIPOCAS simulations, no tendency was observed regarding wave heights. The annual mean and maximum Hs are respectively stable and highly variable. The surge level measured in the harbour of Sète presents a global trend of increase of 2.9 mm/y that is mostly due to the sea level rise in the area. Deducing this global trend, no tendency is observed on the surge level over time. As a consequence, the analysis performed seems to demonstrate that there is no tendency in storm intensity (in term of wave heights and storm surge level) during the last decades.

The occurrence of storm events, both in the short term measurements and mid term simulations, presents high variability, with increasing and decreasing periods. The above points out the need to have very long time series to be able to observe a climate change effect on storms. The corrected HIPOCAS simulations show a global increase of storm occurrence from 1970 to 2001. However, the variability between successive years remains important and the occurrence of the most energetic class (STORM) is stable. Moreover, the previous (1958-1970) and successive (2004-2008) periods indicate a decrease in storm occurrence. Consequently, the observed tendencies are probably linked to climate variability rather than climate change.

5.4 References

Cazenave, A., Bonnefond, P., Mercier, F., Dominh, K., Tomazou, V., 2002. Sea level variations in the Mediterranean Sea and Black Sea from satellite altimetry. *Global and Planetary Change*, 34:59-86.

Durand, P., 1999. L'évolution des plages de l'ouest du Golfe du Lion au XXème siècle. PhD thesis, University Lumière Lyon 2, 462 p.

Sabatier, F., Samat, O., Ullmann, A. And Suanez, S., 2009. Connecting large-scale coastal behaviour with coastal management of the Rhône delta. *Geomorphology*, 107:79-89.

Ullmann, A., 2008. Surcotes dans le Golfe du Lion et conditions atmosphériques: variabilité contemporaine et future (1905-2100). PhD thesis, University of Aix-Marseille I, 236 p. In french.

6 Italy-Northern Adriatic

Paolo Ciavola, Andrea Valentini, Marinella Masina and Clara Armaroli

6.1 Methods

This section presents an analysis done to detect change in storminess over the last 50 years in the northern Adriatic Sea, based on meteorological measurements. Unfortunately, numerical model outputs that extend so far in the past are generally available with a resolution that is too coarse. Long term numerical models extending in the past also have difficulties in simulating extreme Bora events that are an important characteristic of the Northern Adriatic meteorology. These limitations are reflected over wave hindcasting which uses wind as a wave forcing factor. Regarding the use of wind data coming from offshore stations (i.e. platforms and buoys), they do not cover such a long period as well, and therefore the only solution is to rely on coastal stations. This study carries on and updates a previous analysis performed during the CADSEALAND Project (2004-2006), an INTERREG IIIB CADSES – EU Project.

6.1.1 Meteo, wave and tidal data-sets

The meteorological data-set used in this section has been provided by the Aeronautica Militare – Ufficio Generale per la Meteorologia (UGM). In this analysis only the data-set belonging to the coastal meteorological stations of the SYNOP network was used. The data consist of time series of 3-hourly measurements of standard meteorological surface parameters, such as wind at 10 m above ground, mean sea level pressure and others. These time-series are available for many coastal stations along the Adriatic coastlines; in particular, data from Venezia, Ravenna, Rimini and Brindisi were compiled and used for storminess identification (Fig. 1). The stations of Ravenna and Rimini were used just as meteo data input during the study of the identified storms. In the case of the stations used for this analysis the yearly percentage of missing data is shown in Fig. 2. Considering that after 1960 data recovery improves, time series were studied only from this date onwards.

Measurements are the average over a 10 minute sampling period, both for wind direction and speed. The meteo data-set has been carefully checked and quality controlled. It has been shown by previous authors (Pirazzoli and Tomasin, 1999) that winds below 4 knots present a clear bias due to the improvement/changes in instrumentation occurred with time. For this reason, all the measurements below this threshold were considered as calm in the current analysis.

Regarding directional wave records, they were obtained from a wave buoy located in front of the city of Ancona. These wave measurements are available at <http://www.idromare.it/> and were collected from 1999 to 2004 (since 2004 there is a lack of measurements due to network maintenance and management problems). Data were collected with a measurement frequency of three hours till May 2002, thereafter every thirty minutes. Since 2007 a directional wave buoy is managed by ARPA offshore of Cesenatico <http://www.arpa.emr.it/sim/?mare/boa>.

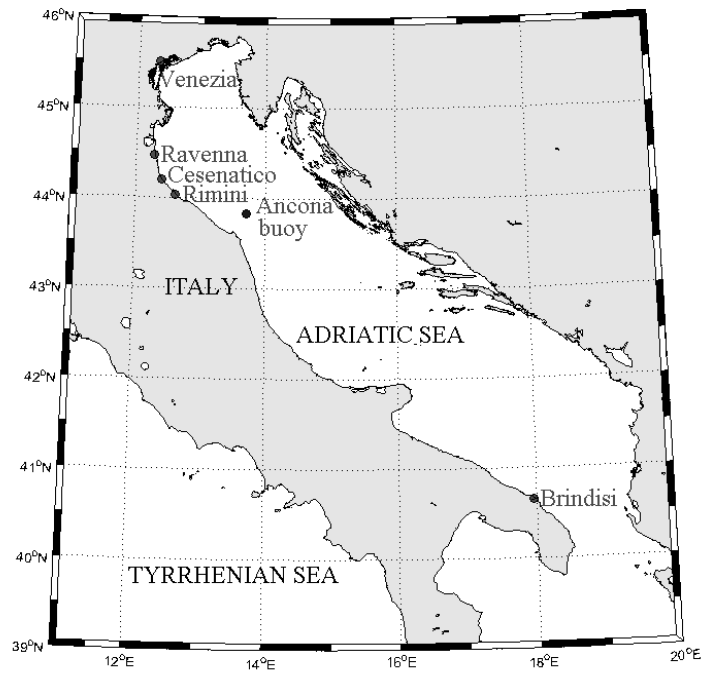


Figure 1. Meteorological stations and localities with wave measurements used in the analysis

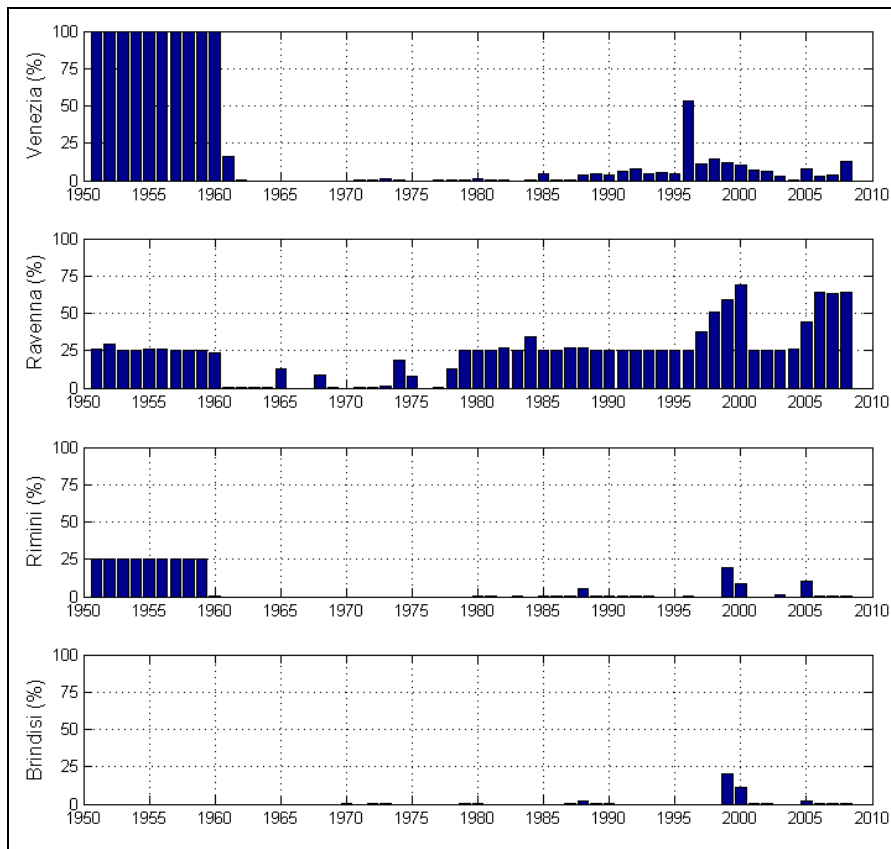


Figure 2. Percentage of missing data in the meteo time series year by year.

The directional wave data-sets (Ancona and Cesenatico) are not characterized by a 100% data recovery rate. Some years (e.g. 2001, 2006) have a percentage of missing data of 20-30%. This is more relevant to the Ancona buoy, while the Cesenatico buoy works on a more continuous basis as it is located inside an offshore fish farm and is less prone to loose the mooring. To notice (Fig. 3) that a gap in the data-set was present between 2006 and mid 2007, this was filled using archived SWAN forecasts by the ARPA-SIMC sea-state forecast system (Valentini et al., 2007). In order to compensate for the short duration of the series, other data sources were used such as non-directional measurements owned by the ENI oil company and by CNR being acquired on offshore rigs respectively located in front of Ravenna and Venezia (see Table 1 for details).

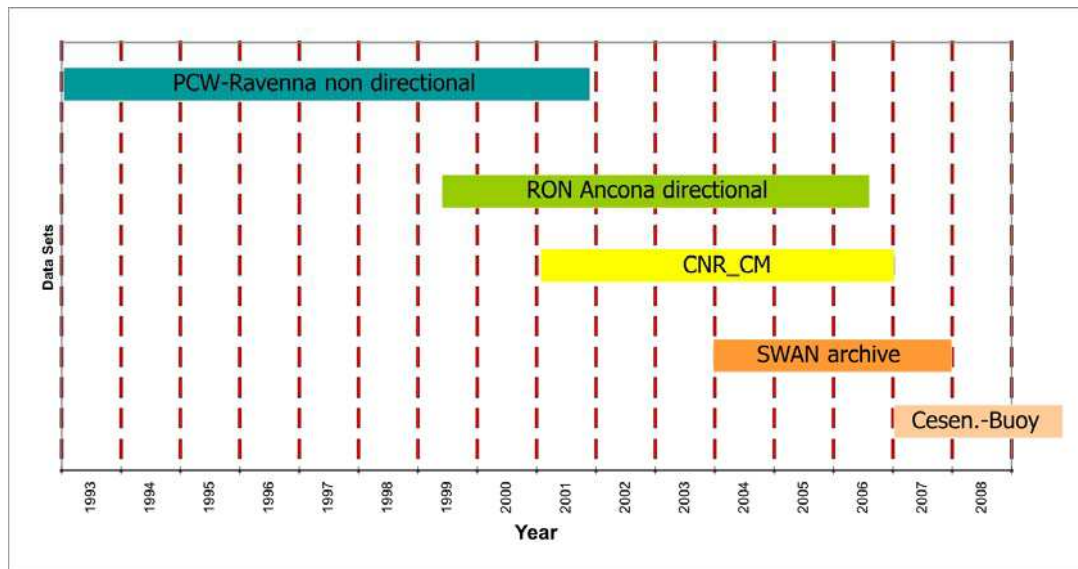


Figure 3. Data sources of wave measurements available for the northern Adriatic

Table 1: characteristics of data measurements used in this analysis.

Station	Latitude N	Longitude E	Water Depth (m)	Period of observation
Venezia Tide Gauge	45° 25.9'	12° 20.2'	-	1923-2008
Venezia meteo	45° 30'	12° 20'	-	1961-2008
Ravenna meteo	44° 28'	12° 17'	-	1951-2008
Rimini meteo	44° 02'	12° 37'	-	1951-2008
Brindisi meteo	40° 39'	17° 57'	-	1951-2008
Ravenna ENI PCW rig	44° 30.7'	12° 21.6'	12.5	1992-2001
Venezia CNR CM rig	45° 18.8'	12° 30.5'	16	2001-2006
SWAN virtual buoy	44° 19.9'	12° 24.0'	10	2005-2008
Ancona Buoy	43° 49.8'	13° 42.8'	75	1999-2006
Cesenatico Buoy	44° 12.9'	12° 28.5'	10	2007-2008

Finally, tidal measurements were obtained from the tide gauge of Venezia, located at Punta della Salute. The tide gauge has the longest tidal dataset available for the Adriatic, further

details can be found for example in Canestrelli et al. (2001), which provide a record of the number of events and the maximum tidal heights which exceeded 1.10 m above the reference level between 1927-1982. The record was extended downloading data available at the Comune di Venezia-Centro Maree (www.comune.venezia.it).

6.1.2 Meteo storminess analysis

In order to analyze the meteorological storminess characterizing the Adriatic Basin, the methodology used by Trigo and Davies (2002) was chosen. The method was originally developed to study a 40 year climatology of meteorological conditions in the Adriatic Sea associated with storm surges in Venezia.

The method of Smits et al. (2005) was applied to three-hourly wave data to isolate sea storm events using a running time-window of 99 hours. The algorithm labels a record and its corresponding wave height value as an event, if the height during the middle hour of the moving window of 99 h equals the maximum wave height of the whole window. This time windows technique is often used in extreme values analysis of wind speed (Smits et al., 2005, Palutikof et al., 1999) and in the current case assumes that events are separated by at least 48 hours. Once the time series of selected events was created, the 90th percentile of the wave height distribution was used to determine the most intense events (i.e. the highest significant wave heights), and their distribution over the years 1999-2004. To notice that this produces a “wave climatology” that is considered representative for the whole period of wind measurements, which is much longer than the wave ones.

Once that the wave events were selected with the procure described above, SYNOP data were used to look for typical meteorological “stormy” conditions, i.e. mean meteorological conditions before and during the wave event selected by means of the procedure described above. For this purpose, Sea Level Pressure (SLP), wind speed and wind direction from all available coastal stations were rearranged to provide an overview during the event and respectively 3, 6, 12, 18, 24 hours. Moreover, a wind climatology was reconstructed for the period of measurements (1999-2004).

On the basis of this analysis, the “stormy conditions” that may produce wave events were defined as:

- NE or SE wind in Venezia (proxy of Bora and Sirocco) during the event.
- Mean sea level pressure difference between Venezia and Brindisi < 2 mb (proxy of Sirocco), 12 hours before the event.
- No SW wind at Ancona during the event.
- No westerly winds in Brindisi during the event.

Such conditions grossly lead to a Sirocco weather type some hours before the event and either Bora or Sirocco weather type during the event. In fact, on some occasions the wind changes

direction from the SE to the NE during the event, a phenomenon that is locally called “dark Bora” (Bora scura). Since the wind speed threshold is rather low (4 knots), many low-intensity events occurring during summertime are (erroneously) included using this selection procedure. Considering that from June till August the wave events are rather infrequent, only data from September till May were considered.

6.1.3 Wave storminess analysis

The wave data were assembled into a homogeneous data-set, using as much as possible the available directional information. Considering that Ravenna is located about halfway between Venezia and Ancona, the wave data from Ancona were transposed there using the relationship between effective fetches. To notice that this method assumes that events at both locations occurred simultaneously. Data from Venezia was not transposed because it is non-directional. Storms were identified using a wave height threshold of 1.5 m, a minimum duration of 6 hours and a minimum gap between events of 3 hours. In this gap evaluation method also missing data are considered. There is no standard on storm thresholds in Italian seas in the literature. According to the Italian Wave Atlas (Corsini and Inghilesi, 2004), the threshold for H_s is fixed at 1.0 m for at least 12 consecutive hours at events are separated by 6 hours of wave height decay. In a specific study for the northern Adriatic Sea, Cavaleri et al. (1996) choose instead 2.0 m. In the current study the threshold and the separation interval were chosen examining the wave height time series for a number of storms. It was observed that the chosen parameters were providing a method that was able to identify events that were recorded qualitatively by coastal authorities as storms that generated either coastal erosion and/or damage and flooding.

Following the approach adopted by Mendoza and Jimenez (2004) and by Armaroli et al. (2006), the total energy (E) of each event was computed using the Significant Wave Height (H_s) integrated over the storm duration (t_1, t_2):

$$E = \int_{t_1}^{t_2} H_s^2 dt \quad [m^2 \cdot hr]$$

Yearly storminess was quantified in two ways. First, to understand if one particular year was more energetic than another one, the cumulative yearly wave energy was computed adding all events. To understand if the energy of events had changed through time, the event specific storm energy was computed, normalizing the total energy of a given year for the number of storms measured in that year.

6.2 Results

6.2.1 Analysis of storm occurrence: long-term wind observations

The meteo data-set from 1960 was investigated to find the simultaneous occurrences of the 4 conditions across the basin to assume the simultaneous occurrence of a wave event. Results of this analysis (Fig. 4) show that there is not a well defined trend in storm occurrence over the

last fifty years. It could be noticed some reduction of the storminess in the period 1998-2000. However, considering that for this period there is a lack of wind measurements for the SYNOP stations of Venezia and Brindisi (Fig. 2), this trend change may be an artefact. Part of the same data-set (1951-2000) was previously investigated by Pirazzoli and Tomasin (1999, 2003), together with data from the SYNOP stations of Trieste, Ancona and Termoli. They carried out some analysis on trends in wind regimes and frequencies eventually linking the results to climatic changes. The main conclusion they reached was a clear decline in the occurrence of easterly winds (Bora winds), that they related to interannual climate variability, such as the NAO or changes in temperature.

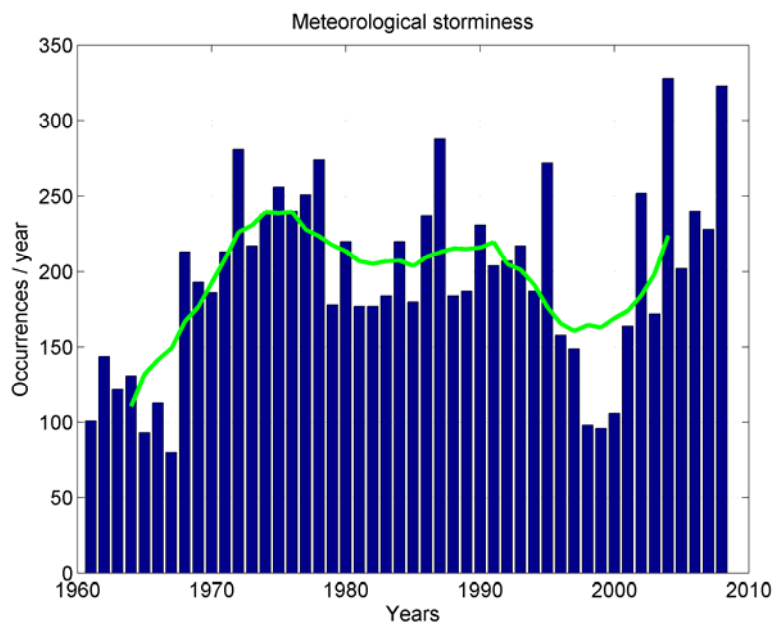


Figure 4. Occurrence per year of storm events (blue bars) and 10-year moving average (green line).

6.2.2 Analysis of storm occurrence: medium-term wave records

For the period 1993-2008 (Fig. 5) the analysis identified 240 storms, with an average duration of 22 hours and a maximum of 94 hours. On average the storms were coming from the direction 66°N (ENE), with an average storm maximum Hs of 2.47 m. The absolute maximum wave height in front of Ravenna was estimated as 5.65 m on 24 September 2004. In Fig. 5 we see that the average Storm Significant Wave Height during all years remained quite constant, while the Maximum Significant Wave Height during storms reached extreme values in 1999 and 2004.

Regarding yearly storminess, one may be tempted to say that from 1999 to 2004 there was an increase. However, it must be remembered that this part of the data-set is referred to the Ancona buoy, located in deep water conditions, while the previous time series (ENI oil rig) refers to shallower water conditions, thus undergoing wave transformation. The normalized wave energy provides instead a clearer picture.

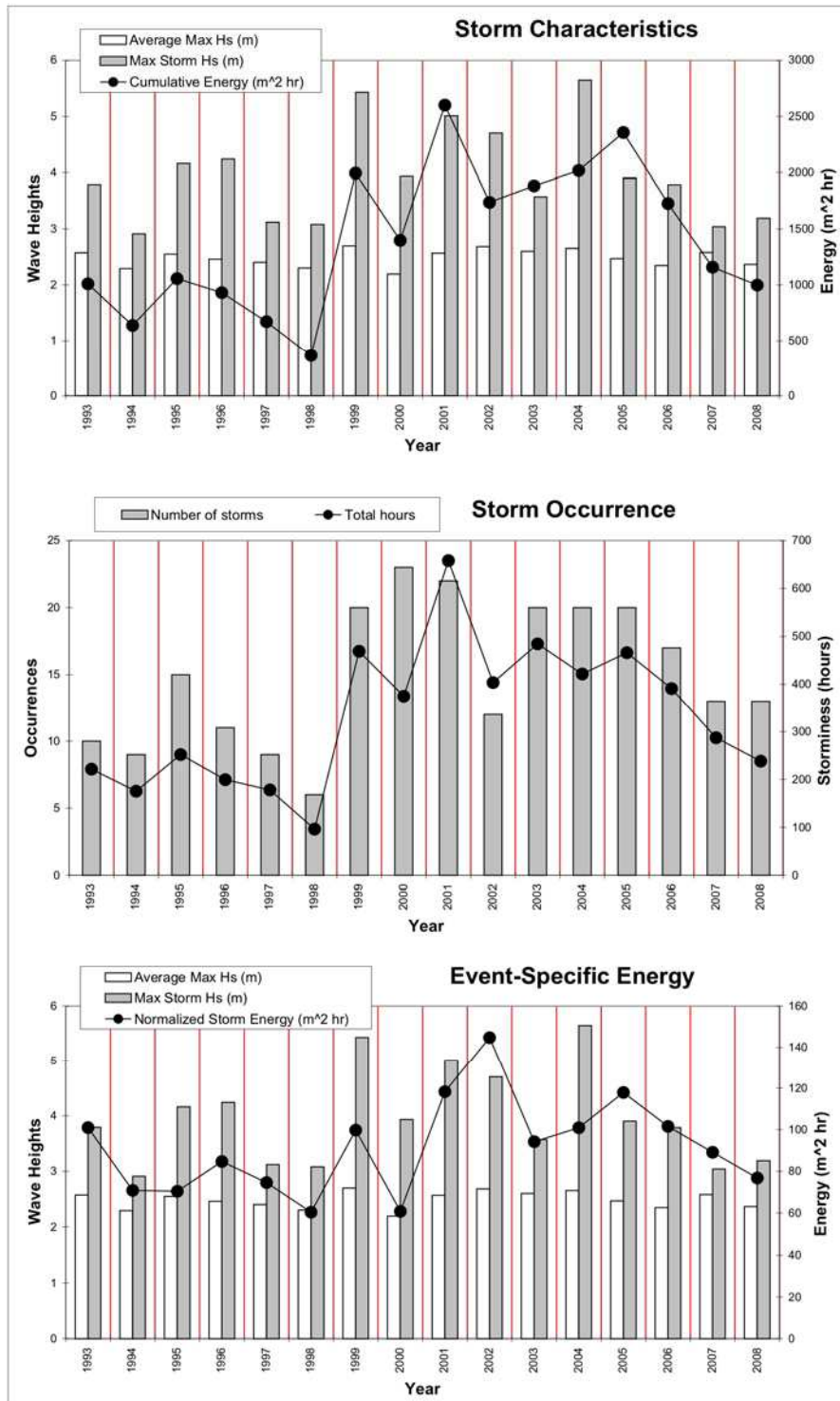


Figure 5. Characteristics of the storms recorded in the period 1993-2008.

The year 2002 results to be extremely energetic, despite the lowest number of observed events. In reality this energy peak is related to a cluster of 4 storms occurred between 7 and 10 December of that year, coming from N-NE and with maximum wave heights up to 4.7 m.

Finally, the apparent decrease in energy from 2006 onwards may be related to the fact that both the SWAN “virtual” buoy and the Cesenatico buoy are located at a -10 m water depth. The diversity in the data sources and the short duration of the time series do not allow to have a clear trend analysis or to adjust trend lines.

6.2.3 Occurrence of storm surges

The time series presented in Fig. 6 show that there was an increase in the last 85 years in the number of events. The maximum tidal levels observed show more variability, with the highest surge (1.94 m) recorded in 1966. The number of events shows a sharp increase coincident with groundwater pumping taking place during 1952-1969. From the mid '90s onwards a new increase is seen. Here it is important to notice the discussion of Fagherazzi et al. (2005) that find a role of climatic variability between the 70s and the early 90s, mitigating the frequency of flooding events.

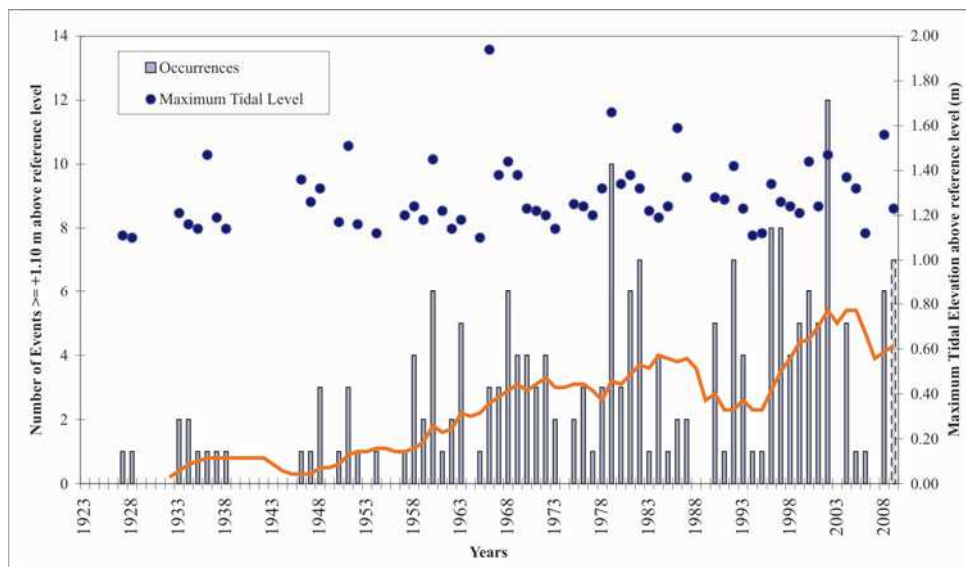


Figure 6. Characteristics of the storm surges recorded at the tide gauge of Venezia (Punta della Salute) in the period 1923-2008. Data from Canestrelli et al. (2001) and by the Comune di Venezia-Centro Maree. The line is the 10-yr moving average of the events observed every year. The reference level is local and corresponds to MSL at the tide gauge (1897 datum).

6.3 Conclusions

The analyses presented here were not able to detect a significant change on storminess over the last 50 years in the Adriatic. Musić and Nicković (2008) tried to use for the Eastern Mediterranean the HIPOCAS database and they came to the conclusion that there may be a slight decrease in extreme wave heights, which somehow could agree with our long-term analysis. However, it must be reminded that their data-set is very limited in the Adriatic, with virtually no validation points in the northern Adriatic. Another comparable approach is that of Lionello and Sanna (2005), which used instead ERA-40 reanalysis for the 1958-2001 time-span, which can be compared well with our analysis. Using linear regression performed upon the time series of monthly averaged Significant Wave Height fields, they detected a statistically

significant tendency to a reduction of H_s in the winter season. They even tried to relate wave variability to larger scale atmosphere circulation patterns controlled by phenomena like NAO and Indian Monsoon, concluding that regional regimes were predominant, in agreement with Camuffo et al. (2000).

Finally, it has been demonstrated by Signell et al. (2005) how important is the horizontal resolution of a meteorological model, when it tries to describe and define local winds (i.e. Bora). In the case of the Northern Adriatic, a model that is too coarse will not be able to resolve the orographic pattern of the surrounding landscapes and, as a consequence, will not identify and localize properly a Bora storm (Pasarić et al., in press). This generates a further limitation to the use of databases of reconstructed wave heights (e.g. HIPOCAS), which are extremely sensitive to the quality of the wind field (Ponce de León and Guedes Soares, 2008).

Regarding the last 15 years, the availability of direct wave measurements offers more reliable information. According to the review of the literature, the analysis presented here is the first of this kind for the Northern Adriatic. Although based on diverse sources of wave measurements, the comparability of data-sets was tested for common storms observed by the Venezia, Ravenna and Ancona data sources and results were satisfactory. The standard deviation of the observed yearly maximum significant wave height during storms is varying between 0.32 and 0.98 m. This may well account for interannual variability.

An issue that possibly deserves further attention is the grouping of extreme events as clusters. The cluster of 2002 has proved that the overall yearly energy budget can be completely overturned. This issue has possible implications for the assessment of past morphological changes and coastal damages. It is important to notice that unlike storm energy, storm surges seem to show a clear increasing trend in the frequency of occurrences in the last 10 years. The joint occurrence of exceptionally high tides even with storms of medium energy may have an important role in causing morphological changes and flooding, possibly more prominent than the absolute wave energy of a single storm.

6.4 Consulted websites

CADSEALAND Project

<http://www.cadses.net/en/projects/apprpro.html?projectId=1506&topic=projects/apprpro&HPSESSID=0e> (accessed on 18 May 2009)

Comune di Venezia-Centro Maree

<http://www.comune.venezia.it/flex/cm/pages/ServeBLOB.php/L/IT/IDPagina/1748> (accessed on 18 May 2009)

APAT Wave Data

<http://www.idromare.it/> (accessed on 18 May 2009)

SWAN set-up at ARPA-SIMC

http://www.arpa.emr.it/dettaglio_documento.asp?id=464&idlivello=64 (accessed on 18 May 2009)

6.5 References

Armaroli, C., Ciavola, P., Caleffi, S., Gardelli, M., 2007. Morphodynamics of nearshore rhythmic forms: an energy-based classification. Proceedings of International Conference on Coastal Engineering, San Diego, CA, USA, vol. 4, pp. 4009-4021.

Cavaleri, L. Bergamasco, A. Bertotti, L. Bianco, M. Drago, L. Iovenitti, A. Lavagnini, G. Liberatore, S. Martorelli, F. Mattioli, Osborne A. R., Pedulli L., Ridolfo M., Sclavo M., Serio M., Tescaro N., Tibaldi S., Tosi E. and Viezzoli D., 1996. Wind and waves in the Northern Adriatic Sea, *Il Nuovo Cimento C*, Volume 19, 1, 1-36.

Camuffo, D., Secco, C., Brimblecombe P., and Martin Vide J., 2000. Sea storms in the Adriatic Sea and the western Mediterranean during the last millennium, *Climatic Change*, 46, 209–223.

Canestrelli, P., Mandich, M., Pirazzoli, P.A., Tomasin, A., 2001. Wind, depression and seiches: tidal perturbations in Venice (1951-2000). Venice, Italy: Comune di Venezia, Centro Previsioni e Segnalazioni Maree, 105 p.

Corsini, S. and Inghilesi, R., 2004. Atlante delle onde nei mari italiani. APAT, Rome, Italy.

Fagherazzi S., Fosser G., D'Alpaos L., D'Odorico P., 2005. Climatic oscillations influence the flooding of Venice, *Geophys Res. Lett.* 32, 19, L19710 10.1029/2005GL023758.

Lionello P. and Sanna A., 2005. Mediterranean wave climate variability and its links with NAO and Indian Monsoon. *Climate Dynamics*, 25: 611–623.

Mendoza E.T. and Jimenez J.A., 2004. Factors controlling vulnerability to storm impacts along the Catalanian coast. Proceedings International Conference of Coastal Engineering, Lisbon, pp. 3087-3099.

Musić S. and Nicković S. , 2008. 44-year wave hindcast for the Eastern Mediterranean. *Coastal Engineering*, 55, 872–880.

Palutikof J. P., B. B. Brabson, D. H. Lister, S. T. Adcock, 1999. A review of methods to calculate extreme wind speed. *Meteorological Applications*, 6: 119-132.

Pasarić Z., Belušić D. and Chiggiato J. (in press). Orographic effects on meteorological fields over the Adriatic from different models, *J. Mar. Syst.* doi:10.1016/j.jmarsys.2009.01.019

Pirazzoli P.A., A. Tomasin, 1999. Recent abatement of easterly winds in the Northern Adriatic. *International Journal of Climatology*, 19:1025-1219.

Pirazzoli P.A., A. Tomasin, 2003. Recent near surface wind changes in the central Mediterranean and Adriatic areas. *International Journal of Climatology*, 23: 963-973.

Ponce de León S. and Guedes Soares C., 2008. Sensitivity of wave model predictions to wind fields in the Western Mediterranean sea, *Coastal Engineering*, 55, 920-929.

Signell, R.P., Carniel, S., Cavalieri, L., Chiggiato, J., Doyle, J., Pullen, J., Sclavo, M., 2005. Assessment of wind quality for oceanographic modeling in semienclosed basins. *J. Mar. Syst.* 53, 217–233.

Smits, A., Klein Tank A. M., Konnen G. P., 2005. Trends in storminess over the Netherlands, 1962-2002. *International Journal of Climatology*, 25: 1331-1344.

Trigo, I. F., and T. D. Davies (2002), Meteorological conditions associated with sea surges in Venice: A 40 year climatology, *Int. J. Climatol.*, 22, 787–803.

Valentini, A., Delli Passeri, L., Paccagnella, T., Patrino, P., Marsigli, C., Deserti, M., Chiggiato, J., and Tibaldi, S., 2007. The Sea State forecast system of ARPA-SIM. *Boll. Geof. Teor. Appl.*, Vol. 48, n. 3, pp. 333-349.

7 Netherlands

Fedor Baart, Marije Smit and Mark van Koningsveld

7.1 Introduction

This study describes an analysis of change in coastal storm occurrence for the Netherlands. Both observed trends in storminess as well as expected climate change impacts on future storm occurrence are examined.

In different studies different measures are used to quantify “storminess”. A storm can be characterised by intensity, frequency and duration of characteristic storm properties like wind speeds. In some studies proxies are used, for example pressure tendencies, surface air pressure and storm surge. Other studies examine wind speeds directly. An overview of different proxies and research methods for determining storminess changes can be found in Carnell et al. (1996); Smits et al. (2005); Bijl et al. (1999). Carnell et al. (1996) concludes that different methods can lead to a different interpretation of the data, and the predicted changes.

In the current work coastal storminess change is assumed to be an underlying variable representing both frequency and intensity of storms directed at the coast. Change in storminess is operationalised (see Bridgman, 1955, chap. 1) as the relative changes in the annual number of storm events. We will compare the storminess changes with storminess changes measured by changes in storm surges.

The availability of data determines the frequency of storms that can be investigated. Low frequency storms require a long period of measurements. For the Netherlands, sets of continuous measurements are available since the 60's. This is just enough to notice big changes in storminess for infrequent (twice per year) events. In case the trend changes in storminess are small, they can only be observed over longer timespans or for higher frequent events. From a short term, tactical perspective, which fits in the operational focus of the MICORE project, the return period of interest for the Netherlands is about once every 2 years. The power of a 40 years dataset is still not enough to examine trends with the order of magnitude as found so far. The study of changes over longer periods using historical records could provide more insight in the changes in the occurrence of storms with a 2 year return period.

We will first examine wind observations at coastal stations over the last decades. These results will be compared with previous analysis of surge levels. Storminess in the context of climate change will be examined using results from scenario studies and reanalysis studies.

7.2 Methods

7.2.1 Observations over the last decades

The relative changes in the annual number of storm events can be examined using decadal length time series of wind speeds collected by weather stations or by proxies of these like pressure measurements. The most important dataset for examining storminess changes in the Netherlands resides at the Koninklijk Nederlands Meteorologisch Instituut (KNMI). The KNMI measures wind speeds at different stations in the Netherlands. Because direct station measurements of storm occurrence and intensity are available, studies doing reanalysis of proxy data (for example Sterl and Caires, 2005) will not be considered as the measure for describing observed changes in storminess. Comparisons between these studies can be found in for example Hurk (2006).

The wind data of the KNMI have been analysed by Smits et al. (2005). They analysed wind data for 13 stations, both coastal as well as inland stations over the period 1962 through 2002. For the current work, only the analysis of the coastal stations is used. Smits et al. (2005) look at the annual numbers of independent wind events that last for several hours. The intensity is determined by the observed hourly peak wind speeds. Frequency is determined by the number of occurrences per year. The study makes an ordinal categorisation of storms where weak events occur on average 30 times per year, moderate wind events are defined as winds which occur on average 10 times (windspeed 6-7Bft), and strong events have an occurrence rate of 2 times per year (windspeed 7-8Bft).

Longer timeseries (100 years), using storm surges as a proxy, were analysed by Bijl et al. (1999). We only look at the high water setup of the Hoek van Holland and Vlissingen stations. The authors define a storminess factor for each station, using four different storm frequencies, by splitting the timeseries in groups of 10 years. For each decade an expected 1/10000 year storm surge is computed. The expected 1/10000 year storm surge over the whole 100 years is subtracted from the decadal storm surge. This is what the authors call the "storminess factor". Note that extrapolation using a Weibull distribution was used to obtain an estimate of the 1/10000 year event. This is done for comparison purposes and does not imply changes in the 1/10000 year storm trend.

7.2.2 Modelled climate change effects

The expected climate change impacts on storm occurrence have been examined using numerical weather prediction models with hypothetical scenarios. An overview will be given of the analysis of climate change scenarios and their expected impact on storm occurrence.

The wind data of the KNMI combined with historic records is also used as a source for the climate change scenarios described in Hurk (2006). This study extrapolates expected wind occurrence using numerical weather prediction models and 4 different climate scenarios.

7.3 Results

7.3.1 Observations over the last decades

The analysis of wind data as observed at different stations in the Netherlands over the period 1962 through 2002 was analysed by Smits et al. (2005) (Fig. 1). For each storm frequency

(number of storms per year), the trend over 40 years was analysed. If for example the moderate storms (10 times per year) occur more often over this period, the trend (% of increase over 10 years) will be positive (e.g. for IJmuiden). If the number of moderate storms decrease over the years, the trend will be negative (e.g. for Hoek van Holland). For identical storm occurrences, the trends are different for the different stations. Note that the 0 axis intersects with the confidence interval meaning that moderate to strong events do not statistically significant decrease. Fig. 2 presents this spatial variability in trends in storm occurrence for the strong storm events (twice per year). The figure presents increasing trends along the Southern part of the Dutch coast and mainly decreasing trends along most of the Holland coast (Western part of The Netherlands). It should be noted that strong winds in The Netherlands generally come from the North Sea (Fig. 3). The presented analysis on wind speeds can therefore be used to understand the trends in storminess of events that may pose a hazard to the Dutch coastal area.

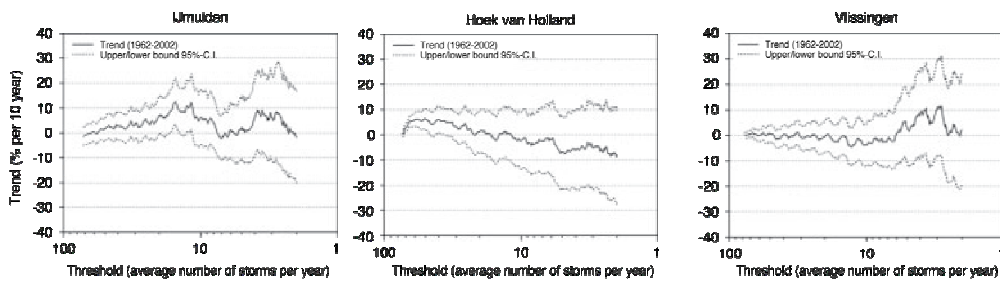


Figure 1. Trends (%/decade) in the annual number of storm events as a function of severity level for three coastal stations (from North to South with geographical locations indicated in Figure 2. Left: IJmuiden, middle: Hoek van Holland, right: Vlissingen). From: Smits et al. (2005)2

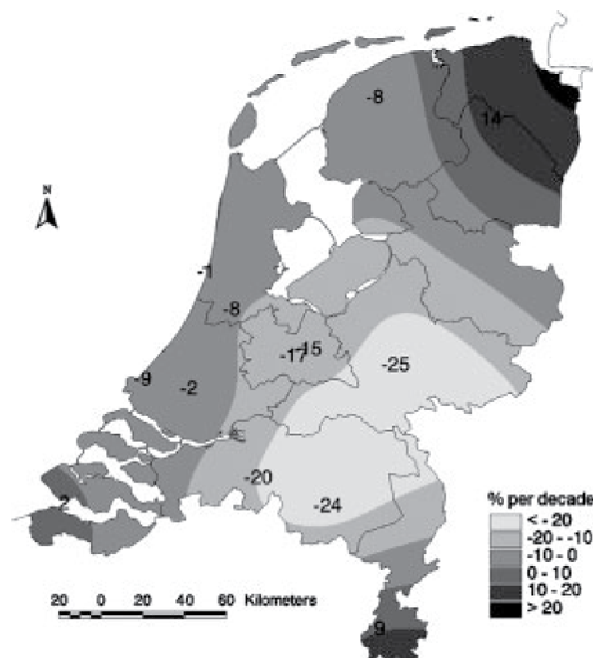


Figure 2. Trends (%/decade) in the annual number of storm events for strong events. From: Smits et al. (2005)

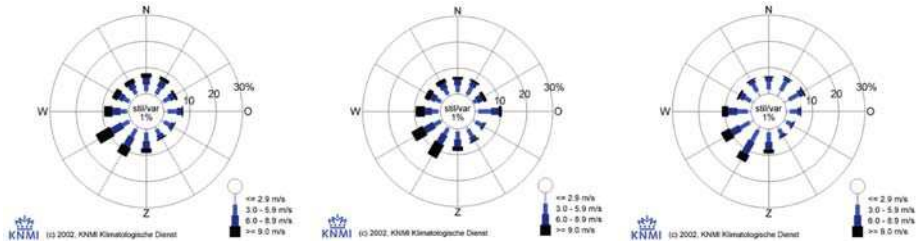


Figure 3. Average (1971-2000) yearly wind climate. Left: IJmuiden, middle: Hoek van Holland, right: Vlissingen. From KNMI (2009)

The analysis of 100 year storm surge variations showed no significant trend for both stations. The results of their analysis, for different storm return periods, show no overall significant trend (Fig. 4).

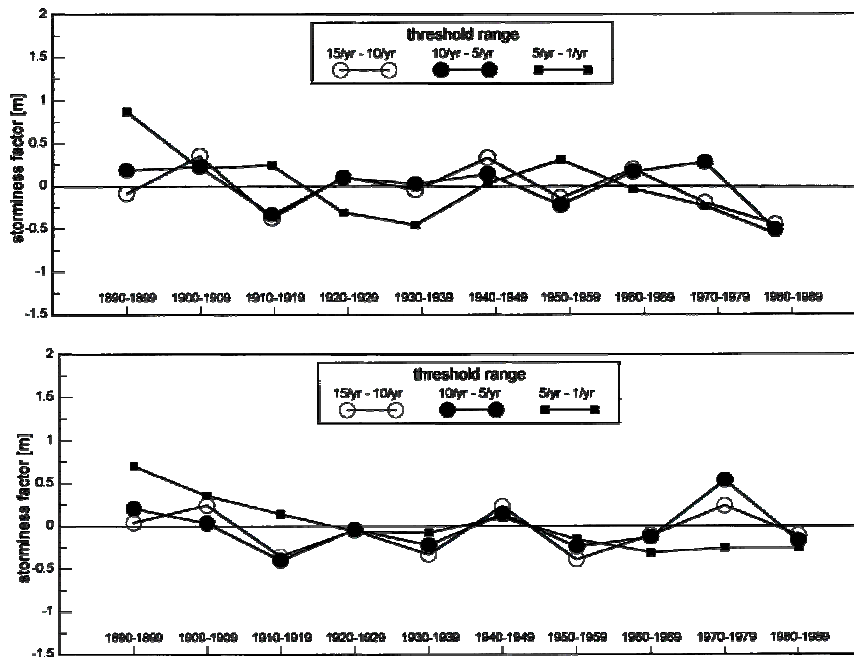


Figure 4. Decadal high water set-up storminess factors. Top: Hoek van Holland, bottom: Vlissingen. From Bijl et al. (1999)

7.3.2 Modelled climate change effects

The only climate change model available so far that looks at wind and is specific for the Netherlands is described by Hurk (2006). The four climate scenarios described in this research vary on two factors: air circulation patterns (constant, increased) and temperature increase. Fig. 5 shows the expected change in the yearly maximum daily mean wind speed until 2050 for the four scenarios. It shows an increase in two scenarios, a decrease in one scenario and one with a constant maximum wind speed.

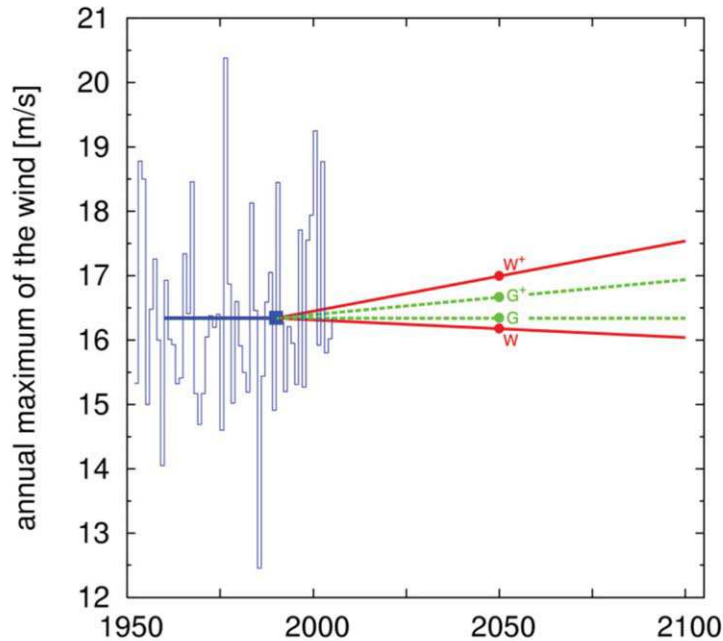


Figure 5. Time series of observed yearly maximum daily mean wind speed (m/s) in IJmuiden, plus the scenario values for 2050. From: Hurk (2006)

7.4 Conclusions

The trends in storminess show a big variation across research methods, region, season and observed period. Observations in the Netherlands show a slight decrease in storminess while reanalysis models show an increase. There are different aspects which can explain these differences which have been discussed by the original authors (see Hurk, 2006; Smits et al., 2005; Bijl et al., 1999) like homogeneity breaks and increase in surface roughness due to population increase.

The statistical power of the dataset is enough to show differences in storminess of storms up to 10 storms per year. Less frequent storms do not show a significant change. While one series of observations alone does not provide enough statistical power to test hypotheses on the decadal trends, doing a meta analysis over several European countries can give more insight into the harder to observe trends in storminess. However with the combination of different research the ambiguity of the definition of storminess will perhaps result in more variation than added explanation. For this meta analysis it is therefore important to aim for a consistent definition of the storminess and focussing on the storminess only in coastal regions.

From a long term, strategical perspective, the coastal defence in the Netherlands is designed with the coastal protections able to withstand storms with a 10000 year return period. The storminess itself can, with a limited reliability, be computed by fitting extreme value

distributions to the observed data. But changes in storminess, for storms with such low frequency, cannot be examined using a series of 40 years of data. To examine trends in return periods the length of the observed timeseries has to be an order of magnitude greater than the return period of the storm.

7.5 References

W Bijl, R Flather, JG de Ronde, and T Schmith, 1999. Changing storminess? An analysis of long-term sea level data sets. *Climate Research*, 11(2):161–172.

P.W Bridgman, 1955. *Reflection of Physicist*. Philosophical Library, New York,

RE Carnell, CA Senior, and JFB Mitchell, 1996. An assessment of measures of storminess: Simulated changes in northern hemisphere winter due to increasing CO₂. *Climate Dynamics*, 12(7):467–476 . ISSN 0930-7575.

Bart van den Hurk, 2006. *KNMI Climate change scenarios 2006 for the Netherlands*, volume WR 2006-01. KNMI, De Bilt,

KNMI. KNMI hydra project, June 2009. URL <http://www.knmi.nl/samenw/hydra/cgi-bin/freqtab.cgi>.

A Smits, AMGK Tank, and GP Konnen, 2005. Trends in storminess over the netherlands, 1962-2002. *International Journal of Climatology*, 25 (10):1331–1344. DOI 10.1002/joc.1195.

A Sterl and S Caires, 2005. *Climatology, variability and extrema of ocean waves: The web-based knmi/era-40 wave atlas*. *International Journal of Climatology*, 25 (7): 963-977.

8 Poland

Kazimierz Furmańczyk, Joanna Dudzińska-Nowak, Barbara Paplińska-Swerpel, Maciej Marek, Monika Kodrans-Nsiah

8.1 Methods

The storminess of the southern Baltic coast, where the Dziwnów Spit is located, was examined using two methods and datasets:

- A. sea level data from the tide gauges situated in the polish harbours;
- B. modelled significant wave height data for an area neighbouring the Dziwnów Spit.

According to the concept applied in Poland, a storm occurs when the wind force exceeds 8 Bft (Majewski et al., 1983). A storm surge occurs when the mean sea level exceeds 570 cm (Majewski et al., 1983; Sztobryn et al., 2005). The Maritime Office, administrative body responsible for the protection of the Polish coast, additionally defined a warning state and an alert state, individually determined for each harbour. For example, the warning state in the Dziwnów harbour is announced when the wind force exceeds 8 Bft or if the water level exceeds 560 cm (60 cm above mean sea level). The alert state, in turn, is declared when the wind force is above 9 Bft or the water level exceeds 580 cm (80 cm above mean sea level). To notice water levels are referred to Polish reference datum.

Changes in the storm, warning and alert state occurrences in the years 1947-2007 were assessed using published sea level data from the tide gauges in the Polish harbours of (from the west to the east): Świnoujście, Dziwnów, Kołobrzeg, Ustka, Władysławowo and Gdańsk (Wisniewski and Wolski, 2008; Furmanczyk and Dudzinska-Nowak, 2009). The tide gauges data were extracted from Majewski et al. (1983) and Sztobryn and Stigge (2005) who described the storm surges from the 1951-1975 and 1976-2000 periods respectively. Further data come from the "Geoserwer" database, Harbour Chronicles, VTS database of Szczecin and Swinoujscie Harbours and data of Institute of Meteorology and Water Management (IMGW) (Wisniewski and Wolski, 2008).

For the purpose of the analysis performed for this report, a storm definition was created being related to the wind waves. A storm was defined as an event starting when the significant wave height exceeds 1 m and ending when it drops below 1 m.

A long-term wave observation programme was never conducted along the Polish coast in the Baltic Sea. Wave measurements at a number of locations have been collected by the Institute of Hydro-Engineering of the Polish Academy of Sciences (IBW), but the periods of the measurements did not exceeded several month. Therefore, in this study modelled significant wave height data were used. The multi-decadal (1958-2001) high-resolution homogeneous data set was generated in the framework of the EU-project HIPOCAS (Cieslikiewicz and Paplinska-Swerpel, 2005, Cieslikiewicz et al. 2005). The wind waves over the Baltic Sea were

modelled using the WAM model (WAve Model; WAMDI Group, 1988). The wave model was driven with the wind fields derived from the atmospheric REMO model (REgional MOdel; Feser et al. 2001) forced with NCEP (National Centres for Environmental Prediction) reanalysis (Kalnay et al. 1996). The set up of the wave hindcast system was described in details in Cieslikiewicz and Paplinska-Swerpel (2008). The available wave measurements were used for the hindcast validation. The comparison of the measured and modelled significant wave heights revealed that the significant wave heights were properly reproduced by the model for all locations. In the current analysis the HIPOCAS data for the western Polish coast were used.

To analyse the significance of the obtained results the F-statistics were used. All statistical tests were performed at 1 and 59 degrees of freedom.

8.2 Results

Wisniewski and Wolski (2008) gathered and analysed all existing data on the storm surges and showed that the annual occurrence of storm surges along the entire Polish coast (Fig. 1) increased over the last 60 years. A similar trend (Fig. 2) is visible in the annual occurrence of alert states declared at minimally one coastal station in Poland (Furmanczyk and Dudzinska-Nowak, 2009). In the western part of the Polish coast, the 1973-1996 “Geoserwer” database contains records of 62 surges that caused the sea level to rise to the alert state at least one coastal station (Swinoujscie or Kolobrzeg). When considering these stations only, the increasing trend of storm surges is less distinct (Fig. 3). If the analysis is restricted to situations when the alert state was declared at all stations, no trend is observed (Fig. 4; Furmanczyk and Dudzinska-Nowak, 2009).

Nevertheless, the annual occurrence of the surges shows a tendency to increase with time. The increase in warning state surges is small, contrary to the significant increase in the number of the alert state surges (Fig. 5; Furmanczyk and Dudzinska-Nowak, 2009). The increases in the annual storm surge occurrence and in the number of alert states minimally at one station along the entire or western Polish coast are significant at the confidence intervals of $p=0.0000007$, $p=0.00127$ and $p=0.000939$ respectively. The trend in the number of alert states at all Polish stations is slightly insignificant ($p=0.291$).

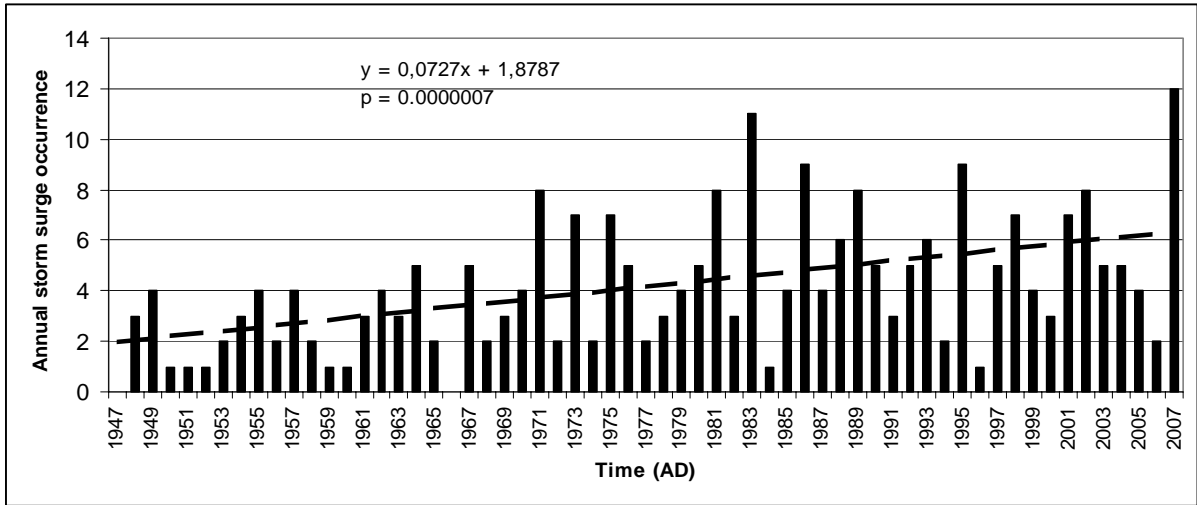


Figure 1. Annual storm surges occurrence along the entire Polish coast during the 1947-2007 period (Wisniewski and Wolski, 2008).

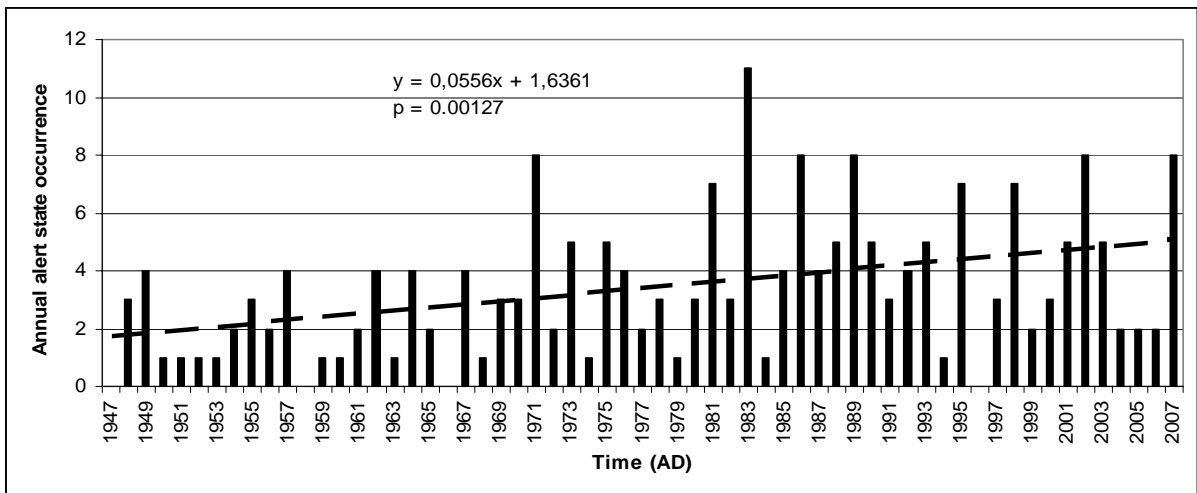


Figure 2. Number of storm surges causing declaration of alert state at minimally one station along the entire Polish coast (after Furmanczyk and Dudzinska-Nowak, 2009; data from Wisniewski and Wolski, 2008).

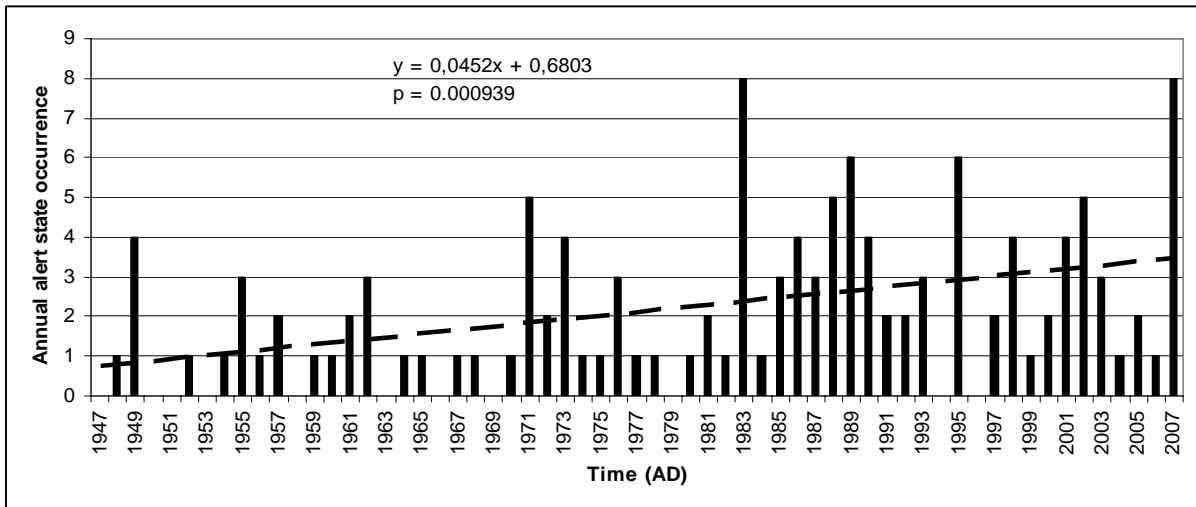


Figure 3. Number of storm surges causing declaration of alert state at minimally one station on the western Polish coast (Swinoujscie and Kolobrzeg) (after Furmanczyk and Dudzinska-Nowak, 2009; data from Wisniewski and Wolski, 2008).

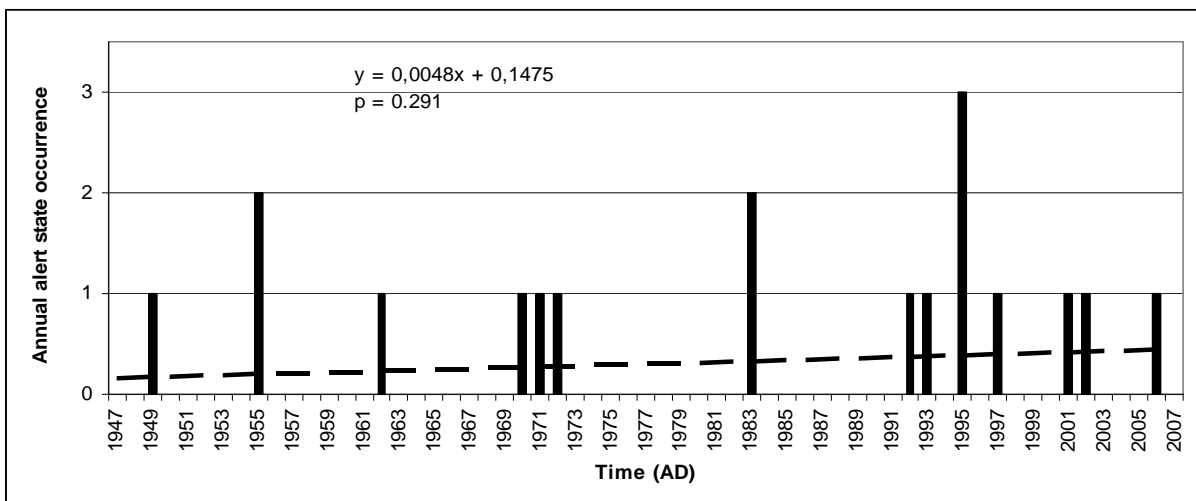


Figure 4. Number of storm surges causing declaration of alert states at all of the Polish coastal stations (after Furmanczyk and Dudzinska-Nowak, 2008; data from Wisniewski and Wolski, 2009).

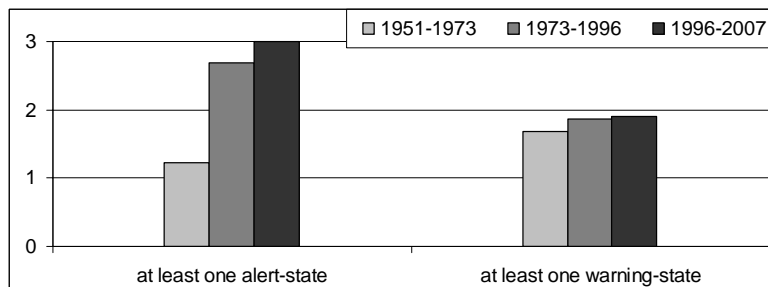


Figure 5. Average annual occurrence of the alert and warning states in different periods of time (after Furmanczyk and Dudzinska-Nowak, 2009).

The storm analysis was performed for the 1958-2001 period. For each year the annual occurrence of storms with significant wave height above 1 m was calculated, along with the individual and cumulative duration of such events. Furthermore, the mean storm energy and cumulative storm energy per year were calculated. Storm energy was estimated by multiplying the square of the event's significant wave height (above 1 m), with its duration [$\Sigma(H_s)^2 * t$]. The results are presented in Figs. 6-10.

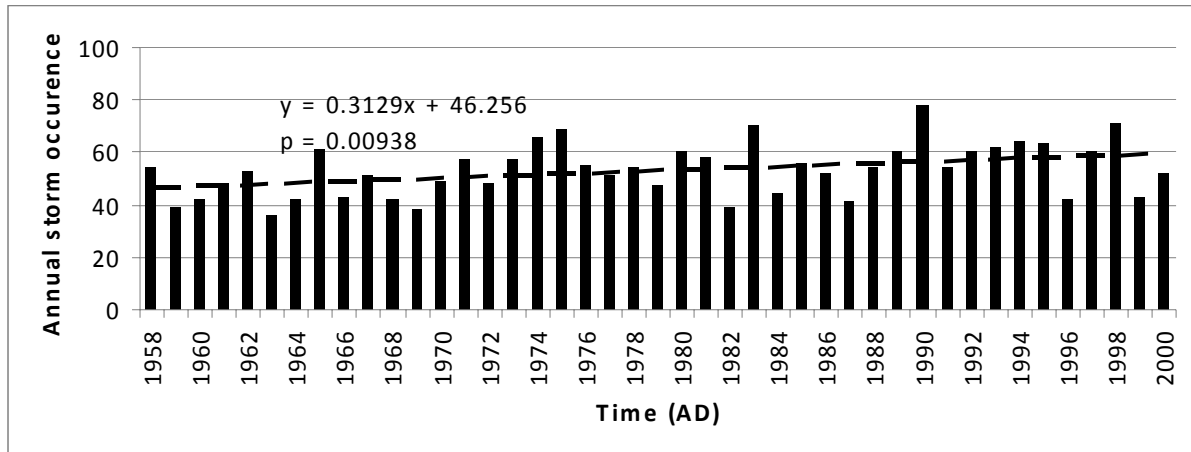


Figure 6. The annual storm occurrence along the western Polish coast during the 1958-2000 period.

During the studied 40-year period, the annual storm occurrence and thus the cumulative storm duration and cumulative storm energy per year significantly increased (for confidence intervals of $p=0.00938$, $p=0.00854$, $p=0.00887$ respectively) (Figs. 6-8). The average storm duration and the mean storm energy increases for the same time period seem to be insignificant ($p=0.452$ and $p=0.489$ respectively) (Figs. 9-10).

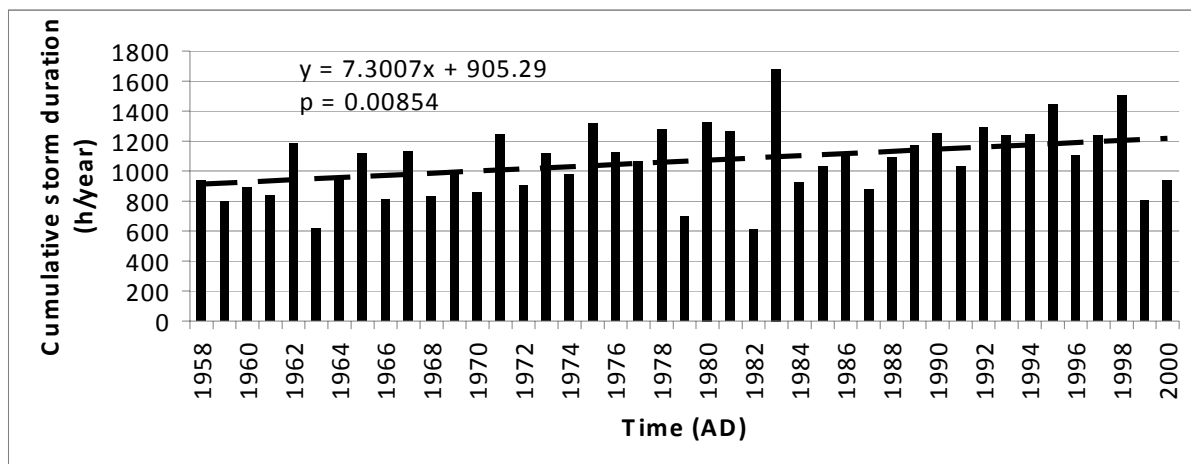


Figure 7. The cumulative storm duration per year along the western Polish coast during the 1958-2000 period.

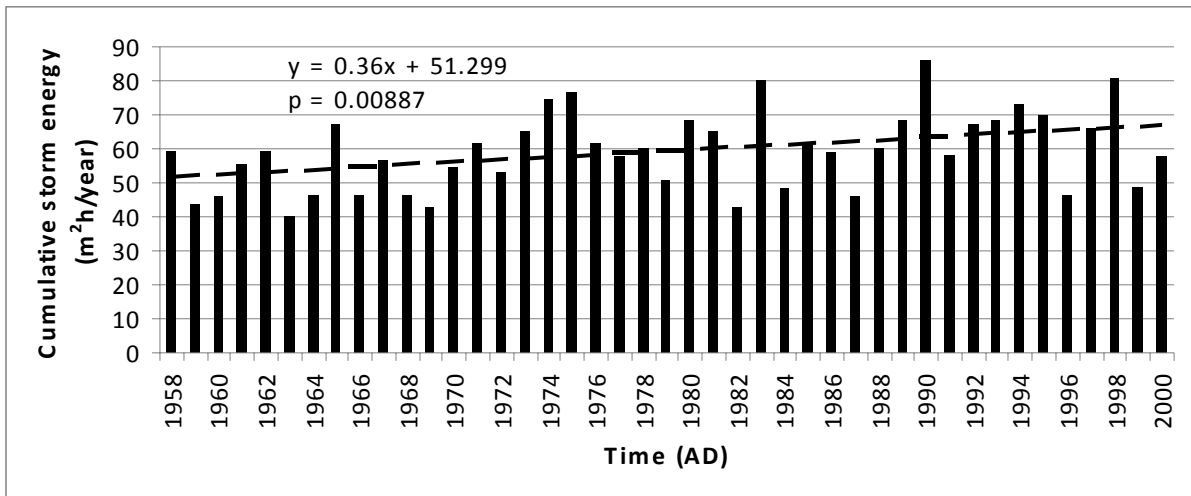


Figure 8. The cumulative storm energy per year along the western Polish coast during the 1958-2000 period.

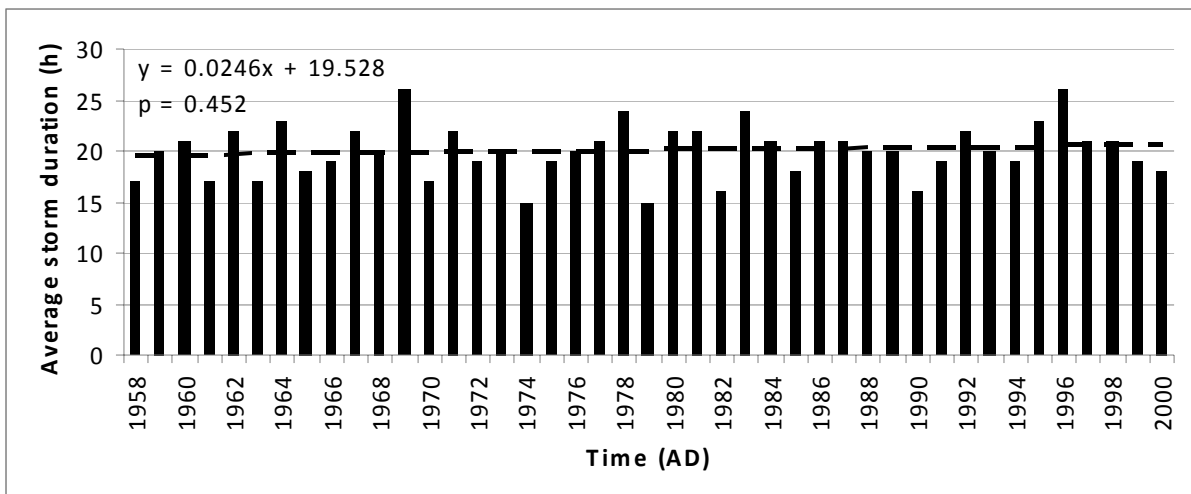


Figure 9. The average storm duration for the western Polish coast during the 1958-2000 period.

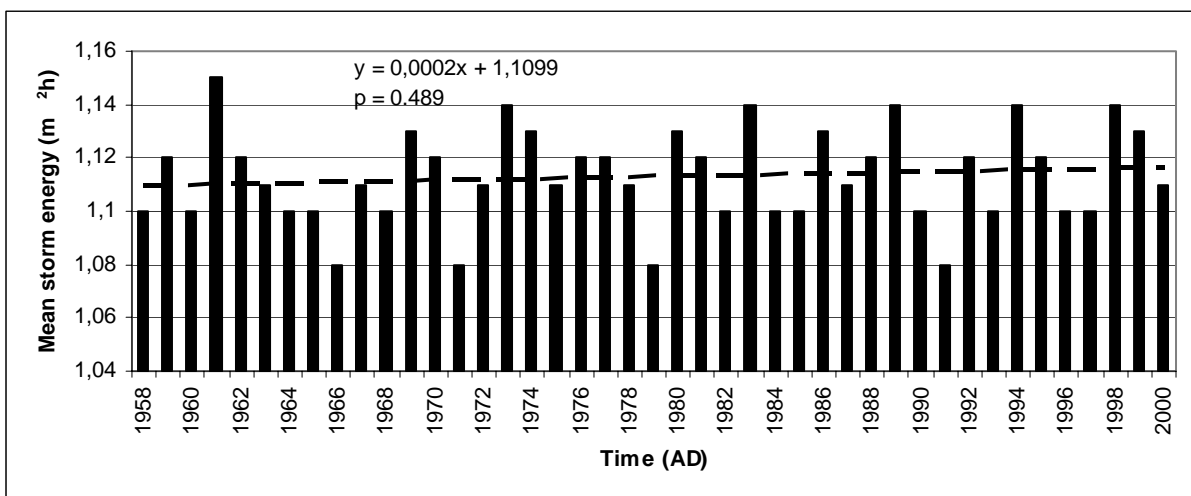


Figure 10. The mean storm energy for the western Polish coast during the 1958-2000 period.

8.3 Conclusions

The results of the performed analysis showed an increase in storminess on the southern Baltic coast, as suggested by the:

- significant increase in annual occurrence of the storm surges since 1947;
- significant increase in annual occurrence of the alert states per year;
- significant raise of annual occurrence of storms with the significant wave height above 1 m which was followed by an increasing cumulative storm duration and cumulative storm power per year.

The average storm duration and the mean storm power did not change significantly during the analysed period.

8.4 References:

Cieślíkiewicz, W., Paplińska-Swempel, B., 2005. Rekonstrukcja falowania wiatrowego na Bałtyku w okresie 1958-2001. *Inżynieria Morska i Geotechnika*, R. 26, 4, pp 313-321.

Cieślíkiewicz, W., Paplińska-Swempel, B., Soares, C. G., 2005. Multi-decadal wind waves modeling over the Baltic Sea. In McKee Smith, J. (ed.) *Coastal Engineering 2004. Proceedings of the 29th International Conference*, Vol. 1, pp 778-790.

Cieślíkiewicz, W., Paplińska-Swempel, B., 2008. A 44-year hindcast of wind wave fields over the Baltic Sea. *Coastal Engineering* 55, pp 894-905.

Feser, F., Weisse, R., von Storch, H., 2001. Multi-decadal atmospheric modelling for Europe yields multi-purpose data. *EOS Transactions*, 28, pp 305-310.

Furmanczyk, K., Dudzińska-Nowak, J., 2009. Effects of extreme storms on coastline changes: a southern Baltic example. *Journal of Coastal Research*, SI 56, pp 1637-1640.

Kalnay, E., Kanamitsu, M., Cistler, R., Collins, W., Deaven, D., Gandin, L., Iredell, M., Saha, S., White, G., Woollen, J., Zhu, Y., Chelliah, M., Ebisuzaki, W., Higgins, W., Janowiak, J., Mo, K. C., Ropelewski, C., Wang, J., Leetma, A., Reynolds, R., Jenne, R., Joseph, D., 1996. The NCEP/NCAR 40-year reanalysis project. *Bulletin of American Meteorological Society*, 77, pp 437-471.

Majewski, A., Dziadziuszko, Z., Wiśniewska, A., 1983. *Monografia powodzi sztormowych 1951-1975*. IMGW. Wyd. Komunikacji i Łączności. Warszawa. 214p.

Sztobryn, M., Stigge, H. J., Wielbińska, D., Weidig, B., Stanisławczyk, I., Kańska, A., Krzysztofik, K., Kowalska, B., Letkiewicz, B., Mykita, M., 2005. *Storm Surges in the Southern Baltic Sea*

(Western and Central Parts). Berichte des Bundesamtes fur Seeschifffahrt und Hydrographie Nr 39/2005.

WAMDI Group, 1988. The WAM model – A third generation ocean wave prediction model. *Journal of Physical Oceanography*, 18, pp 1775-1810.

Wiśniewski, B., Wolski, T., 2008. Katalog wezbrań i obniżeń sztormowych na polskim wybrzeżu Bałtyku, jako zdarzenia ekstremalne. In: Furmańczyk, K. (ed.) ZZOP Tom 3. Morze – Ląd wzajemne relacje.

9 Portugal-Western coast

Alexandre Quadrio and Rui Taborda

9.1 Methods

This report is based on data from the HIPOCAS project “Hindcast of Dynamic Processes of the Ocean and Coastal Areas of Europe”, which has produced a database of 44 years of wind, sea-level and wave data along the European waters. Puertos del Estado (Spain) used HIPOCAS data to produce SIMAR-44 data set, which corresponds to WAM model results performed for the North Atlantic from 1958 to 2001, using a fine grid in the North East Atlantic coastal areas of Europe (details can be found in Pilar et al., 2008). From these data, six nodes were selected with the intention to provide information along the western Portuguese coast (Fig. 1). The data include time series of significant spectral wave height (H_{m0}), mean period (T_m), peak period (T_p) and mean wave direction, with a three hour time step.

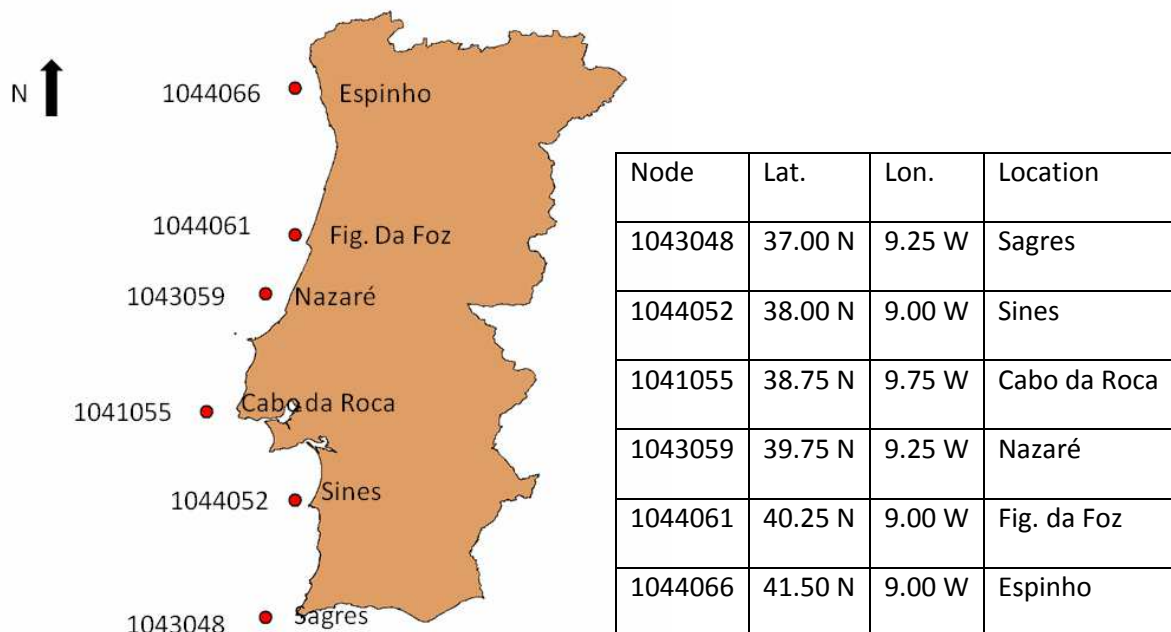


Figure 1. Node coordinates and location.

9.1.1 Storm definition

The storm definition for the Portuguese west coast follows the works of Costa (1994) and Ponce (2008):

- Significant wave height over 5 m.
- Minimum time between storms, i.e., the time interval to consider a new event: 12 h.

- No low limit on the storm duration was considered.

Storm data were retrieved from raw data and subsequently treated and analyzed. Storm energy was calculated using a discrete approach according to the formula:

$$E = \int_{t_1}^{t_2} H_s^2 dt$$

Changes in storminess were studied by analysing several time series: number of storm days, number of storms and average wave height from 1958 to 2001. Trend analysis in this study was carried out by fitting a simple linear model to the time series.

In order to try to extend the study to the late XIX century, SIMAR-44 data were also compared with published data for the northwest coast derived from qualitative historical sources (Andrade et. al, 1996; Pedrosa and Freitas, 2008).

9.1.2 Model validation

Model validation has been undertaken through comparisons with data from Figueira da Foz wave buoy (data from Instituto Hidrográfico, obtained through the National Information System of Littoral Resources, SNIRLIT - <http://geo.snirh.pt/snirlit/site/consulta.php>). Despite the slight tendency of the SIMAR-44 data to overestimate wave height, the results show a good agreement (Fig. 2 and table 1). Additional validation made by Pilar et al, 2008, is also shown in table 1.

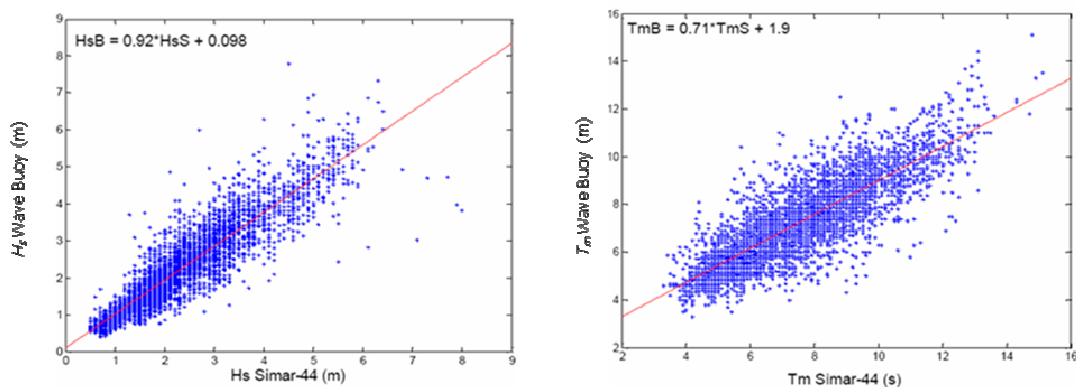


Figure 2. Comparison of SIMAR-44 significant height (left) and mean period (right) with Figueira da Foz wave buoy records from 1993 to 1995.

Table 1 – Error parameters obtained for the correlation between SIMAR-44 data and the wave buoy records for the 1993-1995 and 1988-2001 (intermittent) periods, for this study and Pilar et al, 2008, respectively (v – bias; rms – root mean square, Si – dispersion index, r – correlation coefficient, n – number of records).

Source	Location		v	Rms	Si	r	N
This study	Fig. Foz	H_s (m)	0.095	0.477	0.217	0.91	8687
		T_m (s)	0.242	1.109	0.155	0.84	
Pilar et al. (2008)	Fig. Foz	H_s (m)	-0.425	0.725	0.348	0.927	5934
		T_m (s)	-0.349	1.405	0.193	0.859	
	Sines	H_s (m)	-0.095	0.456	0.270	0.905	31646
		T_m (s)	-0.044	1.361	0.208	0.822	

Average stormy days from hindcast analysis were also matched against buoy records compiled by Costa (1994) for the 1986-1993 period (table 2). Results show a quite good agreement at both sites.

Table 2 – Comparison between hindcast and buoy wave data for the observed storm regime at Figueira da Foz and Sines locations.

Average stormy days per year	Buoy	SIMAR-44
Figueira da Foz	19.9	16.7
Sines	9.3	9.0

9.2 Results

The results are presented considering both spatial and temporal storminess variability. Table 3 summarizes modal and storm wave climates along the western Portuguese coast. From these results it is possible to acknowledge the high energetic characteristics of this coastal stretch which is fully exposed to the Northeast Atlantic swell; average wave height is generally slightly above 2 m with storm waves that frequently exceed 10 m. The wave regime at Sines (node 1044052) is influenced by the presence of the Cabo da Roca, to the north, which results in a slightly milder wave regime; however, despite being less frequently affected by storms, storm intensity is similar to other western coastal locations.

Table 3 – Long-term modal and storm wave statistics along the western Portuguese coast.

	Grid Node	1043048	1044052	1041055	1043059	1044061	1044066
Modal	Tp Avg (s)	10.9	11.0	11.0	11.1	11.1	11.1
	Hs (m)	2.3	1.9	2.3	2.2	2.1	2.2
Storm conditions	Hs Max (m)	13.4	14	14.4	13.7	11.9	12.7
	Max Duration (h)	243	138	252	195	192	198
	Average Duration(h)	25	24	27	26	25	28
	Total Days	487	253	556	509	403	593
	Storms per year	10.5	5.6	11.2	10.7	8.7	11.7
	Tp Max (s)	21.4	23.9	23.9	21.6	21.6	21.7

Numerical results of trend analysis for all nodes are represented in table 4, while time series are only displayed for the northernmost node (Espinho – 1044066; Figs 3 to 5).

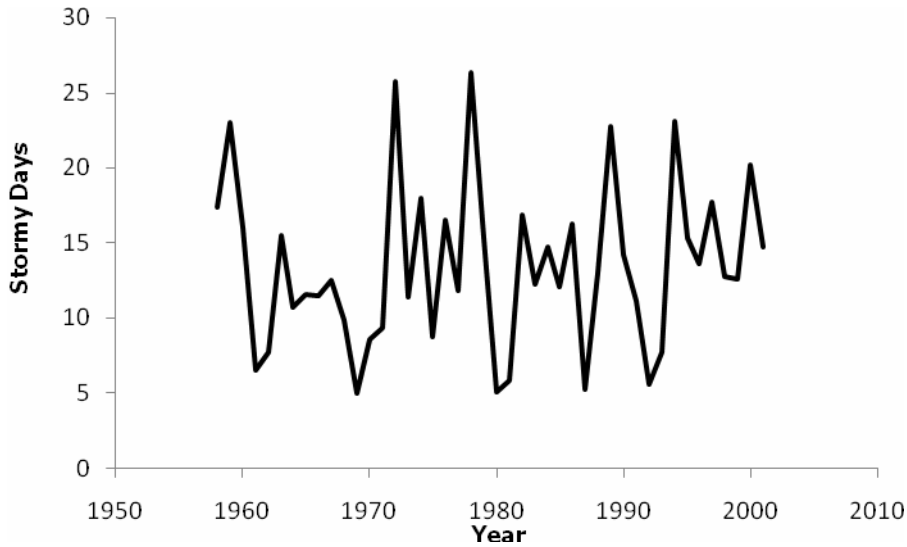


Figure 3. Time series of number of stormy days offshore Espinho (SIMAR-44 1044066 node).

For what concerns the number of stormy days offshore Espinho, values show a relatively large variation with a minimum of 5 days and a maximum of 26 (in 1972 and 1978, respectively). This corresponds to a coefficient of variation, $cv= 0.41$, with the annual average of storm days for the studied period being approximately 13.4 days. Linear regression revealed a non significant positive trend ($y = 0.0414x - 68.505$; $r^2 = 0.0094$).

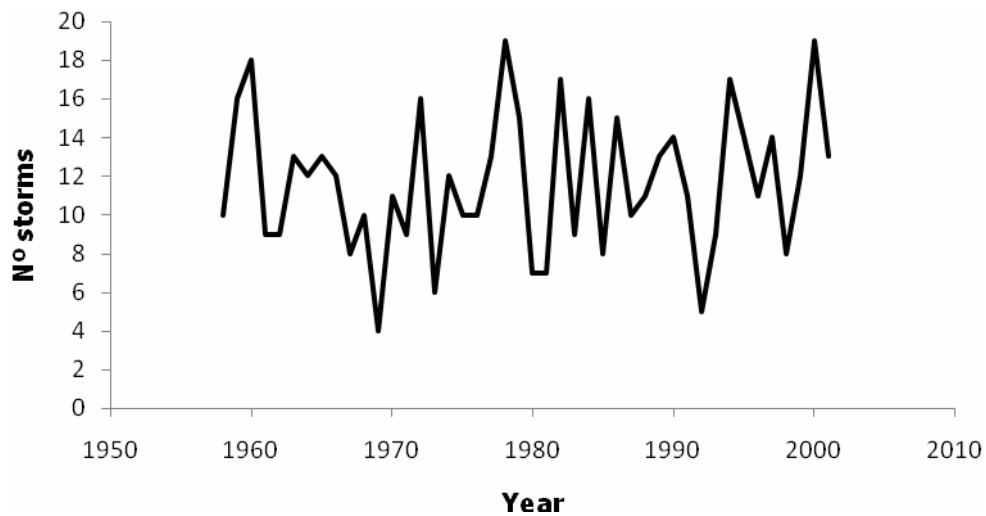


Figure 4. Time series of number of storms per year offshore Espinho (SIMAR-44 1044066 node).

The number of storms has a long term average of about 12 storms per year, with a large interannual variability, ranging from four to nineteen; the lower value occurred in 1969 while the higher values took place in 1978 and 2000. The values here are less scattered; $cv=0.31$. No obvious trend could be identified ($r^2 = 0.0109$).

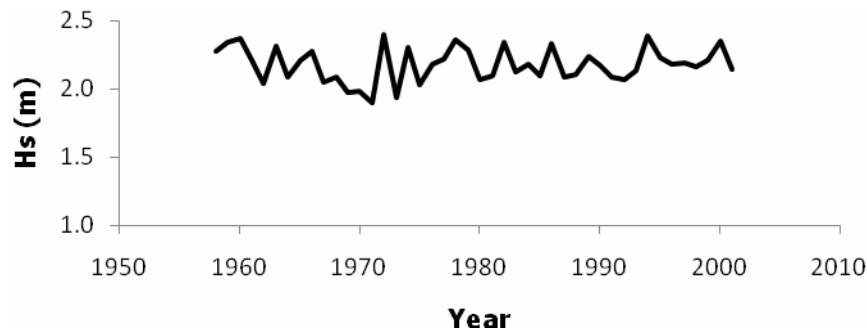


Figure 5. Time series of average wave height offshore Espinho (SIMAR-44 1044066 node).

The average wave height displays an overall mean of 2.2 m, with a relative lower inter-annual variability ($cv=0.06$; values range from 1.9 to 2.4m). Once more, the linear trend shows non significant correlation ($r^2 = 0.0013$).

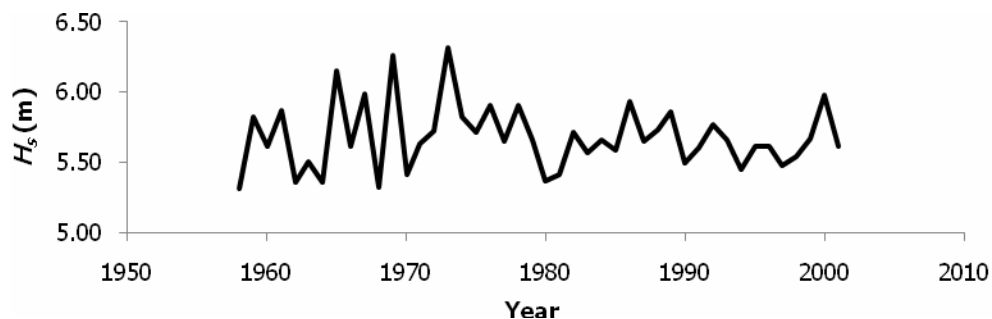


Figure 6.- Time series of average wave height during storms offshore Espinho

For average H_s during storms again there is little variability with values ranging from 5.3 to 6.3m, 5.7m being the average and $cv=0.04$. Again, poor correlation is evident ($r^2=0.0021$).

Table 4 summarizes the regression trends for the temporal evolution of the number of storms, stormy days, and average storm energy, per year, at all sites. Results show very low correlation values for all storm parameters at all nodes, therefore, objectively, there is no reason to support the existence of any long-term trend in the wave storminess along the west Portuguese coast. Nevertheless, it is worthwhile to note that the computed trend displays a different behaviour along the coast; generally the southerly stations (Sines e Sagres) display an opposite trend (for all storm parameters) in comparison to the northerly ones.

Table 4 – Linear regression results for the number of storms, stormy days and average storm energy, per year, at all sites.

Node	Storms/Year		Stormy Days/Year		Storm Energy/Year	
	Slope	r ²	Slope	r ²	Slope	r ²
1043048	-0.0186	0.0041	0.0117	0.001	1.2385	0.0013
1044052	-0.0302	0.0159	-0.0071	0.0007	2.4373	0.003
1041055	0.0016	0.0004	0.0236	0.0037	-1.3809	0.0013
1043059	0.0273	0.0096	0.03	0.0069	-1.1792	0.0145
1044061	0.0325	0.0157	0.0217	0.0046	-1.4852	0.0289
1044066	0.0298	0.0109	0.0414	0.0094	-1.6932	0.0035

The comparison of SIMAR-44 data with published data for the Portuguese northwest coast derived from documentary sources (Andrade et al., 1996; Pedrosa & Freitas, 2008) elicits the following comments.

It was not possible to find any clear correspondence between Andrade et al. (1996) stormy data with the SIMAR-44 hindcast record. This is due not only to differences in the reference time frame, quinquennial intervals in the former case without a clear definition of the intervals timeframe, but essentially to marked differences between the two datasets; for example the noticeable decline in the number of storms from 1960 onwards deduced from documentary records data conflicts with SIMAR-44 data, where at best a very slight negative trend can be observed for the overlapping period. Although the authors try to deduce an arguable positive trend on storm occurrence, inter-annual variability seems to clearly dominate the signal, which concurs with our findings.

The term “Marine Invasion” was used by Pedrosa and Freitas (2008), to describe high magnitude storm events with overwashing and inundation. Assuming that the “Marine Invasions” can be considered a storminess proxy, no consistent trend in storm occurrence was detected. There is a moderate qualitative agreement between the number of marine invasions recorded at Espinho presented by and the storminess obtained from hindcast wave data (fig 9). In the 1960s no marine invasions occurred, which matches a period with milder conditions both in what concerns the number of stormy days and number of storms in the SIMAR-44 data. In 1978 and 1984 a maximum of three episodes of marine invasions were recorded at Espinho; both years correspond to higher than average storminess in SIMAR-44 data. This agrees and extends the conclusions deduced from model data to the middle of XIX century insofar as an absence of trend and the presence of oscillations are concerned.

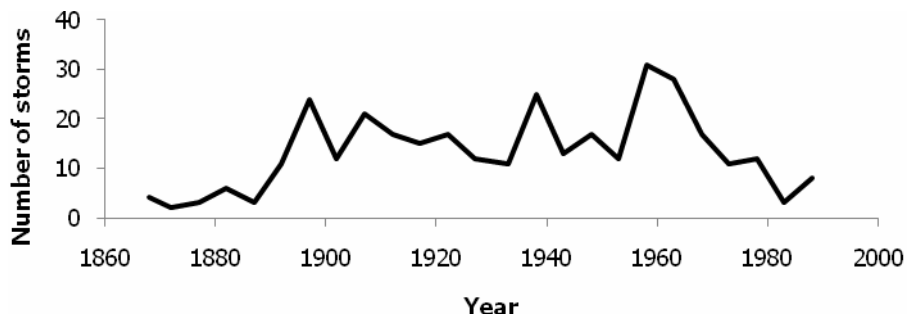


Figure 7. Number of storms in quinquennial intervals obtained through newspaper sources for the north-western Portuguese coast. (Adapted from Andrade et al., 1996)

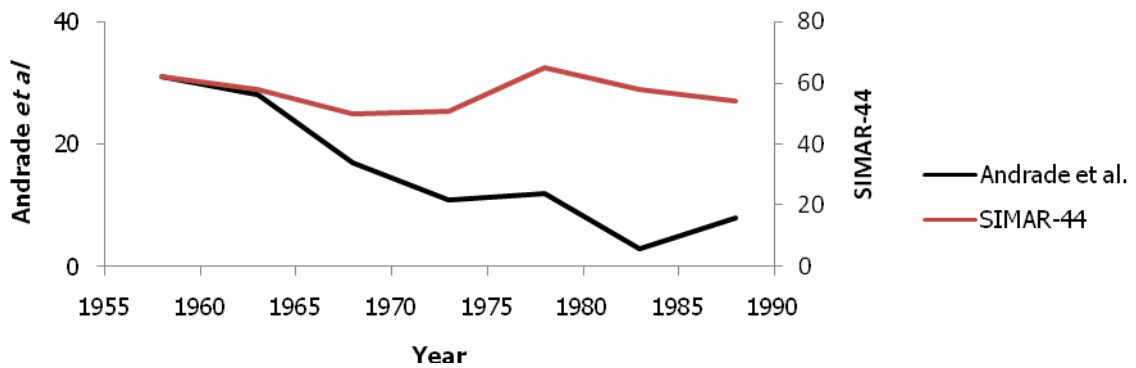


Figure 8. Comparison of number of storms time series offshore Espinho (SIMAR-44 1044066 node) with the number of storms presented by Andrade et al., 1996.

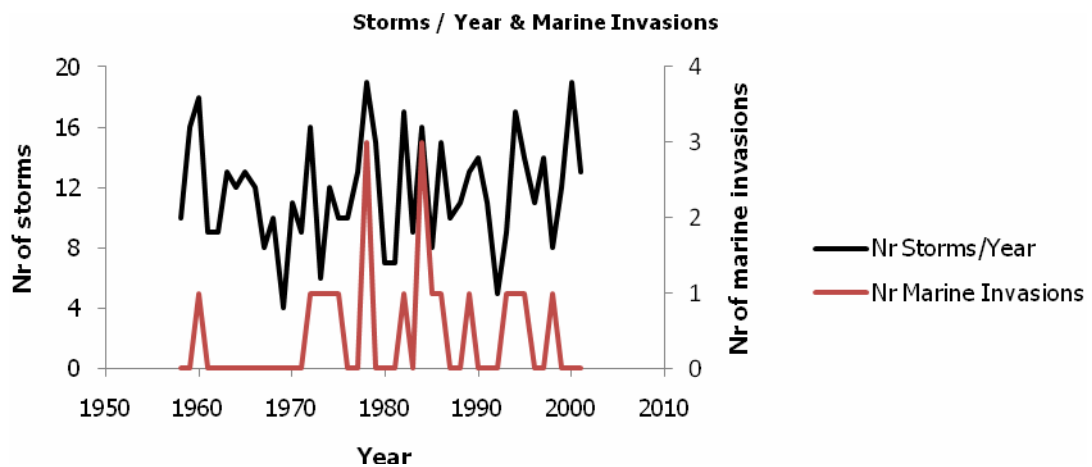


Figure 9. Comparison of number of storms time series offshore Espinho (SIMAR-44 1044066 node) with the number of "Marine Invasions" presented by Pedrosa and Freitas, 2008.

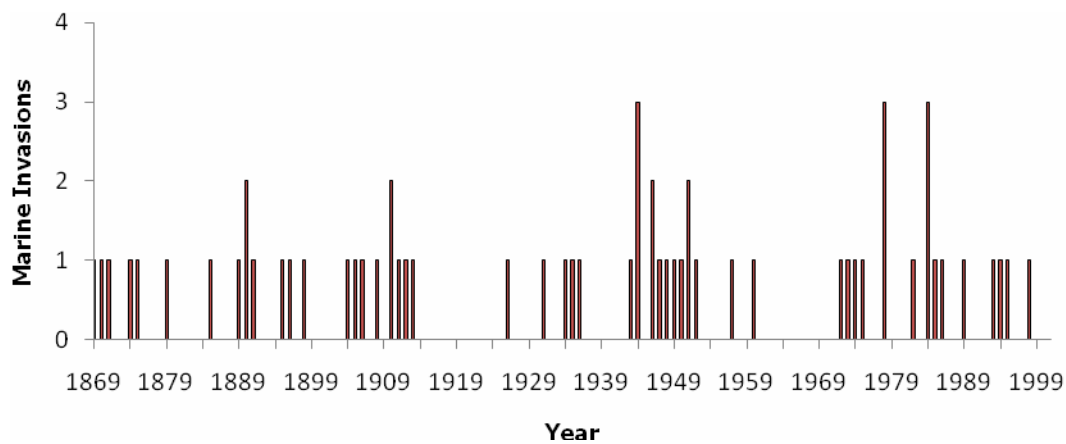


Figure 10. Number of marine invasions in Espinho, adapted from Pedrosa and Freitas, 2008.

9.3 Conclusions

The analysis of hindcast wave data over the last 50 years at the western coast of Portugal showed that storminess has undergone considerable changes, showing significant variations at annual and quasi-decadal timescales, but with no significant trend. The comparison of hindcast data with storminess historical records was inconclusive; nevertheless the analysis seems to support an extension of the former conclusions to the middle of the XIX century. These results are in agreement with the findings of Matulla et al. (2008) for the European storminess.

9.4 References

Andrade, C., Teixeira, S., Reis, R. and Freitas, C., 1996. The record of storminess of the Portuguese NW coast in newspaper sources. In: TAUSSIK, J. and MITCHELL, J. (Eds.), Partnership in coastal zone management. Cardigan, UK, Samara, 159-166.

Costa, M., 1994. Agitação Marítima na Costa Portuguesa, Anais do Instituto Hidrográfico, nº13, 34-40.

Matulla, C.; Schoner, W.; Alexandersson, H; von Storch, H. ; Wang, X. L., 2008. European storminess: late nineteenth century to present, *Climate Dynamics*, 31, 125–130.

Pedrosa, A., Freitas, C., 2008. *Journal of Iberian Geology* 34, 253-270.

Pilar, P., Guedes Soares, C., Carretero, J.C., 2008. 44-year wave hindcast for the North East Atlantic European Coast. *Coastal Eng.* 55, 861–871.

Ponce, E., 2008. Coastal Vulnerability to Storms in the Catalan Coast, PhD thesis, Universitat Politècnica de Catalunya.

10 Portugal-Southern coast

Luis Pedro Almeida, Michalis Vousedoukas and Óscar Ferreira

10.1 Methods

The significant wave height (H_s) from two distinct sources was considered for the present analysis:

- wave measurements obtained from a directional wave rider buoy (see Fig. 1 for location) operated by the Portuguese Hydrographical Institute and located offshore of Sta. Maria Cape (Faro). Data were available from 1995 to 2008 and the acquisition frequency was 3 hours, increasing to 30 minutes when the H_s exceeded 3 m.
- the nearest HIPOCAS project (Hindcast of Dynamic Processes of the Ocean and Coastal Areas of Europe) grid point (Fig. 1) provided wave data from 1958 to 2001, with a time-step of 3 hours.

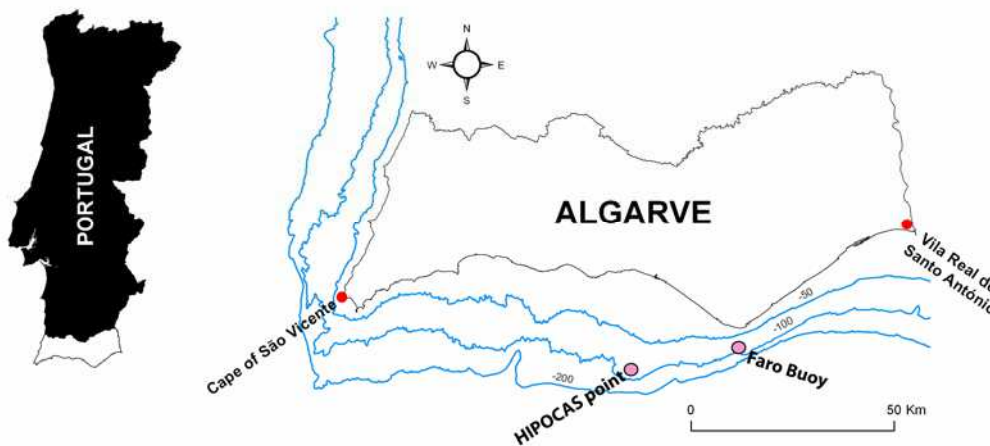


Figure 1. Study area and localization of data sources.

Since the measured data covered only a period of 13 years, which was considered too short for the scope of the present study, the data was also used as ground truth to validate and improve the HIPOCAS estimations.

Storm conditions were considered when the significant wave height exceeded 3 m, according to the definition by Pires (1998) and Costa et al. (2001) while different time thresholds were tested to separate consequent storm events (independence analysis, see Fig. 2). The obtained data (from both series) was then used to analyse changes on the number of storms per year, storm occurrence and wave height from 1958 until 2008 (50 years).

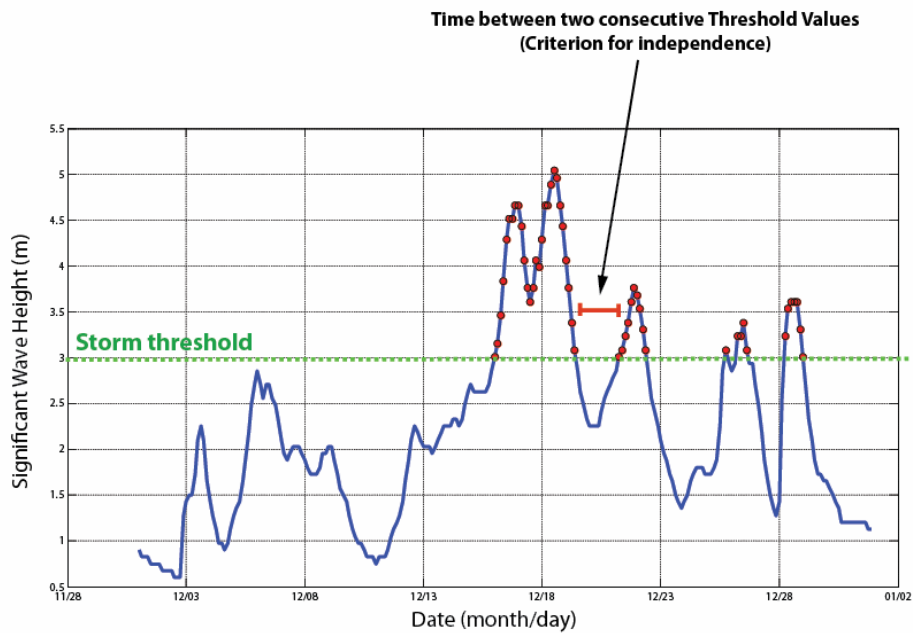


Figure 2. Example of the Storm Threshold and Independence Criterion.

10.2 Results

10.2.1 Validation/modification of Hindcast data (HIPOCAS)

A least square fit was applied between the two datasets and a linear correlation was found and found a statistical significance at 0.01 level, according to which the HIPOCAS data were corrected (see also Figure 3):

$$H_{SO_{HIPOCAS}} = \frac{H_{so_{HIPOCAS}}}{1.33}$$

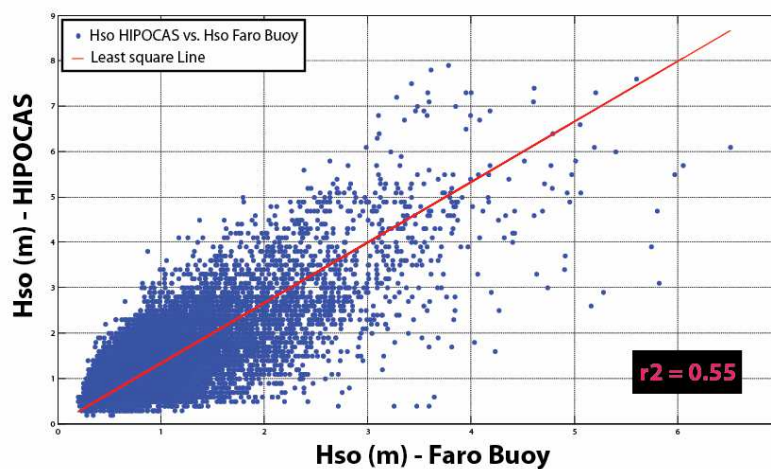


Figure 3. Dispersion Diagram between Faro Buoy and HIPOCAS significant wave height. In the black rectangle is the value of the determinant coefficient (r^2) resultant from this correlation which show significance for 0.01 level

Following the HIPOCAS correction, storm conditions were identified and separated into storm events, considering time limits of 10, 14, 18, 22, 26, 30 and 34 hours. The total number of storms calculated using those different independence classes are shown in Fig. 4 and the results confirmed that the corrected HIPOCAS data have a better agreement to the measured ones than the original data. The classes 10, 30 and 34 hours were the ones that performed better and were considered in the further analysis of both datasets on the grounds of (1) Number of Storms \ Year and (2) Number of Days with Storms \ Year.

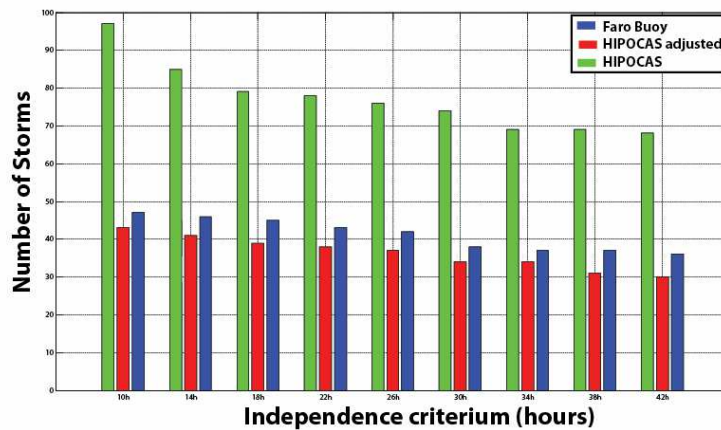


Figure 4. Number of storms vs independence criterion. The green bars represent the HIPOCAS data without the adjustment.

The results again show that the corrected HIPOCAS data show a good agreement with the buoy measurements and the highest correlation is observed for the class of independence criterion of 34 hours (see also Table I). This result is close to the 30 hours chosen by Morton et al. (1997) and Dorsch (2008) for the definition of storm independence criterion.

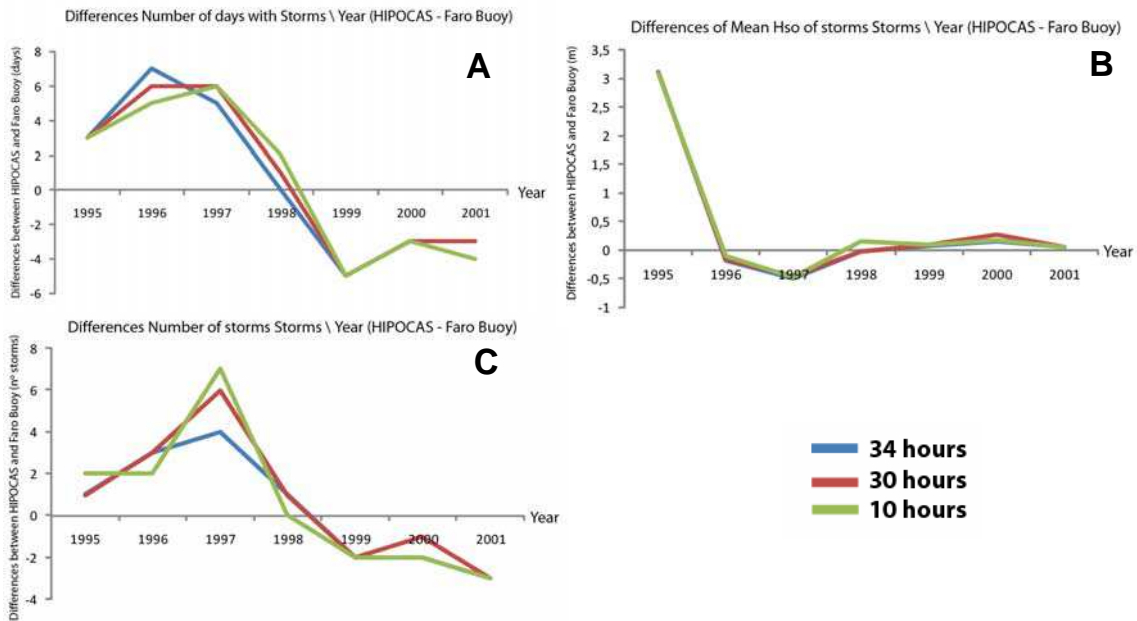


Figure 5. Differences of number of days with storms \ year (A), mean significant wave height of storms \ year (B) and number of storms \ year (B) between HIPOCAS and Faro Buoy using 3 classes of independence criterion (10, 30 and 34 hours).

Table I. Percentage of difference between the sums of the results, using the 34 hours independence criterion.

	HIPOCAS	Faro Buoy	Differences	Percentage (%)
Nº of Days (Total)	72	76	-4	6
Nº of Storms (Total)	34	36	-2	6
Mean Hso of Storms (Mean)	3.49	3.38	0.11	3

10.2.2 Historical Storminess Analysis

Given that the corrected HIPOCAS data seemed to be consistent to measured conditions, the final historical storminess analysis used data from 1958 to 2008, obtained from the concatenation of the (pre-1995) HIPOCAS and Faro buoy datasets.

10.2.2.1 Number of Storms \ Year

The number of storms \ Year series, as well as a moving average are shown in Fig. 6. The data showed a very slightly positive trend showing an increase in one half of a storm in 50 years (Fig. 7), however with no statistical significance for the tested levels ($r^2 = 0.03$ for $p = 0.01$ and 0.05), while Sum of Sin analysis identified two major modes of change: a) a big amplitude one with peaks occurring every 40 years (1963 and 2002), b) a lower amplitude mode with period of ~ 10 years for maxima (1976, 1988 and 1996) and ~ 12 years for minima (1968, 1980 and 1992).

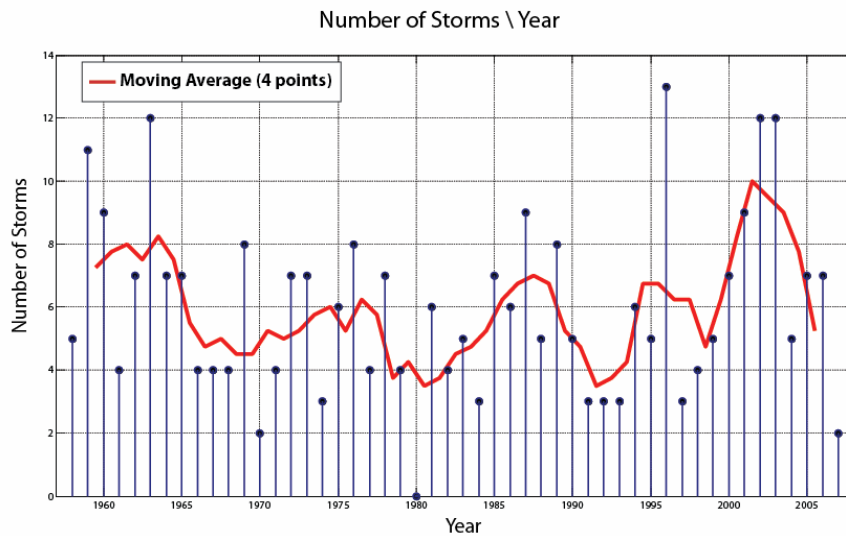


Figure 6. Number of storms \ Year along the entire dataset with a 4 points moving average.

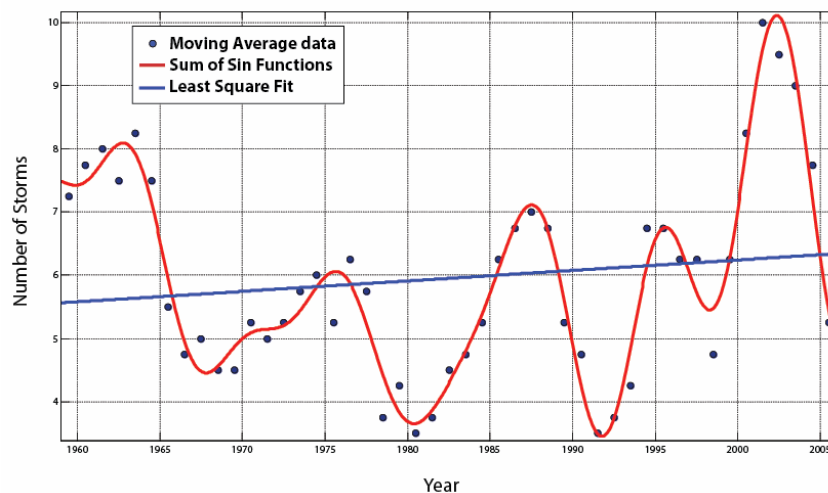


Figure 7. Moving average (4 points) of the Number of storms \ Year along with the fit of two different models, the Least Square Fit and the Sum of Sin functions.

10.2.2.2 Number of days with Storms \ Year

Following a similar approach, the number of days with Storms \ Year series were analysed (Fig. 8 and 9) and again two periods of increased activity were observed on 1962 and 2000. In this case the data showed a general negative trend with a decrease in 2 days in the number of days with storms in 50 years, nevertheless the statistical significance of the correlation (with $r^2 = 0.01$) was tested for 0.01 and 0.05 levels and no significance was obtained.

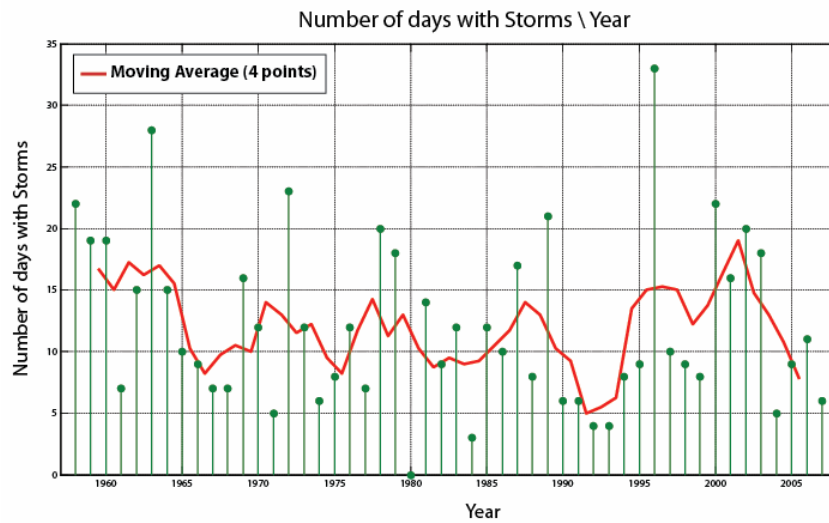


Figure 8. Number of days with storms \ Year along the entire dataset with a 4 points moving average.

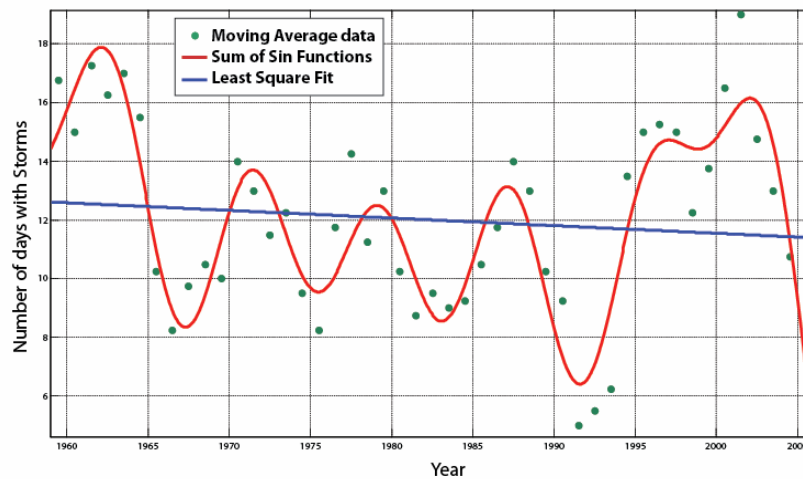


Figure 9. Moving average (? points) of days with storms \ Year along with the fit of two different models, the Least Square Fit and the Sum of Sin functions.

10.2.2.3 Significant Wave Height Trend

Significant wave height exceedence values for each year were estimated considering four different percentiles (50, 80, 99, and 99.8%), and are shown in Fig. 10, along with the moving average lines. The percentile analysis showed that percentiles 50% and 80% lie below 1 m and 1.5 m, respectively not representing storm conditions. Storm conditions (>3 m) correspond to the 99th percentile, while the 99.8th one corresponds to waves over 3.5 m and sometimes reaching more than 5 m.

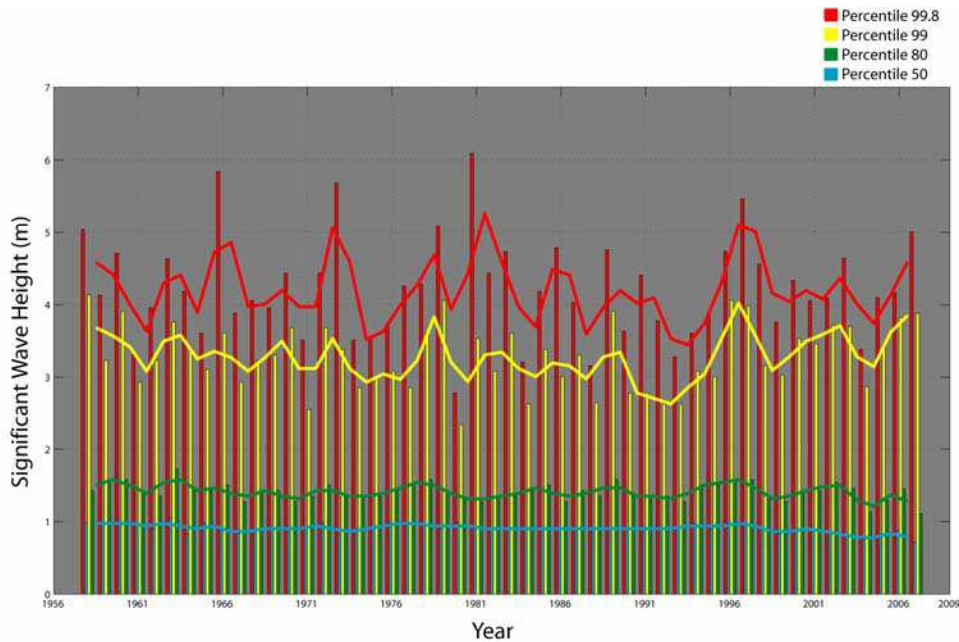


Figure 10. Annual values of significant wave height for the four classes of percentiles (50, 80, 99 and 99.5th). The lines represent the moving average (3 points) of each percentile.

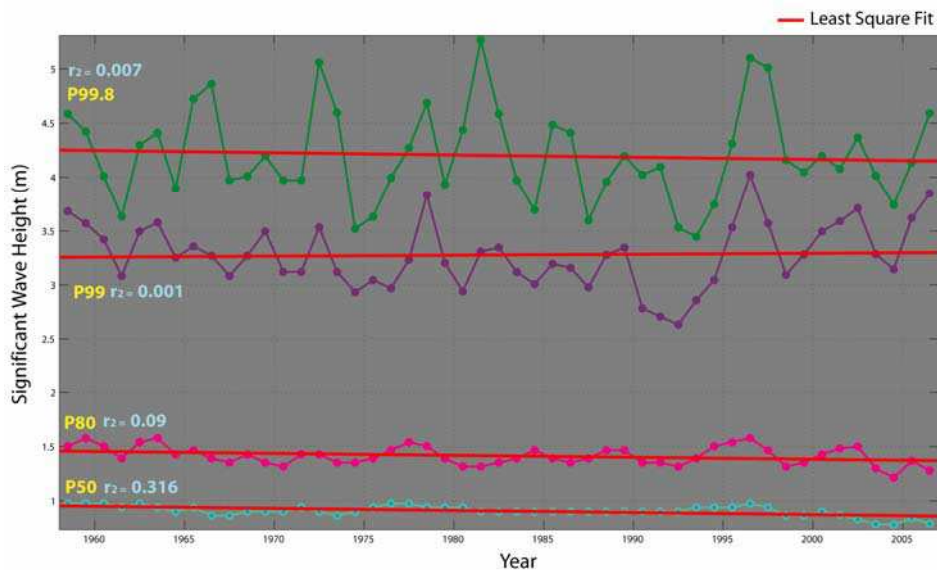


Figure 11. Least square fit computed for the moving average points of each percentile and the value of the determinant coefficient (r^2) for each correlation

Least square fit analysis (Fig. 11) showed that the 50, 80 and 99.8th percentiles showed a negative trend, while the opposite occurred for the 99th percentile value. For each correlation the significance was tested for 0.01 and 0.05 levels and, from all the results, just the 50th percentile show a significant correlation for 0.05 levels. The remains percentiles did not show significance for any of the tested levels.

10.3 Conclusions

The HIPOCAS data were compared and corrected on the grounds of wave measurements from the study area and the corrected values provided robust wave information from 1958 till present.

The conditions defining a storm used for this study were significant wave height exceeding 3 m and a minimum interval between storms of 34 hr.

From all the trends computed just the percentile 50th of the significant wave height show significance for the 0.05 level, showing a decreasing in 0.2m in 50 years. The remains trend analyzes did not show significant results for the tested levels (0.05 and 0.01) however a descriptive interpretation of the results allow the verification different cycles with a general trend of a decrease in the number of storms by year and a decrease in the days with storms in the last 50 years.

10.4 References

Costa, M., Silva, R. and Vitorino, J., 2001. Contribuição para o estudo do clima de agitação marítima na costa portuguesa. Proceedings of 2ª Jornadas Portuguesas de Engenharia Costeira e Portuária, International Navigation Association PIANC, Sines, Portugal.

Dorsh, W., Newland, T., Tassone, D., Tymons, S. and Walker, D., 2008. A statistical approach to modelling the temporal patterns of ocean storms. *Journal of Coastal Research*, 24(6):1430-1438.

Morton, I. D., J. Bowers, and G. Mould. 1997. Estimating return period wave heights and wind speeds using a seasonal point process model. *Coastal Engineering* 31:305–326.

Pires, H.O., 1998. Preliminary Report on the wave climate at Faro – Project INDIA. Instituto de Meteorologia – Instituto Superior Técnico, pp. 37.

11 Spain-Atlantic Andalusia

Pedro Ribera, D. Gallego, and C. Peña

11.1 Introduction

Cádiz is located in the southernmost area of the Iberian Peninsula (Fig. 1) with its coast facing the Atlantic Ocean. It has been widely demonstrated that storms over this region, as much as over most of the western half of the Iberian Peninsula, are closely related to low pressure systems coming from the Atlantic between October and March (Trigo et al., 2002; Trigo et al., 2004; Trigo, 2006; Gallego et al., 2007). On a multi-annual scale, the North Atlantic Oscillation (NAO: Hurrell, 1995 and 1996) dominates the atmospheric variability over the area. When the NAO is on its positive phase (higher than normal pressure over the Azores and lower than normal pressure over Iceland) winters in the Cadiz area are dryer than normal and paths of active systems are deviated towards higher latitudes. During NAO negative phases, the opposite situation is found, and winters are usually stormier in Southern Europe (Hurrell, 1995).

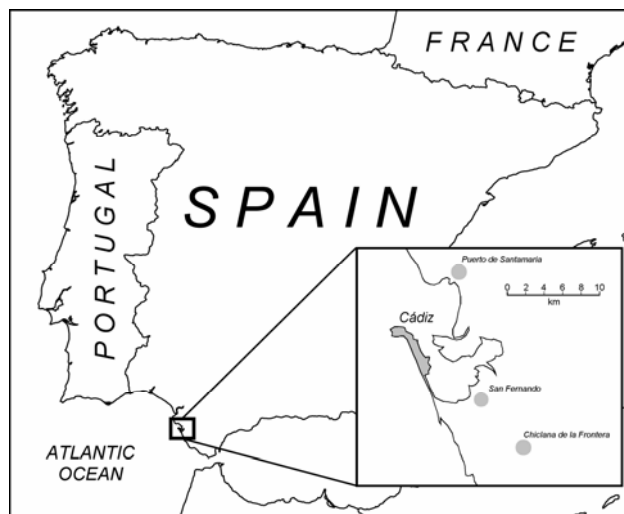


Figure 1. Location of Cadiz

11.2 Data and methods

In order to characterise the occurrence of storms in Cadiz two different data sources were used:

- Wave height data were taken from the HIPOCAS database (HIIndcast of dynamic Processes of the Ocean and Coastal Areas of Europe). These data stem from high resolution numerical modelling and they are considered the best available source for long term wave data (Guedes et al. 2002). We choose the nearest grid-point to Cadiz and selected the significant wave height (H_{m0}) as the parameter to represent the

strength of the storm. HIPOCAS data have been used at daily scale and they cover the period 1958-2001.

- In order to reconstruct the number of storms for years prior to 1958 (starting of the HIPOCAS data), wind records from the ICOADS database (International Comprehensive Ocean-Atmosphere Data Set) have been used. This database consists of millions of individual marine wind observations covering the entire globe. We selected those records inside the square represented in Fig. 2 and computed the wind averages on a daily basis. The square was chosen to represent the atmospheric disturbances coming from the west related to storm occurrence in Cadiz. The ICOADS database covers the period 1850-2008. The 20th Century is well represented with the exception of the World War I and II years. For years prior to 1902, the number of wind record is significantly reduced but still valuable up to 1880.

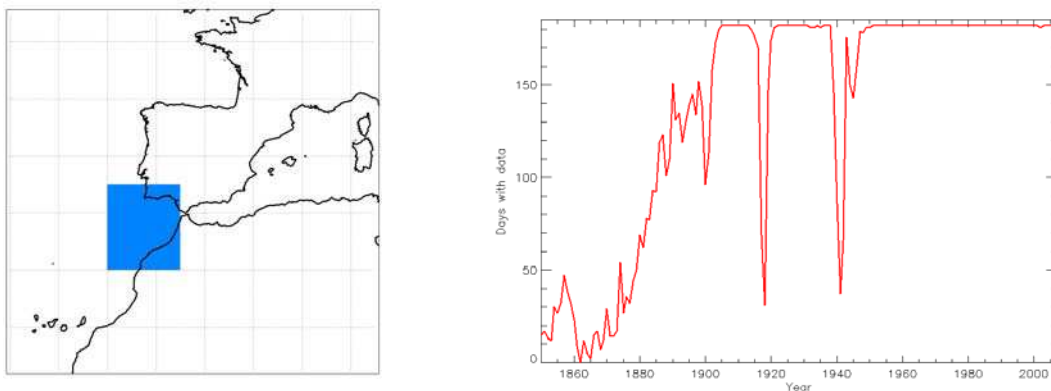


Figure 2. Area selected to compute wind averages from the ICOADS database (left) and number of winter (October-March) days with ICOADS wind observations inside the selected square (right).

11.3 Results

11.3.1 Storm definition

The storm threshold used by the Spanish National Port Authority for instrumental data from the coastal buoy in Cádiz is a wave height equal or higher than 1.5 meters. This limit, notwithstanding, is rather low and occurs for more than 10% of the year. To assess the storm definition criterion, five different storm categories (1 to 5) were defined using percentiles 90, 92, 94, 96 and 98 of the HIPOCAS wave height series, which corresponded to wave heights of 1.8 m, 2.0 m, 2.2 m, 2.5 m and 3.1 m respectively. The limit of 1.5 m will be denoted as “category 0”.

Table 1 shows the correlation coefficients between the total number of storm stratified by categories and the ICOADS wind for the winter months. Clearly, the maximum correlation between wind and wave height is observed for westerly winds. Storm categories 0 to 2, when

wind comes from the west, are well correlated with wind intensity, being characterized by correlation coefficients higher than 0.6. For category 0 storms, almost 46% of the total wave height variance is explained by the wind and the percentage of the variance explained for category 2 storms is very close to 40%. Storms for winds from the North and East seem to be rather independent from wind speed, while storms when the wind blows from the South are in an intermediate level, with correlation coefficients near 0.5. It must be stressed that while wind and wave height are significantly correlated, the level of explained variance is not enough to allow the reconstruction of individual storm events at daily scale.

*Table 1. Pearson correlation coefficient between storm days series and wind speed series with data for winter months. Correlation coefficients are not included if less than 20 storm days were identified. Correlations statistically significant at $p < 0.01$ and $p < 0.05$ are indicated by ** and * respectively.*

	Cat. 0	Cat. 1	Cat. 2	Cat. 3	Cat. 4	Cat. 5
East	0.31**	0.25**	0.26*	0.24	---	---
South	0.54**	0.52**	0.48**	0.49**	0.52**	0.49**
West	0.68**	0.64**	0.63**	0.59**	0.56**	0.52**
North	0.29**	0.34**	0.34**	0.29*	0.46*	---

Concerning to the total number of storms, table 2 shows that most storms occur when wind blows from the west and that the proportion increases for higher categories. But even more interesting is that winter storms represent between nearly the 80% and more than 90% of the yearly storms, depending on the category (table 2, last line).

Table 2. Number of storms as a function of the storm category and wind direction (October to March). The last line includes the relationship between winter storms and annual storms when wind comes from the West (it is expressed as a percentage of the annual number of storms).

	Cat. 0	Cat. 1	Cat. 2	Cat. 3	Cat. 4	Cat. 5
East	354	150	80	43	15	3
South	480	339	256	199	133	58
West	1143	920	744	604	443	242
North	357	157	95	51	23	4
W / (E+S+N)	0.96	1.42	1.73	2.06	2.59	3.72
W winter storms (%)	78.88	83.26	85.52	88.30	90.04	92.02

11.3.2 NAO relationship

As discussed in the introduction, the NAO exerts a strong influence over the storm track across Southern Europe. Any analysis of storm occurrence in Cadiz must take into account this pattern. Table 3 shows the correlation coefficients between the NAO and the storm series during south and westerly wind episodes. The NAO modulation is rather constant for storm categories 0 to 3. The strongest storms, categories 4 and 5, seem to be less correlated to the NAO. For wind coming from the west, the greater correlation with the NAO is reached for storms of category 1 ($r = -0.62$), the correlation slowly decreases for greater categories, with

values of -0.49 and -0.38 for categories 4 and 5 respectively. Results for the annual number of storms are very similar (table not shown).

*Table 3. Pearson correlation coefficient between series of stormy days and the NAO for winter months. Correlation coefficients are not included if less than 20 storm days were identified. Correlations statistically significant at $p < 0.01$ and $p < 0.05$ are indicated by ** and * respectively.*

	Cat. 0	Cat. 1	Cat. 2	Cat. 3	Cat. 4	Cat. 5
South	-0.39**	-0.36**	-0.37**	-0.32**	-0.29**	-0.26*
West	-0.59**	-0.62**	-0.57**	-0.54**	-0.49**	-0.38**

11.3.3 Transfer function

These previous results show that the vast majority of the winter storms in Cadiz are related to westward winds. In addition, these winds are those with the strongest relation between wave height and wind. Moreover, the NAO exerts a strong modulation over the number of storms coming from the west. All the above justify the reconstruction of the number of storm days by constructing a transfer function between wind and wave height according to the following steps:

- Adjust the transfer function for the days with westward wind occurrence.
- Adjust the transfer function for the cold season (October to March).
- Adjust the parameters of the transfer function independently for NAO positive and negative years.
- Use annual scale to convert wind force into number of storms (the level of wave height variance explained by the wind shown in tables 4 and 5 makes it not possible to reconstruct individual storm events).

It should be remembered that table 2 indicates that the winter storms originating from westward winds (those with greater coastal impact and more related to the wind) constitutes the vast majority of the storms in Cadiz. This predominance increases as larger storm categories are considered (see last row in table 2). Additionally, the comparison of a three years period of observed data for Cadiz and the HIPOCAS data shows a good agreement between wave height in HIPOCAS and in the observed data, even when HIPOCAS produces a slight underestimation of real data (Medina-Santamaría et al., 2004). As a compromise, in subsequent analysis, we have chosen the category 2 as the threshold for storm occurrence in HIPOCAS data. This corresponds to a significant wave height larger or equal to 2.0 m.

A quadratic adjustment of the HIPOCAS wave height as a function of the ICOADS wind speed was performed after calibration using the values from the common period HIPOCAS-ICOADS 1958-2001. A different set of parameters was computed for NAO negative and positive years. Fig. 3 shows the comparison between pure HIPOCAS data (1958-2001, dark blue) and the reconstruction using the transfer function (1850-2008, light blue) for the category 2 storms.

Shaded areas indicate the percentage of missing data for wind (same as Fig. 1). With the exception of the World War I and World War II periods, almost the entire 20th Century is well represented. The years corresponding to the 19th century are not well represented because of the high percentage of missing wind data, so the reconstruction is dubious from 1880 to 1902 and essentially unusable before the year 1880.

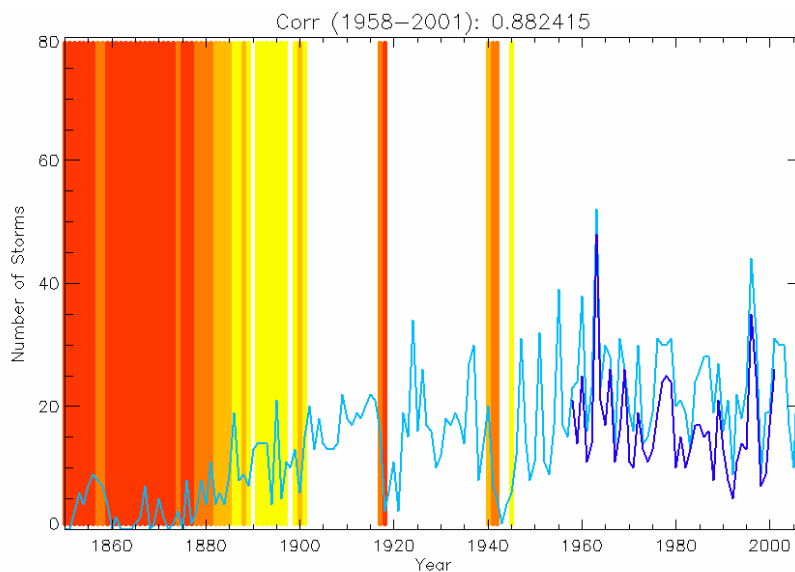


Figure 3. Number of winter storms estimated from wind speed (light blue) between 1850 and 2008. HIPOCAS data (1958-2001) is also shown (dark blue). Shaded areas indicate the percentage of missing wind data in 20% intervals, no shadow indicates lower than 20% of missing data and increases from yellow to red).

The transfer function has a very good performance, as suggested by the HIPOCAS and reconstructed series correlation ($R=0.88$, $p<0.01$) for the calibration period. However the transfer function tends to overestimate the number of storms. In this sense, while the reconstruction captures very accurately the interannual variability, the estimation of the absolute number of storms should be used cautiously.

Fig. 4 shows a moving trend analysis for several periods ending in 2008 and starting from 1902 onwards for the reconstructed series. When the entire series is considered (i.e. the 20th Century), a significant ($p<0.01$) but small increase in the number of storms (between 1 and 1.5 storm / decade) is found. However, when the trends are computed for periods starting in the 1950's and 60's a negative tendency in the number of storms per year is evident. This decrease is not statistically significant due both to the shorter period of study and to the evident increase in the interannual variability on the number of storms (see the last 40 years of the series of the number of storms in Fig. 3 both for HIPOCAS and reconstructed data). The increase in variability is displayed not only for the HIPOCAS data but for the reconstructed series from 1960 onwards. When the trend of the number of storms is computed using only HIPOCAS data (dark blue line in Fig. 3, 1958-2001 period) the trend is -0.12 storms/year (not

statistically significant), in very good agreement with the reconstructed series for the same period.

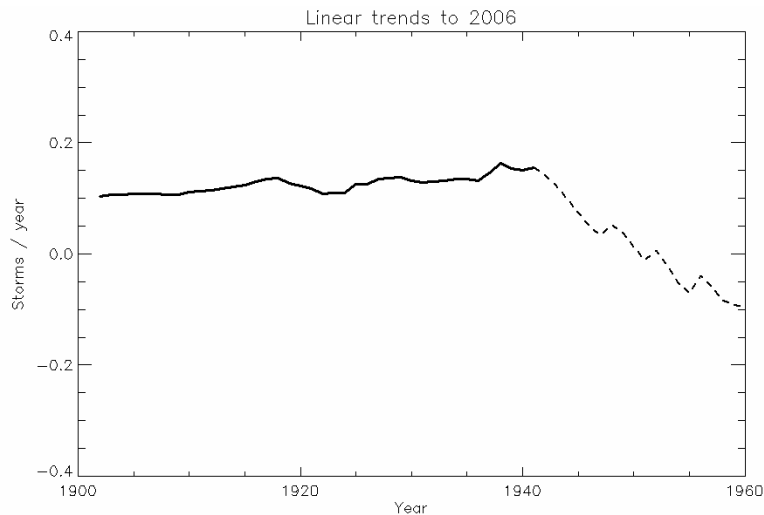


Figure 4 moving trends of the reconstructed wave height series for different periods all ending in 2008. x-axis indicates the first year of the period used to compute the trend. The last x-axis value of 1960 indicates the 1960-2008 trend. Significant trends ($p < 0.01$) are indicated by continuous and thicker line.

11.4 Summary

From this analysis, a number of conclusions can be summarised as follows.

The storms in Cadiz are clearly related to westward wind component. The transfer function between wave height and storms was done for the westward winds.

For HIPOCAS data in Cadiz, an adequate threshold for storm occurrence corresponds to the 92nd percentile of the significant wave height (H_m0) distribution. This corresponds to $H_m0 = 2.0$ m (0.5 m higher than the conventional 1.5 m limit for buoy data in Cadiz).

In Cadiz, it is not recommendable to use the relationship between wind force and wave height to reconstruct individual storm events. Although it has been evidenced that wind and wave height are closely related, the variance of the wave height explained by the wind is not enough to achieve this goal.

However, the total number of storms per winter can be well simulated by using a transfer function to convert average daily wind observations into the number of storms per year. Interestingly, the trend in the annual number of storms is very accurately reproduced for the calibration period so we can be confident in the reconstruction of the tendencies for the entire 20th Century.

Due to the presence of missing data, the reconstruction for period 1880-1902 should be cautiously interpreted. However, compared to the 20th Century, this period is characterised by a very low number of storms (see Fig. 3).

While the HIPOCAS data shows a decreasing trend in the period 1958-2001 (not statistically significant), when the reconstruction for the entire 1902-2008 is analysed it becomes evident that along the entire 20th Century a slight, but significant increase (1 to 1.5 storms per decade) in the annual number of storm has occurred.

11.5 References

Gallego D., García-Herrera R., Calvo N. and Ribera P., 2007. A new meteorological record for Cadiz (Spain) 1806-1854. Implications for climatic reconstructions. *J. Geophys. Res.*, 112 (D12108).

Guedes Soares, C., Weisse, R., Alvarez, E. and, Carretero J.C., 2002. A 40 Years Hindcast in European Waters, Proceedings of the 21st International Conference on Offshore Mechanics and Arctic Engineering (OMAE 2002), ASME (2002) Paper OMAE2002-2860.

Hurrell, J.W., 1995. Decadal trends in the North Atlantic Oscillation: regional temperature and precipitation'. *Science, New Series*, 269, 5254, 676-679.

Hurrell, J.W., 1996. Influence of variations in extratropical wintertime teleconnections on Northern Hemisphere temperature. *Geophys. Res. Lett.*, 23, 6, 665-668.

Medina-Santamaría R. et al., 2004. Impactos en la costa española por efecto del cambio climático. Fase I: evaluación de cambios en la dinámica costera española. Fase I A: recopilación de información. Technical Report. OECC - Ministerio de Medio Ambiente.

Trigo I.F. 2006. Climatology and interannual variability of storm-tracks in the Euro-Atlantic sector: a comparison between ERA-40 and NCEP/NCAR reanalyses'. *Climate Dynamics*, 26: 127-143. DOI 10.1007/s00382-005-0065-9.

Trigo R.M., T. J. Osborn, J. M. Corte-Real, 2002. The North Atlantic Oscillation influence on Europe: climate impacts and associated physical mechanisms'. *Climate Research*, 20: 9-17.

Trigo R.M., D. Pozo-Vazquez, T.J. Osborn, Y. Castro-Diez, S. Gamiz-Fortis and M.J. Esteban-Parra, 2004. North Atlantic Oscillation influence on precipitation, river flow and water resources in the Iberian Peninsula. *Int. J. Climatol.* 24: 925-944.

12 Spain-Catalan coast

José A. Jiménez and Eva Bosom

12.1 Introduction

One of the potential effects of climate change on our coasts is the increase in wave storminess. This could produce an increase in the frequency and intensity of induced hazards such as erosion and inundation events, especially in sensitive coastal zones. Within this context, the main aim of this chapter is to identify and characterise the time evolution of storminess along the Catalan coast (NE Spanish Mediterranean).

The structure of the report is as it follows: (i) subchapter 12.2 presents an overview of the study area and the data used; (ii) subchapter 12.3 describes how storminess is measured; (iii) results are shown in subchapter 12.4 and, finally; (iv) subchapter 12.5 briefly states the main findings.

12.2 Study area and Data

The Catalan coast is located in the NE Spanish Mediterranean (Fig. 1). It is about 700 km long and it comprises a large variety of coastal types such as cliffs, large bays, deltas, embayed beaches and long sandy beaches.

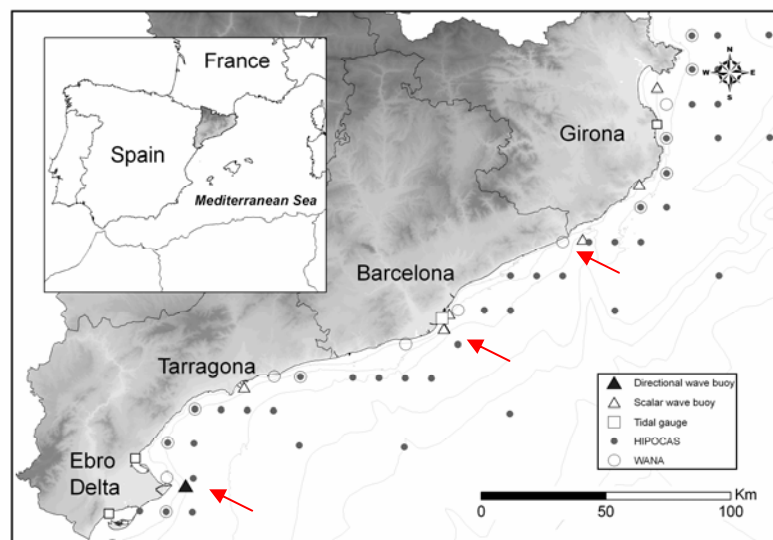


Figure 1. Area of study (arrows indicate wave buoys used in this study). Dots indicate the distribution of hindcasted (HIPOCAS) data "points" in the area.

Main wave data used to characterize storms were obtained from records of a wave buoy network, XIOM (www.boiescat.org) along the Catalan coast. In this work we have selected data recorded by buoys deployed at three locations to characterize the spatial variability of storm wave conditions along the coast: Tordera delta at the N, Llobregat delta at the central part and Ebro delta at the S (Fig. 1). Since recorded wave time series are relatively short to make a

reliable trend analysis (first records were obtained in 1984 –Tordera and Llobregat- and 1990 - Ebro-), they were supplemented with hindcasted data. These simulated data were obtained within the framework of the HIPOCAS project (Guedes Soares et al. 2002) and they cover the period from 1958 until 2001. The combination of both datasets provides the opportunity to perform a significant analysis of the time evolution of storminess in the area since they jointly cover a period of 50 years, from 1958 to 2008.

The main problem of combining measured and modelled data is to assess whether they are equivalent or not. As an example, Fig. 2 shows a comparison of simultaneous recorded and modelled –hindcasted- data in the Ebro delta area. As it can be seen clearly, although they are related, there is a huge dispersion in such a way that, for a given hindcasted H_s value any recorded H_s can be found. When we restrict the comparison to storm conditions, although the dispersion decreases, is still significant (Fig. 2).

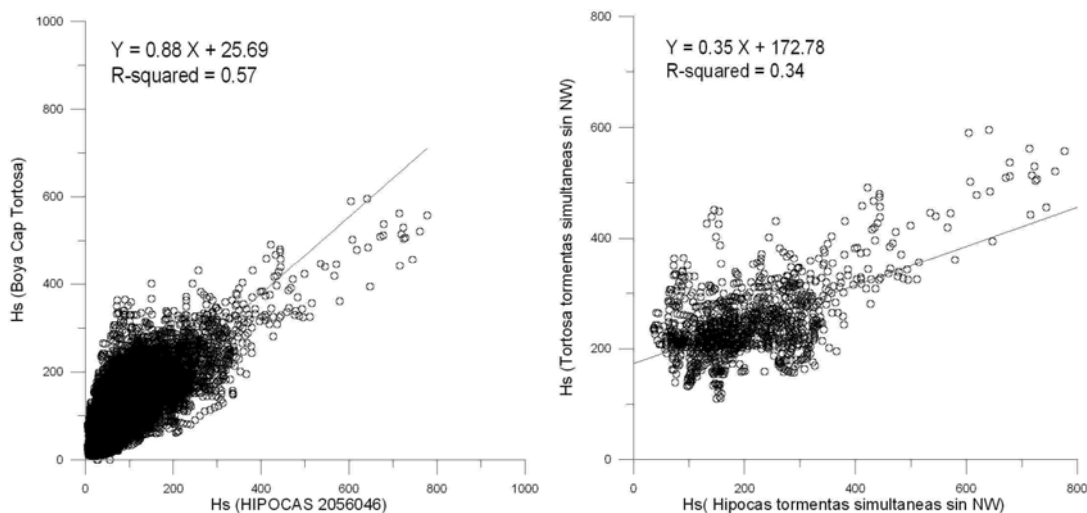


Figure 2. Comparison of simultaneously measured and hindcasted (HIPOCAS) wave data in the Ebro delta area (left: all wave conditions, right: stormy conditions – $H_s > 1.5$ m-).

Thus, before applying any trend analysis to wave conditions it is necessary to build consistent time series in such a way that analyzed data will not be conditioned by its origin.

Due to this, we performed a calibration of HIPOCAS data to obtain an uniform storm time series covering the period 1958-2008. In essence, the procedure was to identify for each location, periods of time simultaneously covered by observational and hindcasted data. The first step was to identify simultaneous wave data defining storms in both time series which are then used to calibrate the hindcasted wave parameters (H_s at the peak of the storm, associated T_p , and storm duration, τ). It has to be stressed that without this calibration the time evolution of wave characteristics should be restricted to periods covered by homogeneous data, i.e. HIPOCAS data from 1958 to 2001 and buoy records from 1984/1990 until present. The analysis presented here corresponds to reconstructed (calibrated +recorded) wave parameters unless otherwise specified.

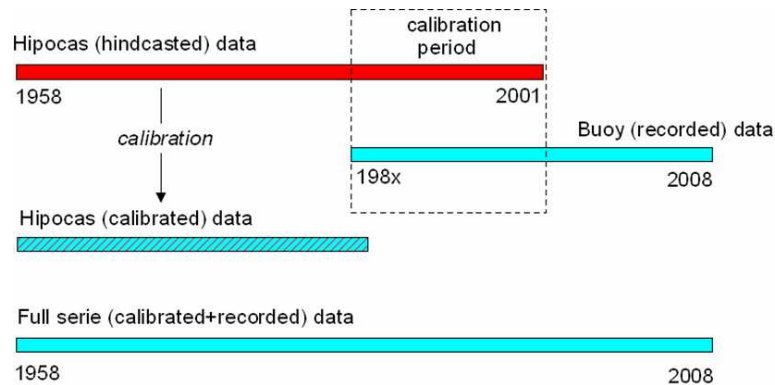


Figure 3. Procedure for building time series for trend analysis.

A storm is defined here as the wave event during which H_s exceeds a threshold value of 2 m during a minimum period of 6 hours. These values were recommended by Mendoza and Jiménez (2006) to define storms inducing a measurable coastal morphodynamic response.

For the purpose of this analysis, we characterize storminess by means of the characteristics of the annual maximum wave storm (H_s , T_p , θ , τ) of the corresponding climatic year, defined as the period from September 1st of a given year to August 31st of the following one. We implicitly assume that the annual maximum storm can be used as a proxy of the maximum potential induced hazards of the current year. Once characteristics defining annual maximum storms (H_s , T_p , τ) are identified in both simultaneous time series, they are compared by means of linear regression. In this procedure, HIPOCAS data is taken as the independent variable and recorded data is the dependent one. This results in a set of linear equations that are used to convert each parameter (H_s , T_p , τ) in the HIPOCAS storm dataset to “real” data. After that, the entire time series is reconstructed by adding the HIPOCAS calibrated storms to values extracted from the recorded time series.

12.3 Storminess variables

To analyze the time evolution of storminess we have selected two set of parameters: (i) those characterizing the wave storm properties and, (ii) those characterizing the storm-induced hazards.

12.3.1 Wave variables

The basic variables used to characterize storminess along the Catalan coast are wave parameters defining the annual maximum storm: H_s at the peak of the storm, T_p associated to H_s , θ wave direction at the peak of the storm and τ , the storm duration ($H_s > 2$ m).

12.3.2 Storm-induced hazards

To characterize storm-induced hazards we have selected the three main induced morphodynamic processes during storm impacts: beach profile erosion, inundation and sediment transport potential.

12.3.2.1 Beach profile erosion

The storm-induced beach profile erosion potential is parameterized following Mendoza and Jiménez (2006) who related the storm-induced eroded volume due to the impact of a storm to a simple predictor, $JA \cdot \tau$, where JA is a parameter characterising beach profile changes proposed by Jiménez et al. (1993) and τ is the storm duration.

$$\Delta V \propto JA \tau \propto \left(|D - D_{eq}|^{0.5} \tan \beta \right) \tau \quad (1)$$

where D is the dimensionless fall velocity parameter (Dean, 1973), D_{eq} is its value at equilibrium, $\tan \beta$ is the beach slope and τ is the storm duration. Since here we are mainly interested in quantifying the storm contribution to beach erosion (whatever the characteristics of the beach will be), we restrict the parameter BE to storm wave variables, i.e.

$$BE = \sqrt{H/T} \tau \quad (2)$$

12.3.2.2 Beach inundation

The storm-induced inundation potential is parameterized in terms of the wave-induced run-up during the peak of the storm. To do this, we use the run-up formula proposed by Stockdon et al (2006) which is given by

$$Ru_{2\%} = 1.1 \left(0.35 \tan \beta (H_s L_0)^{1/2} + \frac{(H_s L_0 (0.563 \tan \beta^2 + 0.004)^{1/2})}{2} \right) \quad (3)$$

Again, since here we are mainly interested in quantifying the storm contribution to inundation (whatever the beach slope will be), we restrict the parameter to storm wave variables, i.e.

$$I = \sqrt{HT^2} \quad (4)$$

12.3.2.3 Sediment transport

The sediment transport potential during the storm has been parameterized in terms of the cumulative wave power during the storm, which, after removing all the constants in the formulation can be written as

$$TP = H^2 T \tau \quad (5)$$

12.4 Results

Figures 4, 5 and 6 show the time evolution of the main wave variables defining the maximum annual storm for each site. The existence of any long-term trend was analysed through linear regression by the least squares method using wave parameters (H_s , T_p , τ) as dependent variables and time as the independent one. Obtained results are shown in table 1, where it can be seen that none of the calculated trends are statistically significant, i.e. according to these data, no long-term (decadal) trend in annual maximum storm conditions along the Catalan coast can be detected during the last 50 years.

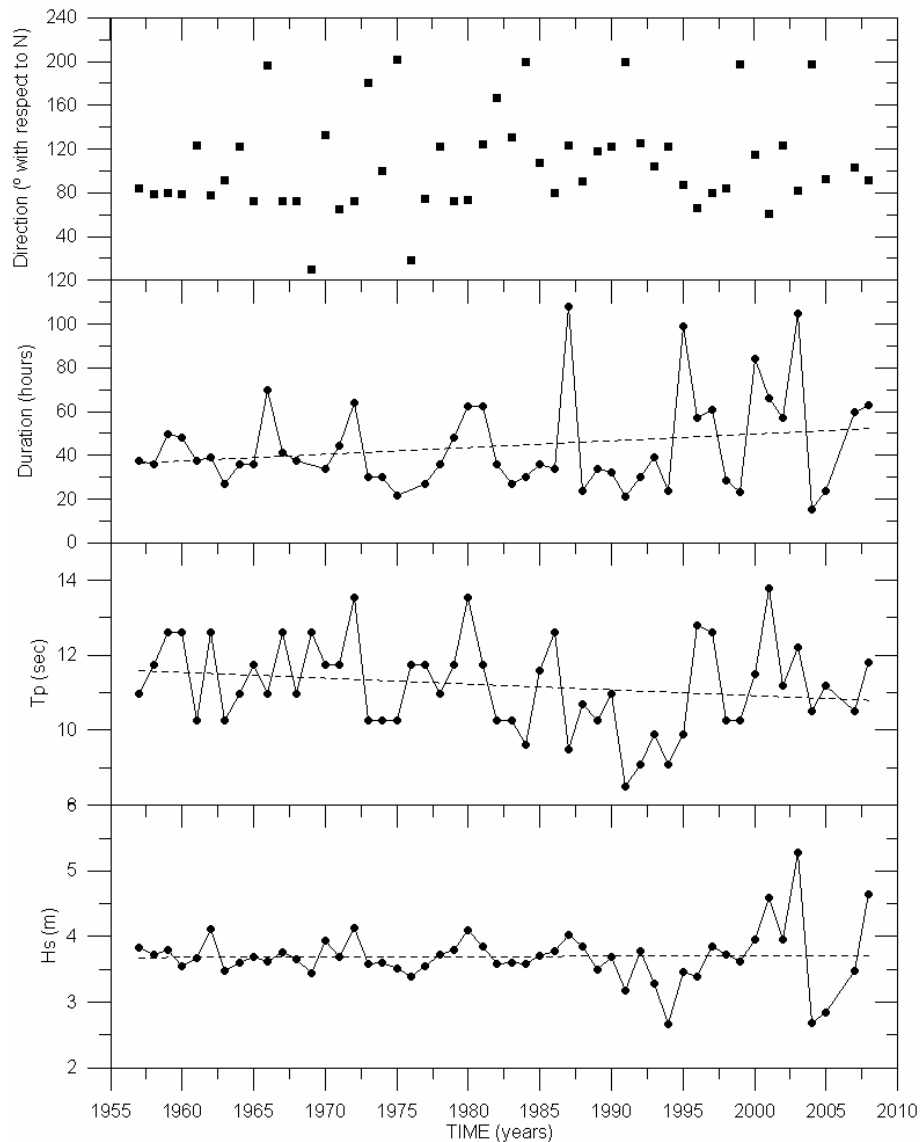


Figure 4. Long-term variations of wave variables defining the annual maximum storm at the Tordera delta during the period 1958-2008 (main trend analysis parameters are shown in table 1).

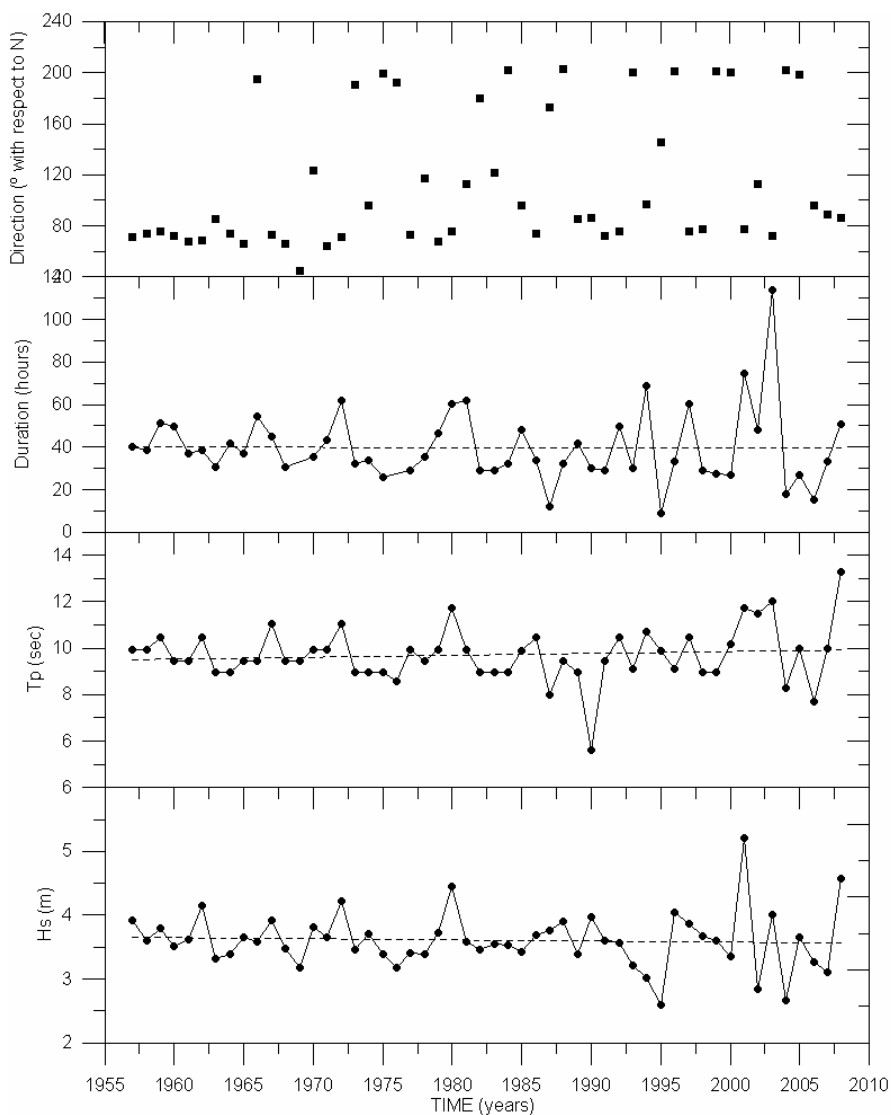


Figure 5. Long-term variations of wave variables defining the annual maximum storm at the Llobregat delta during the period 1958-2008 (main trend analysis parameters are shown in table 1).

Table 1. Trend analysis of wave variables defining the annual maximum storm for each site during the period 1958-2008. Slope is the calculated trend by least squares fitting. Associated *t* test-derived *p* values (in parentheses) <0.05 indicate that the associated *r*² (in bold) are statistically significant.

site	variables	slope	r ² (p value)
Tordera	Hs (m)	0.00068	0.001 (0.868)
	Tp (s)	-0.0155	0.037 (0.178)
	D (h)	0.308	0.046 (0.138)
Llobregat	Hs (m)	-0.0018	0.004 (0.672)
	Tp (s)	0.0081	0.011 (0.465)
	D (h)	-0.0048	0.000 (0.977)
Ebro	Hs (m)	-0.0062	0.036 (0.180)
	Tp (s)	-0.0144	0.051 (0.107)
	D (h)	0.453	0.061 (0.077)

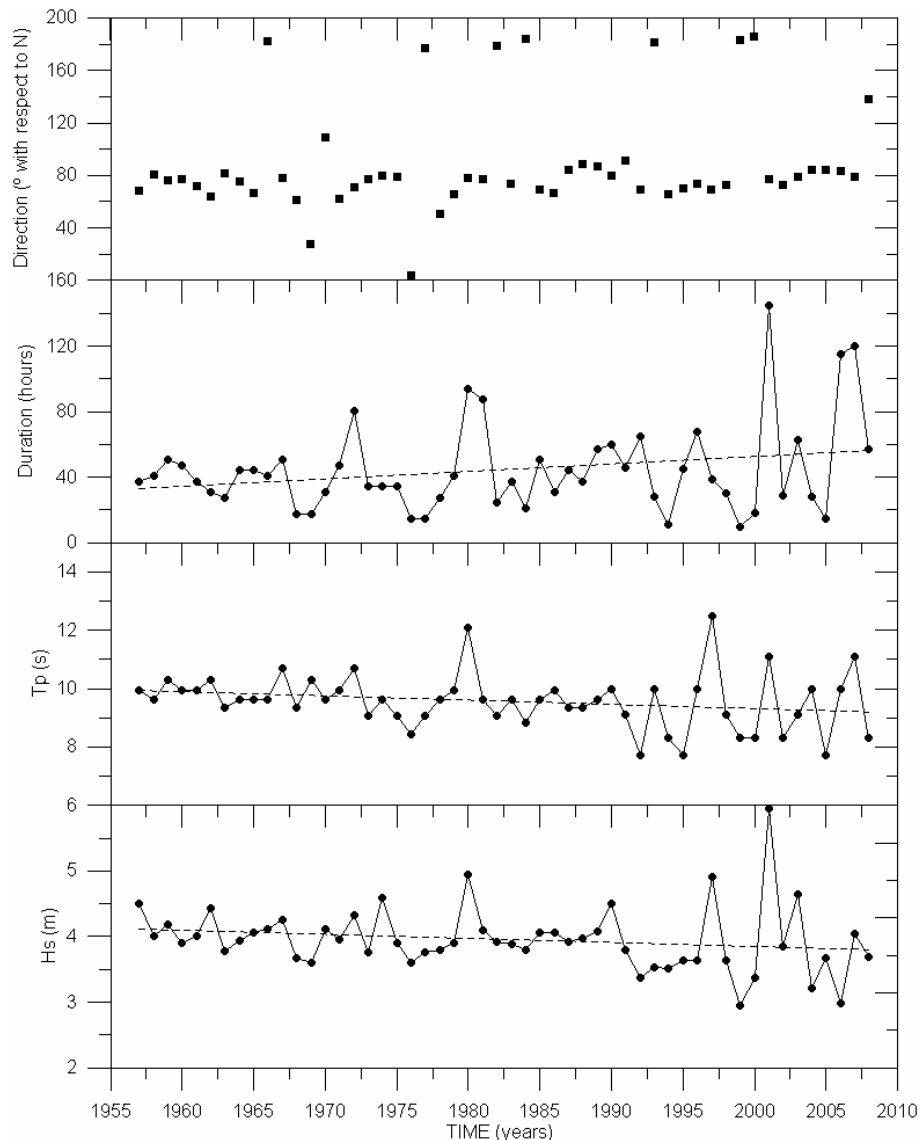


Figure 6. Long-term variations of wave variables defining the annual maximum storm at the Ebro delta during the period 1958-2008 (main trend analysis parameters are shown in table 1).

An overall measure of the magnitude of storminess in each site during the period 1958-2008 is shown in table 2 in form of basic statistics of reconstructed annual maximum storms time series.

According to these data, the S and N areas (Ebro and Tordera respectively) are the sites with larger storminess values (in terms of H_s and storm duration) whereas the central coast of Catalonia (here characterized by Llobregat data) can be considered the mildest energetic area. Thus, it is expected that storm-induced coastal hazards will be more important in the N and S areas whereas the central part of the Catalan coast will be subjected to lowest intensity hazards. However, it has to be mentioned that this will strictly be true in the case of an alongshore uniformity in coastal geomorphology. In reality, the hazard intensity will be jointly

conditioned by the intensity of storm characteristics (the ones analyzed here) and the coastal geomorphology which will control the magnitude of the coastal response to the storm forcing.

Table 2. Basic statistics of annual maximum storms at each site during the period 1958-2008 (μ : mean; σ : standard deviation; max: maximum value).

variables	site			
		Tordera	Llobregat	Ebro
Hs (m)	μ	3.70	3.61	3.96
	σ	0.42	0.44	0.50
	max	5.28	5.21	5.95
Tp (s)	μ	11.20	9.71	9.57
	σ	1.21	1.19	0.97
	max	13.8	13.3	12.5
D (h)	μ	44.3	39.8	44.7
	σ	21.6	17.5	27.7
	max	108	114	145

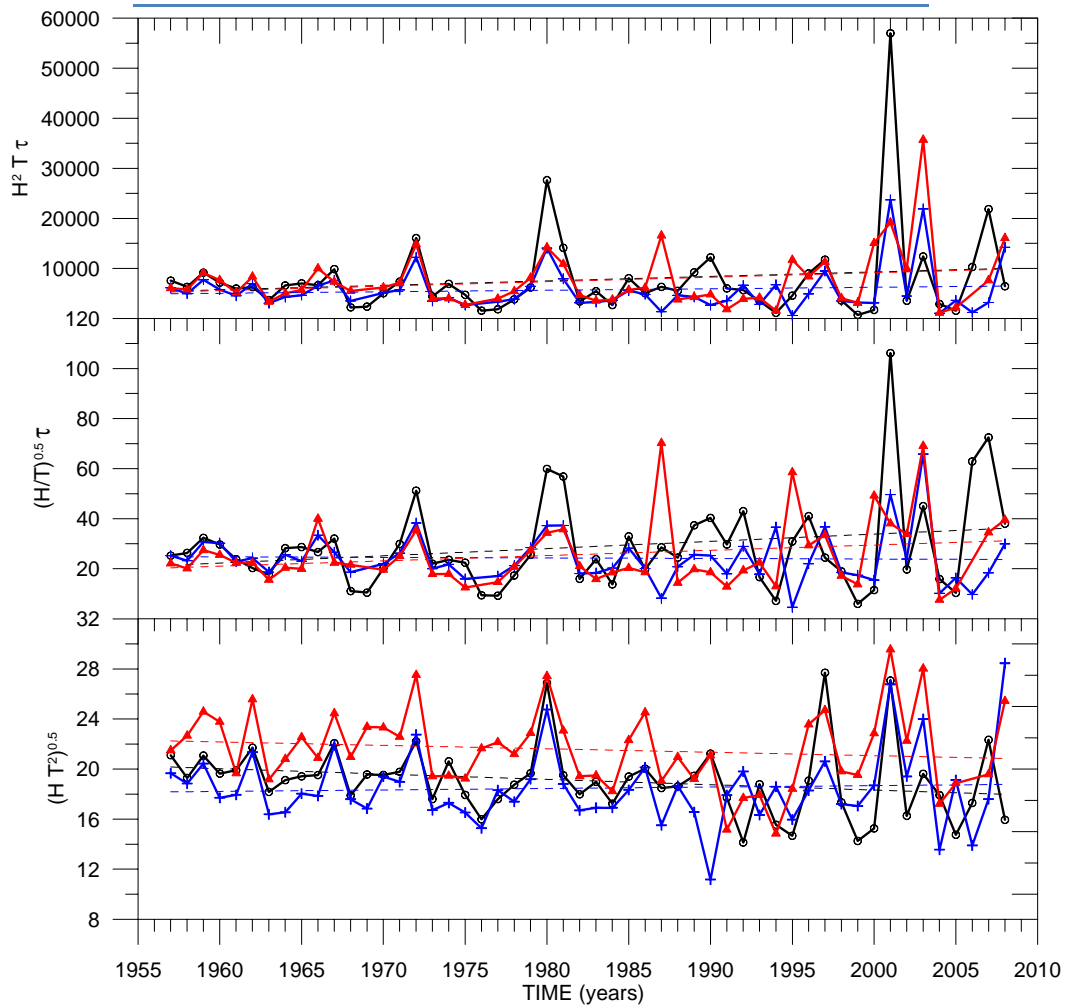


Figure 7. Long-term variations of storminess variables characterizing induced hazards (bottom: inundation; middle: beach erosion; top: sediment transport) in each site (black: Ebro; blue: Llobregat; red: Tordera).

Fig. 7 shows the time evolution of the variables used to characterize storm-induced hazards along the Catalan coast, whereas the numerical values obtained in the analysis are shown in table 3. As in the case of basic wave variables, storm-induced hazards do not show any statistical significant trend during the analyzed period in such a way that we can state that according to our data and, accepting that storminess can be schematized in terms of the annual maximum storm, no long-term trend can be detected during the last 50 years.

Table 3. Trend analysis of storm-induced processes (hazards) for the annual maximum storm for each site during the period 1958-2008. Slope is the calculated trend by least squares fitting. Associated t test-derived p values (in parentheses) <0.05 indicate that the associated r2 (in bold) are statistically significant.

site	variables	slope	r ² (p value)
Tordera	BE	0.211	0.0552 (0.104)
	I	-0.0274	0.0172 (0.359)
	TP	89.26	0.0519 (0.115)
Llobregat	BE	-0.0225	0.0011 (0.818)
	I	0.0116	0.0034 (0.681)
	TP	29.98	0.0103 (0.484)
Ebro	BE	0.289	0.0578 (0.086)
	I	-0.0427	0.0512 (0.107)
	TP	89.11	0.0249 (0.264)

Although no long-term trend has been detected in none of the analyzed time series used to characterize storminess along the Catalan coast, this does not mean that time series do not reflect any temporal pattern. In order to investigate the possibility of the existence of such pattern, we have analyzed time series in a different way. Thus, we have obtained for each variable characterizing storm-induced hazards a time series of its anomaly, which is defined as the actual yearly value minus the mean value of the parameter (averaged during the entire time period, i.e. 50 years). This will highlight years where the intensity of induced hazards are above the mean (positive anomalies) –energetic years- and mild years, when the hazards’ intensity is low (negative anomalies).

Figures 8, 9 and 10 show the 50 year anomaly time series for beach erosion, inundation and transport potential respectively. They show the same trend than the original ones, i.e. no statistically significant trends are detected. However, if we divide these time series in decades and, we obtain an averaged value for each 10 years period (table 4), we can identify time periods during which the considered hazard significantly varies.

This could be used to identify periods where we should expect larger values of storm-induced hazards and/or damages. Thus, for instance, the last decade (period 1999-08) can be characterized as the period showing the largest storm-induced beach erosion potential along the Catalan coast, being especially larger at the N and S ends. This fact also coincides with the fact that during this period is when larger damages have been reported along the Catalan coast due to the impact of storms.

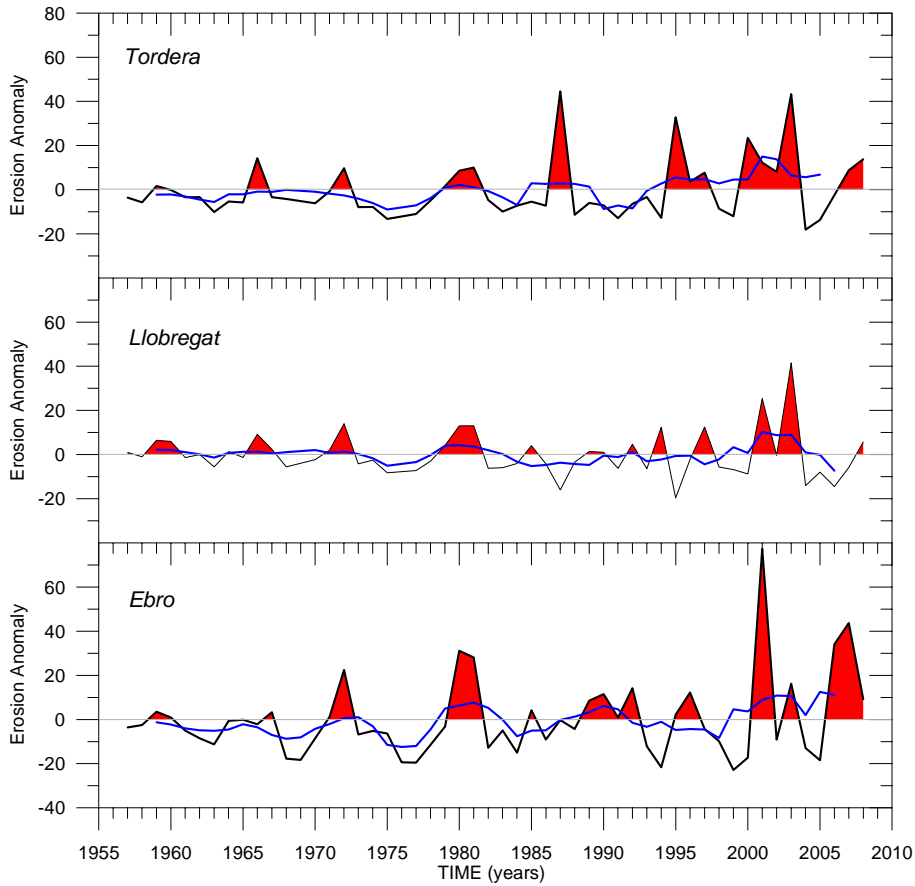


Figure 8. Long-term variations of storm-induced beach profile erosion anomaly at each location. Blue line is the 5-years running average anomaly.

Table 4. Averaged values of storm-induced hazard anomalies for periods of 10 years at each location along the Catalan coast.

Anomaly	Period	site		
		Tordera	Llobregat	Ebro
Erosion	1957-78	-2.437	0.942	-3.623
	1969-78	-5.277	-1.454	-7.211
	1979-88	1.874	-0.571	1.375
	1989-98	-1.314	-0.830	0.166
	1999-08	7.318	1.434	10.019
Inundation	1957-78	0.655	0.213	0.839
	1969-78	0.432	-0.526	-0.111
	1979-88	0.174	0.116	0.608
	1989-98	-2.322	-1.229	-0.504
Transport	1999-08	1.032	1.384	-1.000
	1957-78	-978	-243	-1191
	1969-78	-1530	-650	-2321
	1979-88	178	-237	711
	1989-98	-1975	-1198	-1065
	1999-08	4660	2246	4105

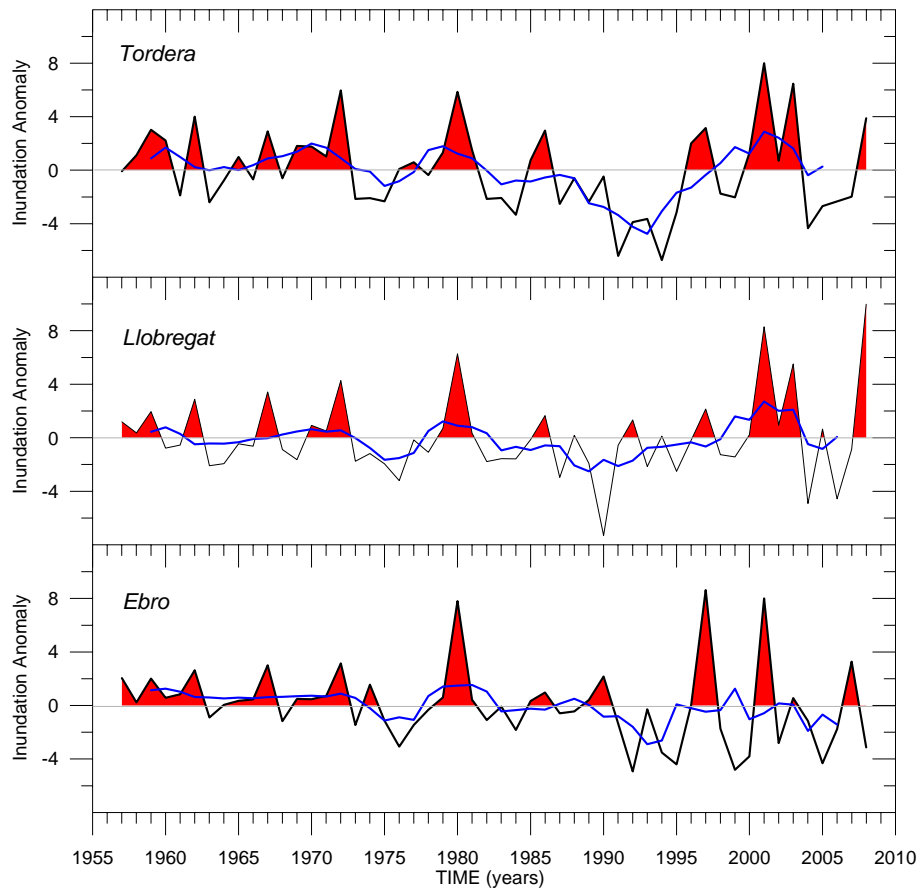


Figure 9. Long-term variations of storm-induced inundation anomaly at each location. Blue line is the 5-years running average anomaly.

As a final exercise and to further explore this apparent increase in hazards' intensity, we obtained the 5-years running averaged time series of morphodynamic responses (erosion, inundation and wave power, Fig. 8, 9 and 10). These series filter out short-term variations and reinforce the influence of clustered years (periods with similar hazards' intensity).

By applying the same trend analysis to these series, we obtained the results showed in table 5. As it can be seen, there are some series where a statistically significant trend has been detected. Thus, in the southern part of the Catalan (Ebro delta) coast, analyzed hazards (characterized by the 5-year running average of anomalies) show increasing beach erosion and sediment transport potential trends and a slightly decreasing inundation trend. In the northern part (Tordera delta), increasing erosion and sediment transport potential trends have been detected. On the other hand, hazards in the central part of the coast did not show any trend in intensity.

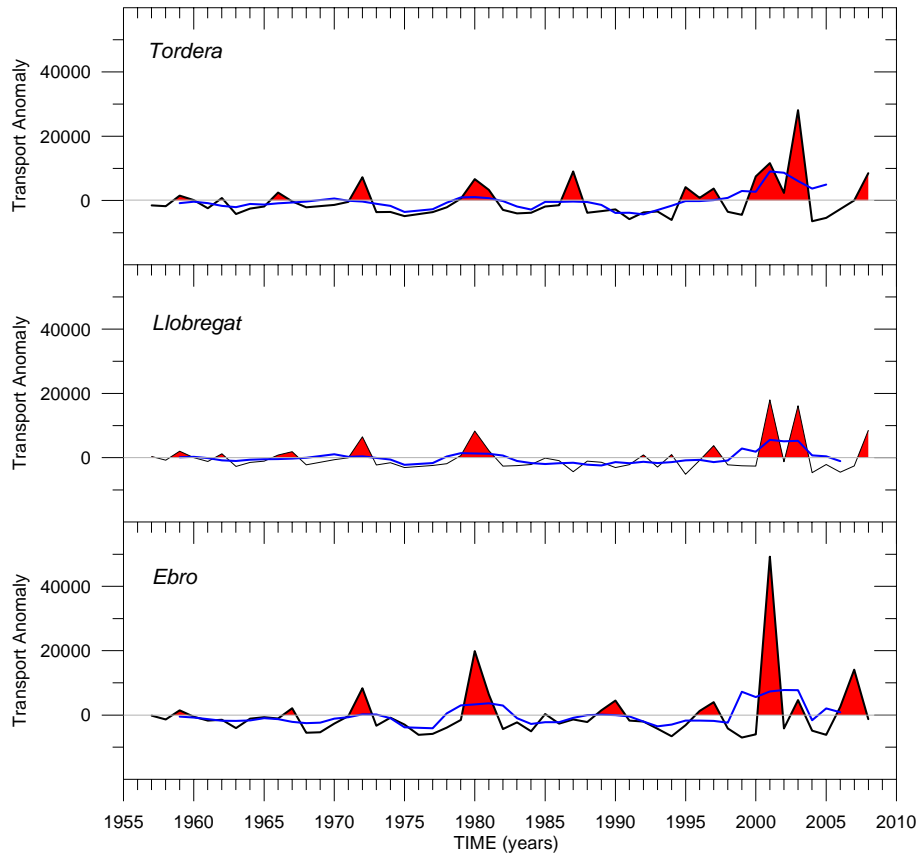


Figure 10. Long-term variations of storm-induced sediment transport anomaly at each location. Blue line is the 5-years running average anomaly.

Table 5. Trend analysis of 5-years running averaged time series of induced processes (hazards) for annual maximum storm for each site during the period 1958-2008. Slope is the calculated trend by least squares fitting. Associated t test-derived p values (in parentheses) <0.05 indicate that the associated r² (in bold) are statistically significant.

site	variables	slope	r ² (p value)
Tordera	BE	0.206	0.298 (0.000)
	I	-0.032	0.072 (0.066)
	TP	90.49	0.201 (0.001)
Llobregat	BE	-0.0000	0.00 (0.999)
	I	0.0033	0.002 (0.783)
	TP	30.7	0.054 (0.112)
Ebro	BE	0.239	0.284 (0.000)
	I	-0.041	0.312 (0.000)
	TP	91.81	0.174 (0.003)

12.5 Summary and Conclusions

In this report we have analyzed long-term changes in storminess along the Catalan coast. This was done by analysing reconstructed 50-years long time series of wave data. Storminess was characterized by the annual maximum storm, being the main variables defining the storm H_s, T_p, θ and τ. In addition to this, storminess was also analyzed considered the main storm-

induced hazards, i.e. beach profile erosion, inundation and sediment transport potential. This was done by proposing a set of parameters reflecting the contribution of the forcing (storm) to such processes.

The trend analysis applied to basic storm properties and hazards time series does not reflect any statistically significant trend and, in consequence we could conclude that for the analyzed period (1958-2008) no systematic change in storminess can be detected along the Catalan coast.

However, if morphodynamic hazards are analyzed by comparing their averaged value over periods of decades, the last decade (1999-2008) can be identify as the most hazardous in terms of beach erosion and sediment transport along the Catalan coast, and, especially for the northern and southern parts.

To further analyze this apparent clustering, 5-years running averaged time series of morphodynamic hazards anomalies were built and subjected to a trend analysis. In this case, the above mentioned behaviour was reinforced and, statistically significant increasing trends in beach erosion and sediment transport potential were obtained for the northern (Tordera delta) and southern (Ebro delta) parts of the Catalan coast.

12.6 Acknowledgements

We thank the Department of Territorial Policy and Public Works of the Autonomous Government of Catalonia and Ente Público de Puertos del Estado (Spanish Ministry of Public Works) for supplying wave data used in this study.

12.7 References

Dean, R.G., 1973. Heuristic Models of Sand Transport in the Surf Zone. 1st Australian Conf on Coastal Engineering, Sydney, 208 -214.

Guedes-Soares, C., Weisse, R., Carretero, J.C., and Alvarez, E., 2002. A 40 years hindcast of wind, sea level and waves in European waters. Proc. 21st Int. Conf. on Offshore Mechanics and Arctic Engineering, (OMAE 2002), ASME, New York, Paper OMAE2002-28604.

Jiménez, J.A., Sanchez-Arcilla, A. and Stive, M.J.F., 1993. Discussion on prediction of storm/normal beach profiles. Journal of Waterway Port Coastal and Ocean Engineering, 19(4): 466-468

Mendoza, E.T. and Jiménez, J.A., 2006. Storm-Induced Beach Erosion Potential on the Catalanian Coast. Journal of Coastal Research, SI 48: 81-88.

Stockdon, H.F., Holman, R.A., Howd, P.A. and Sallenger, A.H., 2006. Empirical parameterization of setup, swash and runup. Coastal Engineering, 53: 573–588.

13 UK

Luciana S. Esteves, Jon J. Williams, and Jenny Brown

13.1 Methods of analysis

The UK study site is located in NW England and analyses presented here are focussed on the Eastern Irish Sea and Liverpool Bay. Trends and observations obtained from the analysis of relevant time-series data (i.e. water level, surge levels, wave heights, wind speed and barometric pressure) available for MICORE UK are described. HIPOCAS results are not available for the Eastern Irish Sea; therefore the data used here were obtained from other sources, as described below.

13.1.1 Measured water level and surge - Tide Gauges

Water level data within the study area are available from Heysham (54°01'54.5"N, 02°55'12.9"W) and Liverpool Gladstone Dock (53°26'58.8"N, 03°01'05.3"W). From Heysham, data are available since 1964 and from Liverpool Gladstone Dock, since 1991. However, water levels at Liverpool have been measured for longer time-period by other tide gauges. Changes in extreme water levels have been analysed for the period 1768-1999 (Woodworth and Blackman, 2002) and change in sea level have been analysed using data from 1901-2004 (Woodworth et al., 2009). Here, trends of maximum water levels (tide + surge) and surge levels (difference between observed water level and predicted tide level) are analysed. Water levels above 10 m (CD) have been suggested to cause intense dune erosion (Pye and Blott, 2008); therefore trend analysis is performed here using water levels above 10m (CD).

13.1.2 Measured wind, barometric pressure and waves

Mean and maximum monthly wind speeds are available from 1929 to 2002 from Bidston Observatory. Daily mean wind speeds and barometric pressure and significant wave height data available for the period 03/04/2001 to 31/01/2009 from the Irish M2 met-ocean wave buoy³ (located 53.4800°N, 05.4250°W) have also been analysed. A shorter time-series (starting on 16/04/2004) of wind data is available from the Hilbre Island met station located at the mouth of the Dee Estuary (53° 22.94'N, 3° 13.60'W).

13.1.3 POLCOMS-WAM model

A nested POLCOMS-WAM system model was used to produce wave-surge results for the Eastern Irish Sea and Liverpool Bay for an 11-year period (01/01/1996 – 01/01/2007). The tide-surge interaction was modelled using the POLCOMS set up in a one-way nested approach from the 1/9° by 1/6° Operational Continental Shelf surge model to the 1.85 km Irish Sea model. POLCOMS technical description can be found on the Proudman Oceanographic Laboratory website⁴ and details of the Liverpool Bay model application is provided in Brown and Wolf

³ <http://www.marine.ie/home/publicationsdata/data/buoys/>

⁴ http://cobs.pol.ac.uk/modl/metfcst/POLCOMS_DOCUMENTATION/

(2009) and Wolf (2008). Surge predictions in the eastern Irish Sea have been calibrated using the November 1977 and January 2007 storm surge events (Brown and Wolf, 2009). The operational surge model has been regularly validated using data from the national tide gauge network⁵. The WAM results for the northeast Atlantic model have been validated for significant wave height (H_s), zero-crossing period (T_z) or peak period (T_p) using data obtained from 19 buoys and platforms. The Irish Sea POLCOMS-WAM model results for total water level and surge residual have been validated using data obtained from 19 tidal gauges and wave parameters measured in five locations.

13.1.4 ERA-40 waves, wind and barometric pressure

ERA-40 data available for the period 1960-2007 were used to extend the time-series of trend analysis of changes in storminess. However, the results should be considered with caution as wind and waves are underestimated for medium to large values in ERA-40 data, especially in enclosed seas such as the Irish Sea (Caires and Sterl, 2005). Furthermore, availability of ERA-40 data for the Irish Sea is limited to only one point in the 1.5° wave data and four points in the 1° met-data. These limitations resulted in only 10 events showing wave heights above 3 m and none above 4 m from 1960 to 1990. Considering that the wave height typically exceeds 3 m during 5–10 events per year and exceeds 4 m from 1–5 times per year (Wolf, 2008), ERA-40 wave data are unreliable for the Eastern Irish Sea. Therefore, only met data results are presented here. Trend analyses are conducted here identifying storm events showing barometric pressure <980 mb and wind speeds >17 m/s.

13.2 Results

According to Lowe and Gregory (2005), the coarse resolution of coupled climate models impede the simulations of individual storm surges and predictions for the next 50 to 100 year can be made only regarding the average frequency of events exceeding a certain water level (i.e. return period) based on present and future climate conditions. Using a fine-resolution regional climate model and the POL storm surge model, Lower and Gregory (2005) analysed changes in the height of 50-yr return period storm surge around the UK using SRES A2 and B2 for future climate conditions by 2080. These predictions indicate that cyclonic systems moving from the west will continue to dominate during the winter and the number of low pressure systems crossing the UK will increase from five to eight per winter for SRES A2. Additionally, the storm tracks will move southwards resulting in reduction of wind speeds in the north of the UK and increase in the south. Along the southern Irish Sea, the surge height is determined mainly by the inverted barometer effect, while along the northern Irish Sea the wind forcing contributes with 72% of the surge height (Lowe et al., 2001). Therefore, changes in wind speed are likely to directly affect surge heights in Liverpool Bay.

⁵ <http://www.pol.ac.uk/ntslf/surgemonthlyplots>

Analysis of mean and maximum monthly wind speeds measured at Bidston Observatory (1929-2002) (Fig. 1a) or the annual mean and maximum calculated from the same dataset does not show any significant trend. The shorter-term dataset of daily mean wind speeds available from the met-ocean M2 buoy (2001-2009) indicate a slightly trend of increasing wind speeds ($R^2 = 0.34$). Considering wind speeds >17 m/s, the annual number of storm events were assessed using ERA-40 data. An average of six events per year occurred in the period 1960-2007, and a maximum of 18 events was observed in 2007. Fig. 1b indicates an increase in the number of events with wind speeds above 17 m/s per year; however, the trend shows a poor correlation coefficient ($R^2 \sim 0.34$ for third order polynomial). ERA-40 data was used also to identify storms based on events showing barometric pressure below 980 mb. The dataset showed high inter-annual variability (no events occurred in 1969 and a maximum of 12 events were identified in 2002) and a mean value of 6.3 storm events occurring annually; no trend was observed. The average number of storm events per year reduced to 1.4 when both criteria (barometric pressure < 980 mb and wind speeds > 17 m/s) are applied simultaneously and no significant trend was observed (Fig. 1b).

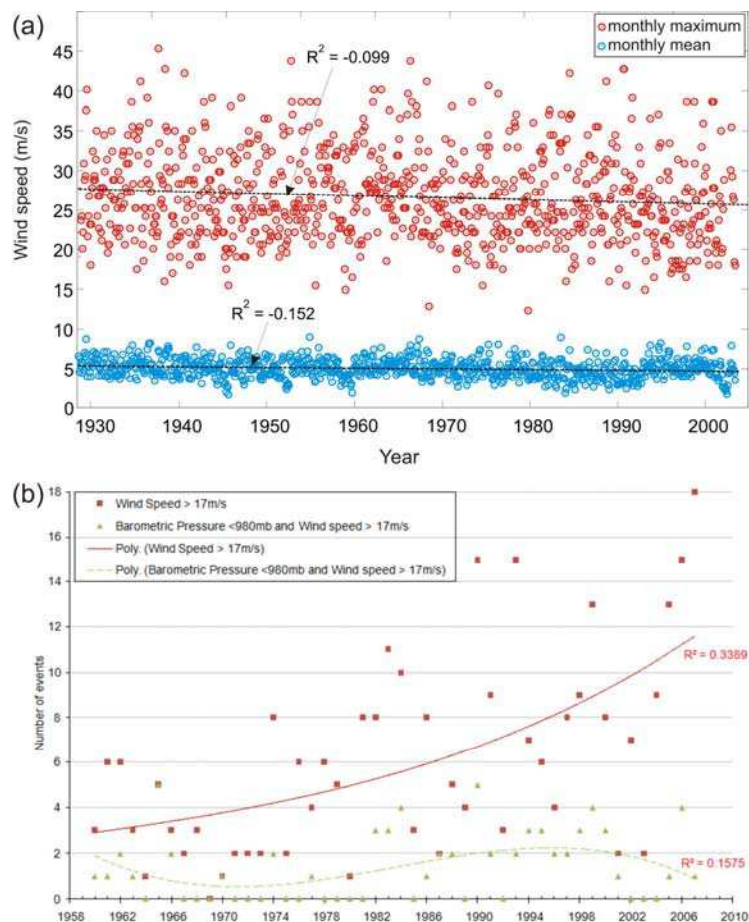


Figure 1. (a) Maximum and mean monthly wind speed from 1929 to 2002 obtained from ERA-40 data for the Eastern Irish Sea showing no significant trend through time. (b) Number of events per year based on wind speeds > 17 m/s (red squares) and wind speeds > 17 m/s and barometric pressure < 980 mb (green triangles).

At present, the 50-yr return period storm surge is 1.5-m for the Eastern Irish Sea and is predicted to increase between 0.2 m and 0.4 m due to climate change for the MICORE UK study site when predicted sea level rise (33 cm for SRES A2 and 25 cm for SRES B2) and rates of land movements are included (Lowe et al., 2001; Lowe and Gregory, 2005). However, when only changes in atmospheric storminess are considered, SRES A2 results in a slightly reduction of surge height in the south and a slightly increase in the north. The authors compare results with other similar studies and conclude that there is still a low confidence in any particular model attempting to simulate changes in storminess due to climate change. Model results from Lowe and Gregory (2005) indicate that sea level rise might be the factor determining an increase of up to 0.4 m in present surge levels in the Eastern Irish Sea by 2080. Therefore, it is relevant to include predictions of sea level rise in this report. Analysis of tidal records from Liverpool for the period 1901-2004 indicates a sea level trend of 1.6 ± 0.17 mm/yr or 1.8 ± 0.13 mm/yr depending on the method applied (Woodworth et al., 2009). For the UK, it is estimated that sea level will rise of 75 cm by 2080 for a high emission scenario (Hulme et al., 2002; Woodworth et al., 2009). This is more than double the 33 cm of sea level rise used in the modelling of increased surge levels presented by Lowe and Gregory (2005) and could represent a larger increase in surge levels for the MICORE study site.

A recent study by Pye and Blott (2008) indicates that increasing rates of dune erosion along the Sefton Coast are associated with periods of more frequent occurrence of extreme water levels. The authors indicate that, although these periods are correlated with the lunar nodal cycles, the meteorological forcing has had an effect. Other studies suggest that water levels trends in the UK are influenced by inter-annual and decadal variations, potentially driven by the 'inverse barometer effect' and the North Atlantic Oscillation (Woodworth et al., 2009; Woodworth and Blackman, 2002), which can significantly affect trends based on relatively short time periods. High inter-annual variability was observed in the values of annual maximum high water and surge at annual maximum high water at Liverpool in the period 1768–1999, but the dataset did not show any long-term trend over the 232 years (Woodworth and Blackman, 2002). However, the statistical distribution of annual maximum surge-at-high-water values shows highest values in the late-18th and late-20th, indicating a secular trend in distribution shape. Therefore, any analysis using time-series ending in the late 20th century is bound to show positive trends. Woodworth and Blackman (2002) suggest that variability within their dataset is similar to NAO and other indices and cannot yet be attributed to the beginning of a new long-term trend (Woodworth and Blackman, 2002).

Fig. 2a shows water levels above 10 m registered in the tidal records from Heysham for the period 1964 to 2008 and indicates no trend, corroborating with the findings of Woodworth and Blackman (2002) for Liverpool. There is an indication of a slight trend of increasing annual maximum tidal levels at Heysham but the correlation coefficient is poor (Fig. 2b) and it might just be reflecting the secular trend in distribution shape (higher water levels late in the 20th century) described by Woodworth and Blackman (2002). In the tide record from Liverpool (1991-2008), 18 events were identified having tide-surge residual elevation greater than 1.5 m

(Fig. 2c). No significant trend in the frequency of extreme surge levels was found at Heysham or Liverpool.

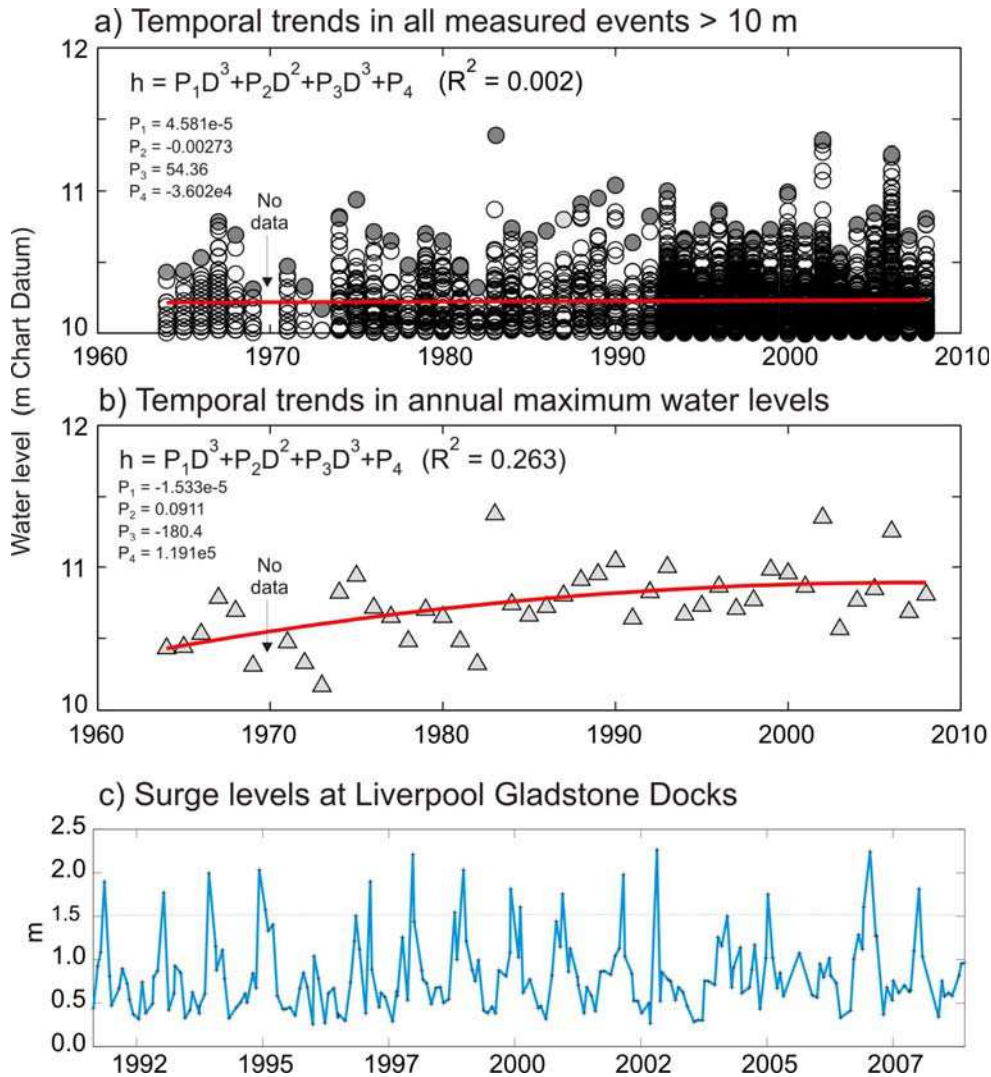


Figure 2. Water levels above 10 m (Chart Datum) observed at Heysham show no significant trend (a). A slightly trend of increasing the frequency of annual maximum water levels at Heysham is observed (b). Surge levels at Liverpool Gladstone Docks (c).

The largest surge residuals along the Sefton coast can reach 2.43 m (Fig.2c) and wave heights accompanying these surge events vary from 2.5 m to 5.6 m. Extreme wave events are defined as showing $H_s > 3$ m, while the extreme 1 in 50 year wave height is estimated to be 5.5 m (Wolf, 2008). No significant trend was observed for frequency of significant wave height (Fig. 3a) or extreme significant wave height ($H_s > 3$ m, Fig. 3b) in Liverpool Bay using POLCOMS results.

Increasing storminess in the North Atlantic at the end of the twentieth century has been suggested by studies based on barometric pressure and/or wind speeds (e.g. Schinke, 1993;

Lambert, 1996). Concomitantly, several studies indicate a high temporal variability (inter-annual and inter-decadal) in the occurrence of storms in the North Atlantic (e.g. Woodworth et al., 2007), which could explain an intensification of storm activity during certain time periods (Lozano et al., 2004; Wang et al., 2008). Lozano et al. (2004) has demonstrated that the North Atlantic Oscillation shows a quasi-decadal variability which agrees well with the changes in number of winter storms in the period 1965-1995. Further complexity to the analysis of changes in storminess is added by the increase in number of intense storms while the total number of storms remains unchanged. This has been observed in the North Atlantic during the period 1979-1997 (Sickmüller et al., 2000). The majority of the datasets analysed here for the Eastern Irish Sea does not indicate significant trends on change in storminess. The slightly trends shown in the number of events with wind speeds > 17 m/s (Fig. 1b) and the annual maximum water levels (Fig. 2b) is likely to be a result of the high temporal variability in storminess (associated with NAO, lunar cycle etc) described above.

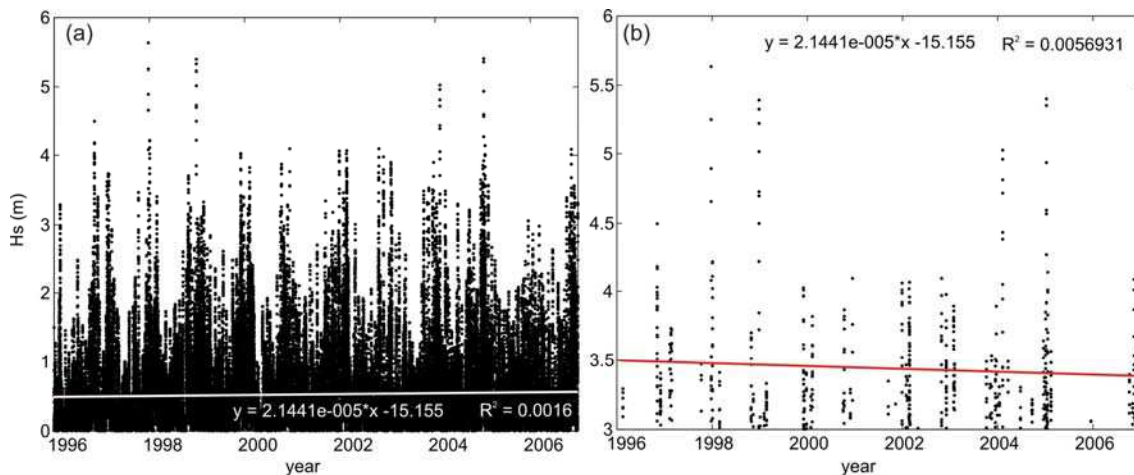


Figure 3. No significant trends were observed for significant wave height (a) or significant wave height >3m (b), values obtained from POLCOMS for Liverpool Bay.

13.3 Summary

Analysis of long-term tidal records and modelling results suggest no significant trends in the frequency or intensity of storms affecting the Eastern Irish Sea. Slightly trends of increasing (a) wind speeds (observed in the datasets from both the Irish M2 buoy and Hilbre), (b) the number of events showing wind speeds above 17 m/s (ERA-40 data) and (c) the annual maximum water levels at Heysham were identified and all showed poor correlation coefficient ($R^2 < 0.35$). These trends might well be reflecting inter-annual or decadal variability due to lunar cycle, NAO or other causes as described in the literature. Considering that surge heights in the northern Irish Sea are largely controlled by wind forcing (Lowe et al., 2001), the confirmation of even a slightly trend of increasing wind speeds might have a direct influence in the extreme water levels observed in the future along the coast of the Eastern Irish Sea. The short time-span of the available atmospheric pressure data does not allow computation of long-term trends or corroboration with the predictions of increasing numbers of low pressure systems

crossing the UK (i.e. Lower and Gregory, 2005). It is probable that the most critical expected impact of climate change in the Eastern Irish Sea is that the heights of the 50-yr return period storm surge are expected to increase by up to 0.4 m when a range 25-33 cm of sea level rise is included in the model predictions (Lowe and Gregory, 2005). Predictions of sea level rise by 2080 reach 75 cm along the UK (Hulme et al., 2002; Woodworth et al., 2009), which could potentially increase the predicted surge level and/or reduce its return period.

13.4 References

Brown, J. and Wolf, J., 2009. Coupled wave and surge modelling for the eastern Irish Sea and implications for model wind-stress. *Continental Shelf Research*, 29(10), 1329-1342.

Caires, S. and A. Sterl, 2005. A new non-parametric method to correct model data: Application to significant wave height from the ERA-40 reanalysis. *J. Atmospheric and Oceanic Tech.*, 22(4), 443-459.

Hulme, M. et al., 2002. Climate change scenarios for the United Kingdom: the UKCIP02 Scientific Report, Tyndall Centre for Climate Change Research, 120 pp.

Lambert, S.J., 1996. Intense extratropical northern hemisphere winter cyclone events: 1899–1991. *Journal of Geophysical Research*, 101, 21319–21325.

Lozano, I., Devoy, R.J.N., May, W. & Andersen, U., 2004. Storminess and vulnerability along the Atlantic coastlines of Europe: analysis of storm records and of a greenhouse gases induced climate scenario. *Marine Geology*, 210, 205-225.

Lowe, J. A. and Gregory, J. M., 2005. The effects of climate change on storm surges around the United Kingdom. *Philosophical Transactions of the Royal Society. Series A, Mathematical and Physical Sciences*. 363, 1313-1328.

Lowe, J.A., Gregory, J.M. and Flather, R.A., 2001. Changes in the occurrence of storm surges around the United Kingdom under a future climate scenario using a dynamic storm surge model driven by the Hadley Centre climate models. *Climate Dynamics*, 18(3-4), 179-188.

Pye, K., and Blott, S.J., 2008. Decadal-scale variation in dune erosion and accretion rates: An investigation of the significance of changing storm tide frequency and magnitude on the Sefton coast, UK. *Geomorphology*, 102, 652–666.

Schinke, H., 1993. On the occurrence of deep cyclones over Europe and the North Atlantic in the period 1930–1991. *Beitr. Phys. Atmosph.*, 66, 223–237.

Sickmüller, M., Blender, R. and Fraedrich, K., 2000. Observed winter cyclone tracks in the northern hemisphere in re-analysed ECMWF data. *Q. J. R. Meteorol. Soc.*, 126, 591–620.

Wang S., McGrath R., Hanafin J. A., Lynch, P., Semmler T. and Nolan P., 2008. The impact of climate change on storm surges over Irish waters. *Ocean Modelling*, 25, 83-94.

Wolf, J., 2008 Coupled wave and surge modeling and implications for coastal flooding. *Advances in Geosciences*, 17, 19-22.

Woodworth, P.L. and Blackman, D. L., 2002. Changes in extreme high waters at Liverpool since 1768. *International Journal of Climatology*, 22(6), 697-714.

Woodworth, P.L.; Teferle, F.N.; Bingley, R.M.; Shennan, I. and Williams, S.D.P., 2009. Trends in UK mean sea level revisited. *Geophysical Journal International*, 176, 19-30.

14 Final Considerations

As a first result, several differences can be highlighted on the approaches chosen by the MICORE partners, due to a variable quality in the available data, in the selection of best proxies for each coastal area and for the length of the time intervals. Despite the wish and effort at the first stages to follow a similar approach for all coastal regions, this proved to be untenable due to differences between datasets. This is explained in detail in the following sections. Table A summarises the approaches and the main results obtained for each studied region.

14.1 Differences in the available datasets

One major problem found by the MICORE partners was the difficulty in accessing long time-series of measured data. For several countries meteorological databases are not publicly available or have restrictions of use, which impede a free distribution of the data. In several cases datasets do not extend further than few years or, at the most, few decades. Data available from few years to a couple of decades are not useful to determine long-term trends that can be assumed to overcome interannual variability or cyclical behaviour. The solution to minimise this problem was to extend the existing databases of measured data by integration of results from hindcast models (mainly for waves) or use of hindcast results alone. The two main differences between the datasets assembled by the partners are therefore the data source (measured versus hindcast) and the size of time series (from 4 years up to 105 years depending on data availability for each regional coastline). For the purposes of these Final Considerations chapter, datasets with less than 30 years will not be considered as indicators of relevant climatic trends. Even so, three decades may be insufficient to overcome long-term cycles (e.g. 18yr lunar cycle) reason why the conclusions presented should be considered with caution considering the limits of the existing and available information. In specific cases, where results were already available from the literature (e.g. Belgium, Poland), the presented conclusions reflect a critical analysis of the conclusions reached by previous authors on the basis of the results presented in their papers/reports. To notice that in these cases the information is often from grey literature and therefore a compilation and analysis released in the public domain constitutes a useful progress on the current knowledge of the topic.

Almost all wind analyses were based on measured data, e.g. Belgium, Italy, Netherlands, Andalusia (Spain), Eastern Irish Sea (UK). For the Bulgarian Black Sea coastline the wind characteristics were reconstructed from reanalysis of hindcasted data and for Catalonia (Spain) hindcast and measured data were used together. All surge and water level analysis were based on measured data. On the contrary, wave analysis for datasets covering more than 30 years was mainly based on hindcasting (e.g. Bulgaria, France - Aquitaine and Mediterranean, Poland, Portugal - West Coast, Spain - Andalusia, and UK - Eastern Irish Sea). Measured data were only used for Belgium, Portugal (South Coast) and Catalonia (Spain) but in the two latter cases validated hindcast data were also used to complement the dataset.

The periods considered for wind analysis range from 46 years (Netherlands) to 105 years (Andalusia – Spain), for surge analysis range from 45 years (Poland) to 100 years (Netherlands), while for wave analysis range from 30 years (Belgium) up to 60 years (Bulgaria). For Italy the wave analysis was not included in this summary because only 18 years of wave records were available.

14.2 Differences in the used proxies

The different European coastal regions are subject to distinct storminess, which can be mainly expressed by surge levels and/or waves. Both are directly related to wind as a forcing agent, although surge levels will also be extremely dependent on changes on atmospheric pressure (e.g. low pressure systems) and, at a different time-scale, to changes induced by sea-level rise. For some coastal regions storm impacts are mainly related with surge levels (e.g. Belgium, Netherlands, Poland, Italy) while for others waves seem to be the most important factor (e.g., Portugal, Spain). Therefore, the use of a single proxy for all coastal regions was not possible, given the particular characteristics of each case. As a consequence, each partner defined specific proxies, based on the available data and on the nature of the studied coastal area.

Wind was used as a proxy for Belgium, Bulgaria, Italy (Northern Adriatic), Netherlands, Spain (Atlantic Andalusia) and UK (Eastern Irish Sea). Surges or water levels were used for Belgium, Italy (Northern Adriatic), Netherlands, Poland and UK (Eastern Irish Sea). Waves were used at all coastal regions with the exception of the Netherlands.

14.3 Differences in the analysis

All partners performed an evaluation of data quality and defined which type of analysis could be made for each data set. Ideally all proxies should provide results on storm duration, storm intensity and storm frequency trends. It was however not possible to analyse storm duration trends for Belgium and Spain (Atlantic Andalusia), storm intensity trends for Spain (Atlantic Andalusia) and storm frequency trends for Belgium. For all other coastal regions it was possible to analyse all firstly defined trends for at least one used proxy. In several cases more than one proxy was used. A solution to minimise problems with the overall analysis based on the used proxies was to reject interpretations based on averaged data (water levels/surges, wave heights or winds) and only use the analysis performed for values above a given and well defined threshold. A total of 54 proxies analyses were made, using surge/water levels, wave height and wind above a defined threshold for the 12 considered coastal regions.

14.4 Storminess analysis

A first conclusion from the concepts expressed above is that integrating and comparing all information at a European level is a rather difficult task, due to differences among data sets, in the used proxies and in the studied periods. As already stated above, the problem regarding the studied periods was minimised in this analysis by only using data sets covering the time span of at least 30 years of records/hindcast and only datasets representing analysis above a defined storm threshold.

Table A is a synthesis of the analysis performed by all partners and incorporates, among other information, the used storm threshold for each proxy, together with trend analysis on the parameters. The main conclusion derived from the table analysis is that a clear trend of storminess change at European level is not evident. The results express a large variability of trends from coastal region to coastal region. The dominant result is the absence of a trend, with most of the used proxies (62%; 36 in 58) showing “no trends”. About 19% (11 in 58) of the used proxies showed an increasing trend on storminess, with only 3 proxies (5%) having a statistically significant increase (for $p < 0.05$). Circa 19% (11 in 58) of the proxies showed a decreasing storminess trend, although none of them statistically significant. A summary of storm trends is presented in Table B.

14.4.1 Storm duration

The storm duration analysis was not performed for Belgium and Spain - Atlantic Andalusia. There was no observed trend for France - Aquitaine and Mediterranean, Italy - Northern Adriatic, Portugal - West Coast, Spain - Catalonia, and UK – Eastern Irish Sea. Non-significant decreasing trends were observed for Bulgaria and Portugal – South Coast, while Poland is the only region showing an increase (not-significant) trend.

14.4.2 Storm intensity

It was not possible to analyse storm intensity evolution for Spain – Andalusia, and there were no observed trends for Belgium (most of the used proxies), Bulgaria, France – Mediterranean, Italy – Northern Adriatic, Netherlands, Portugal – West Coast, Spain – Catalonia, and UK – Eastern Irish Sea. A non-significant decrease was observed for Portugal – South Coast and Belgium (one proxy, wave height higher than 3 m). Non-significant increases were recorded for Belgium (one proxy, surge level), Bulgaria (wind), France Aquitaine and Poland. It is important to note that for some countries (e.g. Belgium and Bulgaria) different proxies showed different trends.

14.4.2.1 Storm frequency

This evaluation was not performed for Belgium and Spain – Catalonia. There was no observable trend for Italy – Northern Adriatic (waves and winds), Portugal – West Coast, and UK – Eastern Irish Sea. Non-significant decreases were found for Bulgaria, Netherlands, Portugal – South Coast, and Spain – Atlantic Andalusia (for waves). An increase in storm frequency was observed in France – Aquitaine and Mediterranean (from the 1970s till 1990s), Italy – Northern Adriatic (one proxy, surges), Poland (significant both for surges and waves) and Spain – Andalusia (significant for wind). Six proxies out of 17 suggest an increase in storm frequency for 5 different coastal regions. However, it must be stressed that 6 proxies show no trend and other 5 indicate a storminess decrease at 4 coastal regions. For one of the regions (Spain – Andalusia) one of the proxies (wind) indicates a significant increase while another one (waves) indicates a decrease, in agreement with the results for the neighbouring region (Portugal – South).

The use of 58 proxy analyses for 12 coastal regions of Europe, including modelled and measured data and the most important storminess indicators (surges, winds and waves), could give indicative values about storminess trends in Europe. However, from the results discussed above it must be stated that there is no general trend of storminess change in Europe, based on the studied coastal regions, used proxies and datasets.

For some coastal regions, specific trends can be pointed out:

Bulgaria – In general shows a decreasing storminess trend, although not significant.

France Aquitaine – In general shows an increasing, not significant, storminess trend.

Poland – In general shows an increasing storminess trend, significant for storm frequency.

Portugal South Coast – In general shows a decreasing, not significant, storminess trend.

The findings of this work also point towards the need of making available into the public domain all European data sets on storminess indicators, as well as to establish monitoring networks for storminess proxies that should be kept active for decades, integrating both new and historical data. Gaps in existing data should be filled with the most advanced and best validated models in order to diminish uncertainties and increase the accuracy of data analysis. At present storminess variability is much higher than the observed trends at the time scale of the performed analysis (more than 3 decades records). Some analysis (e.g. France - Aquitaine, Spain – Andalusia) indicated a direct relationship between storminess and NAO (North Atlantic Oscillation Index). It was however not possible to observe any clear association between storminess changes and global climate change. This does not imply that global climate change consequences (e.g., sea temperature increase, sea level rise) will not have an influence on European storminess and storminess impacts. It mainly means that for the existing and available data sets, those impacts have not been detected or do not have a visible and strong signal at European level.

Table A – Synthesis of the used proxies and analysis for each coastal region. Light and dark grey lines were not used for the overall analysis (analysed period < 30 years and use of average values, respectively). NA – Not available; * mean daily wind speed shows a weak increasing trend ($R^2 = 0.34$); ** <http://www.ecmwf.int/>;

Study site	Period	Proxy	Data type	Data source	Storm threshold	Storm duration trend	Storm intensity trend	Storm frequency trend
Belgium	1955-2006	Wind	Literature (measured)	Climar	Uw > 10,8 m/s	NA	No trend	NA
Belgium	1955-2006	Wind	Literature (measured)	Climar	Uw > 17,2 m/s	NA	No trend	NA
Belgium	1955-2006	Wind	Literature (measured)	Climar	max Uw	NA	No trend	NA
Belgium	1978-2007	Waves	Literature (measured)	Climar	Hs > 2 m	NA	No trend	NA
Belgium	1978-2007	Waves	Literature (measured)	Climar	Hs > 3 m	NA	Decrease, not significant	NA
Belgium	1978-2007	Waves	Literature (measured)	Climar	max Hs	NA	No trend	NA
Belgium	1925-2000	Surge	Literature (measured)	Seamocs	90 % annual surge level	NA	Increase (+ 1 mm/yr)	NA
Bulgaria	1948-2008	Waves	Hindcast	IO-BAS	Hs>1.5m	Decrease - not significant; 2.26 days/decade	No trend max Hs; Increase, not significant, mean Hs 0.003 m/yr	Decrease, not significant; 0.275 storms/decade
Bulgaria	1948-2008	Wind	Reanalysis/RAM (hindcast)	ECMWF/ NCEP/ IO-BAS	Uw>15m/s	Decrease - not significant; 2.26 days/decade	Increase, not significant, max Uw 1.42 ms-1/decade	Decrease, not significant; 0.275 storms/decade

France - Aquitaine	1958-2008	Waves	Hindcast	ERA-40	Hs>4m	No trend	Increase, not significant; 0.004 m/year	Increase from 1970 to 2000 (associated with NAO+) but no trend on a longer timescale
France - Mediterranean	1958-2008	Waves	Hindcast	Hipocas	Hs>3 m	no trend	no trend	Increase from 1970 to 2000, but no trend on a longer timescale
Italy - Northern Adriatic	1993-2008	Waves	Measured	ENI PCW rig,CNR CM rig, SWAN, RON Buoy, ARPA buoy	Hs>1.5m	No trend	No trend	No trend
Italy - Northern Adriatic	1960-2008	Wind	Measured	AM-UGM SYNOPS	Smits et al. (2005)	No trend	No trend	No trend
Italy - Northern Adriatic	1923-2008	Surges	Measured	Comune di Venezia-Centro Maree	Tide>1.1 m	NA	No trend	Increase
Netherlands	1962-2008	Wind	Measured	KNMI (coastal stations)	occurrence rate > 70/year & < 2/year	NA	No trend	Decrease between 5 and 10%/decade
Netherlands	1890-1990	Surge	Measured	RIKZ (coastal stations)	occurrence rate 15/year-10/year, 10/year-5/year, 5/year-1/year	NA	No trend	Slight decrease in frequency (-94.1, 79.7) cm/100 year
Poland	1947-2007	Surges	Literature	Wiśniewski & Wolski, 2008	Sea level \geq 570 cm	NA	NA	Increase, significant (p=0.0000007); 0.727 storms/decade
Poland	1958-2000	Waves	Hindcast	Hipocas	Hs>1m	Increase, not significant (p=0.0452); 0.246h/decade	NA	Increase, significant (p=0.00938); 3.129 storms/decade
Poland	1958-2000	Waves; storm energy	Hindcast	Hipocas	Hs>1m	NA	Increase, not significant (p=0.489); 0.002 hm ² /decade	NA
Portugal - West coast	1958-2001	Waves	Hindcast	Hipocas	Hs>5m	No trend; -	No trend; -	No trend;-
Portugal - South coast	1958-2008	Waves	Hindcast/Measured	Hipocas	Hs>3m	Decrease, not significant; 1 day/decade	Decrease, not significant; 0.2 m/decade	Decrease, not significant; 0.2 storms/decade

Spain-Atlantic Andalusia	1958-2008	Waves	Hindcast	Hipocas	Hm0>2m	NA	NA	Decrease, not significant; -1.2 storms/decade; variability associated with NAO
Spain-Atlantic Andalusia	1902-2007	Wind	Measured	ICOADS	Hm0(transfer function from wind and NAO datawind)>2m	NA	NA	Increase, significant; 1.0 storms/decade; ; variability associated with NAO
Catalonia _N (Tordera)	1958-2008	Waves	Hyndcast+Measured	Hipocas + Tordera wave buoy	Hs>2m	No trend	No trend	NA
Catalonia _Central (Llobregat)	1958-2008	Waves	Hyndcast+Measured	Hipocas + Llobregat wave buoy	Hs>2m	No trend	No trend	NA
Catalonia _S (Ebro)	1958-2008	Waves	Hyndcast+Measured	Hipocas + Ebro wave buoy	Hs>2m	No trend	No trend	NA
UK-Eastern Irish Sea - Heysham	1963-2008	Water level	Measured	BODC	h>10m	No trend	No trend	No trend
UK-Eastern Irish Sea - Gladstone Dock	1993-2008	Water level	Measured	BODC	h>10m	No trend	No trend	No trend
UK-Irish Sea - Princess Pier	1963-1982	Water level	Measured	BODC	h>10m	No trend	No trend	No trend
UK-Eastern Irish Sea - Various locations	1993-2008	Maximum surge residual	Measured	BODC	R>1.5m	No trend	No trend	No trend
UK-Eastern Irish Sea - Hilbre Island	2004-2008	Mean monthly wind speed	Measured	BODC	NA	No trend	No trend	No trend
UK-Eastern Irish Sea - Bidston	1929-2002	Mean monthly wind speed	Measured	BODC	NA	No trend	No trend	No trend
UK-Eastern Irish Sea - Bidston	1929-2002	Maximum monthly wind speed	Measured	BODC	Speed >17m/s	No trend	No trend	No trend
UK-Irish Sea - M2 wave buoy	2001-2008	Daily mean wind speed *	Measured	Irish Marine Institute	Speed >5m/s	No trend	No trend	No trend
UK-Irish Sea - M2 wave buoy	2001-2008	Daily mean barometric pressure	Measured	Irish Marine Institute	P<980mb	No trend	No trend	No trend
UK-Irish Sea - M2	2001-	Significant	Measured	Irish Marine	Hs>3m	No trend	No trend	No trend

wave buoy	2008	wave height		Institute				
UK-Eastern Irish Sea	1960-2007	Significant wave height	Hindcast	ERA40 **	Hs>3m	No trend	No trend	No trend
UK-Eastern Irish Sea	1997-2007	Significant wave height	Hindcast	POL	Hs>3m	No trend	No trend	No trend

Table B – Synthesis of storminess trends (duration, intensity and frequency) for each coastal region. NA – Not available, Grey – No trend, Pink – Increasing storminess, Blue – Decreasing storminess.

Study site	Period	Proxy	Storm duration trend	Storm intensity trend	Storm frequency trend
Belgium	1955-2006	Wind	NA	Grey	NA
Belgium	1955-2006	Wind	NA	Grey	NA
Belgium	1955-2006	Wind	NA	Grey	NA
Belgium	1978-2007	Waves	NA	Grey	NA
Belgium	1978-2007	Waves	NA	Blue	NA
Belgium	1978-2007	Waves	NA	Grey	NA
Belgium	1925-2000	Surge	NA	Pink	NA
Bulgaria	1948-2008	Waves	Blue	Grey	Blue
Bulgaria	1948-2008	Wind	Blue	Pink	Blue
France - Aquitaine	1958-2008	Waves	Grey	Pink	Pink
France - Mediterranean	1958-2008	Waves	Grey	Grey	Pink
Italy - Northern Adriatic	1960-2008	Wind	Grey	Grey	Grey
Italy - Northern Adriatic	1923-2008	Surges	NA	Grey	Pink
Netherlands	1962-2008	Wind	NA	Grey	Blue
Netherlands	1890-1990	Surge	NA	Grey	Blue
Poland	1947-2007	Surges	NA	NA	Pink
Poland	1958-2000	Waves	Pink	NA	Pink
Poland	1958-2000	Waves; storm energy	NA	Pink	NA
Portugal - West coast	1958-2001	Waves	Grey	Grey	Grey
Portugal - South coast	1958-2008	Waves	Blue	Blue	Blue
Spain-Atlantic Andalusia	1958-2008	Waves	NA	NA	Blue
Spain-Atlantic Andalusia	1902-2007	Wind	NA	NA	Pink
Catalonia _N (Tordera)	1958-2008	Waves	Grey	Grey	NA
Catalonia _Central (Llobregat)	1958-2008	Waves	Grey	Grey	NA
Catalonia _S (Ebro)	1958-2008	Waves	Grey	Grey	NA
UK-Eastern Irish Sea - Heysham	1963-2008	Water level	Grey	Grey	Grey
UK-Irish Sea - Princess Pier	1963-1982	Water level	Grey	Grey	Grey
UK-Eastern Irish Sea - Bidston	1929-2002	Maximum monthly wind speed	Grey	Grey	Grey
UK-Eastern Irish Sea	1960-2007	Significant wave height	Grey	Grey	Grey

The MICORE Consortium

	Prof. Paolo Ciavola Coordinator WP7 Leader Italy	Dipartimento di Scienze della Terra Università degli Studi di Ferrara	Phone: +39.0532.97.46.22 Fax: +39.0532.97.47.67 E-mail: cvp@unife.it
	Mr. Marco Deserti Italy	Hydro-Meteorological and Climatological Service of the Emilia Romagna (ARPA-SIM)	Phone: +39.051.52.59.15 +39.051.649.7511 Fax: +39.051.649.75.01 E-mail: mdeserti@arpa.emr.it
	Mrs. Luisa Perini WP6 Leader Italy	Geological Survey of the Emilia-Romagna Region	Phone: +39.051.527.4212 Fax: +39.051.527.4208 E-mail: lperini@regione.emilia-romagna.it
	Prof. Oscar Ferreira WP1 Leader Portugal	University of Algarve CIACOMAR-CIMA	Phone: +351.289.800.900 Fax: +351.289.800.069 E-mail: offerreir@ualg.pt
	Prof. Rui Taborda Portugal	University of Lisbon Fundação da Faculdade de Ciências da Universidade de Lisboa	Phone: +351.217.500.357 +351.217.500.066 Fax: +351.217.500.119 E-mail: rtaborda@fc.ul.pt
	Dr. Javier Benavente Spain	University of Cadiz Department of Earth Sciences	Phone: +34.956.016.447 +34.956.016.276 Fax: ++34.956.016.195 E-mail: javier.benavente@uca.es
	Dr. Balouin Yann WP3 Leader France	BRGM-French Geological Survey Regional Geological Survey of Languedoc-Roussillon Montpellier	Phone: +33.467.157.972 Fax: +33.467.157.972 E-mail: y.balouin@brgm.fr
	Mr. Piet Haerens WP5 Leader Belgium	International Marine Dredging Consultants	Phone: +32.327.092.94 Fax: +32.323.567.11 E-mail: piet.haerens@imdc.be
	Prof. Jon Williams United Kingdom	University of Plymouth, School of Marine Sciences and Engineering	Phone: +44 (0) 1752 585928 Fax: +44 (0) 1752 585998 E-mail: jon.j.williams@plymouth.ac.uk
	Prof. Kazimierz Furmanczyk Poland	University of Szczecin INoM Laboratory of Remote Sensing and Marine Cartography	Phone: +48.91.444.23.51 Fax: +48.91.444.24.51 E-mail: kaz@univ.szczecin.pl
	Prof. Zdravko Belberov Bulgaria	Institute of Oceanology, Bulgarian Academy of Sciences	Phone: +359.52.370.493 +359.52.370.486 Fax: +359.52.370.483 E-mail: belberov@io-bas.bg
	Dr. Albertus "Ap" Van Dongeren WP4 Leader The Netherlands	Stichting Deltares	Phone: +31.15.285.8951 Fax: +31.15.285.8951 E-mail: ap.vandongeren@wldelft.nl
	Dr. Mark Van Koningsveld WP2 Leader The Netherlands	Technical University of Delft Civil Engineering	Phone: +31.6.53.246.297 +31.10.447.8767 Fax: +31.10.447.8100 E-mail: M.vanKoningsveld@tudelft.nl
	Dr. Alejandro Jose Souza United Kingdom	Natural Environment Research Council Proudman Oceanographic Laboratory	Phone: +44.15.17.954.820 Fax: +44.15.17.954.801 E-mail: ajso@pol.ac.uk
	Dr. Pedro Ribera Spain	University Pablo de Olavide Department of Physical, Chemical and Natural Systems	Phone: +34.954.349.131 Fax: +34.954.349.814 E-mail: pribrod@upo.es
	Mrs. Stefania Corsi Italy	Consorzio Ferrara Ricerche	Phone: +39.0532.76.24.04 Fax: +39.0532.76.73.47 E-mail: stefania.corsi@unife.it